CHALMERS

# Subjective perception and prediction model of vehicle stability under aerodynamic excitations

ARUN KUMAR

Department of Mechanics and Maritime Sciences
CHALMERS UNIVERSITY OF TECHNOLOGY
Göteborg, Sweden 2021

THESIS FOR THE DEGREE OF LICENTIATE OF ENGINEERING

# Subjective perception and prediction model of vehicle stability under aerodynamic excitations

ARUN KUMAR

Department of Mechanics and Maritime Sciences

CHALMERS UNIVERSITY OF TECHNOLOGY

Göteborg, Sweden 2021

Subjective perception and prediction model of vehicle stability under aerodynamic excitations
ARUN KUMAR



Thesis for the degree of Licentiate of Engineering 2021:18
Department of Mechanics and Maritime Sciences
Chalmers University of Technology
SE-412 96 Göteborg
Sweden
Telephone: +46 (0)31-772 1000

Chalmers Digitaltryck
Göteborg, Sweden 2021

Subjective perception and prediction model of vehicle stability under aerodynamic excitations
ARUN KUMAR
Department of Mechanics and Maritime Sciences
Chalmers University of Technology

# Abstract

The current automotive era is moving towards electrified vehicle propulsion. As a result, an energy efficient vehicle design becomes one of the top priorities. From an aerodynamics point of view, the vehicle should be more streamlined for minimal aerodynamic drag. Such designs have the potential to enhance vehicle sensitivity when exposed to external disturbances such as unsteady aerodynamic forces and moments created by the flow of air around the vehicle.

Before signing off for production, several on-road test scenarios are conducted by professional drivers to evaluate the new vehicle's performance. Finding vehicle instabilities and proposing solutions to problem's during such late phases of development is challenging in many aspects. The objective of this paper is to correlate and predict the driver's subjective perception on high-speed straight-line driving stability with measurable quantities in the early phase of development.

In this work, different aerodynamic devices were used for generating higher lift and asymmetric aerodynamic forces resulting in substandard straight-line drivability on-road. An inverted wing, an inverted wing with an asymmetric flat plate, and an asymmetric air curtain attached under the bumper were the selected aerodynamic devices paired with and without bumper side-kicks. The side-kicks help define the flow separation, thus improving the drivability of the tested vehicle. Plots of mean and standard deviation and ride diagrams of lateral acceleration, yaw velocity, steering angle, and steering torque are used to understand vehicle behaviour for the paired configurations and relate to the difference of subjective judgment of drivability within each pair. The ride diagram was used to separate the presence of transient behaviour and study its impact on subjective judgement. The qualitative assessment of the resulting trends agrees well with the subjective judgement of the driver.

Clinical tests were conducted using driving simulators, in order to have an in-depth understanding of the subjective perception and responses of drivers towards external disturbances. Both common and experienced test drivers were involved in this test. The results provided an insight towards the disturbance frequencies and amplitudes of interest. From the test data, a model is generated that can predict the drivers' subjective perception after experiencing induced external disturbances. The outcome also shows the impact of drivers' steering action on their subjective perceptions towards these disturbances.

Keywords: Driving simulator, human-vehicle interaction, drivability, unsteady aerodynamics, vehicle stability, prediction model, driver perception.

# Acknowledgements

I would like to start by thanking my academic supervisors Professor Simone Sebben and Professor Bengt Jacobsson for their dedication, support, and guidance throughout my work. Immense gratitude lies towards Dr. Erik Sällström, my industrial supervisor, for his dedicated limitless support in guidance and in improving the quality of my work. I want to thank my second industrial supervisor, Dr. Kaveh Amiri, for his excellent supervision and guidance at any time. I would like to thank Alexander Broniewicz, former project head, who was the first to introduce me to this opportunity, for his resourcefulness and support ever since.

I thank the Swedish Energy Agency and the Strategic Vehicle Research and Innovation Programme (FFI) and Volvo Cars for funding the project.

All my experimental work would not be possible if I had not received support from the following people. The people at Volvo Cars, wind tunnel, Volvo Cars' driving simulator, VTI and Hällered Proving Ground. I would have to especially thank all the Volvo test engineers, especially Dr. Egbert Bakker, for being available when approached. I would also like to thank Sergej Abyzov from DEWEsoft, Tommy Gundersen, and Mikael Fischer from Volvo cars instrument support for helping in the test equipment setup. Special thanks to mechanics at Volvo Cars and Hällered Proving Ground for their patience and ingenuity for vehicle setup.

Furthermore, it would be impossible to move forward without mentioning my former and present colleagues at Volvo Cars Aerodynamics group and Chalmers VEAS group for providing a supportive and friendly environment.

I thank my parents, grandparents, and my whole big family back home, my mother, for all that I have started is from you. To Anju, thank you for being around, supporting me with love, care, and support over my hardships.

# Nomenclature

**Abbreviations**

| | |
|---|---|
| CAN | Controller Area Network |
| CFD | Computational Fluid Dynamics |
| DoF | Degree of Freedom |
| IMU | Inertia Measurement Unit |
| MCA | Motion cueing algorithm |
| MS | Mean Squared Value |
| RMS | Root Mean Square Value |
| SUV | Sports Utility Vehicle |
| VTI | Statnes Väg- och Transportförskninginstitut (Swedish National Road and Transport Research Institute) |

**Symbols**

| | | |
|---|---|---|
| $\beta$ | Vehicle body slip angle | [deg] |
| $\delta_{sw}$, $\delta_{SW}$ | Steering wheel angle | [deg] |
| $\dot{\delta}_{sw}$ | Steering rate | [deg/s] |
| $\theta_{vh}$ | Pitch angle | [deg] |
| $\dot{\theta}_{vh}$ | Pitch velocity | [deg/s] |
| $\tau_{sw}$, $T_{SW}$ | Steering wheel torque | [Nm] |
| $\phi_{vh}$ | Roll angle | [deg] |
| $\dot{\phi}_{vh}$, $\omega_x$ | Roll velocity | [deg/s] |
| $\psi$ | Relative flow angle | [deg] |
| $\psi_{vh}$ | Yaw angle | [deg] |
| $\dot{\psi}_{vh}$, $\omega_z$ | Yaw velocity | [deg/s] |
| $\dot{\omega}_x$ | Roll acceleration | [deg/s$^2$] |
| $\dot{\omega}_z$ | Yaw acceleration | [deg/s$^2$] |
| $\vec{\omega}$ | Vehicle body angular velocity vector | [deg/s] |
| $\vec{a}$ | Vehicle body acceleration vector | [m/s$^2$] |
| $\vec{F}_{aero}$ | Aerodynamic loads | [N & Nm] |
| $\vec{z}_t$ | Road vertical wheel input vector | [m] |
| $a_y$, $\ddot{y}_{vh}$ | Lateral acceleration | [m/s$^2$] |
| $c_{DT}$ | Driver type | [-] |
| $C_{lf}$ | Aerodynamic coefficient of front lift force | [-] |
| $C_{lr}$ | Aerodynamic coefficient of rear lift force | [-] |
| $s$ | Time | [$s$] |
| $V_{mag}$ | Relative flow magnitude | [m/s] |
| $v_x$ | Vehicle longitudinal velocity | [m/s] |
| $w_x$ | Longitudinal wind component | [m/s] |
| $w_y$ | Crosswind component | [m/s] |
| $\ddot{x}_{vh}$ | Longitudinal acceleration | [m/s$^2$] |
| $\ddot{z}_{vh}$ | Vertical acceleration | [m/s$^2$] |

| **Definition** | |
|---|---|
| High Speed | $\geq$ 200 km/h |
| $p2p$ | Peak-to-peak value |
| $std$ | Standard deviation |

# Thesis

This thesis consists of an extended summary and the following appended papers:

**Paper A** Kumar, A., Sebben, S., Sällström, E., Jacobson, B. J. H., and Broniewicz, A. "Analysis of Subjective Qualitative Judgement of Passenger Vehicle High Speed Drivability due to Aerodynamics". *Energies* **12**.14 (2019). DOI: 10.3390/en12142839

**Paper B** Kumar, A., Sällström, E., Amiri, K., Jacobson, B., and Sebben, S. "Prediction of Driver's Subjective Perception and Vehicle Reaction under Aerodynamic Excitations". *Submitted to Vehicle System Dynamics* (2021)

## Division of work

- All instrumentation setup, data acquisition and analysis for Paper A was done by Kumar. The high-speed driving at the test track was performed by Kumar with the support of three experienced test drivers. The first manuscript was written by Kumar then discussed, reviewed, and revised by all authors.
- All instrumentation setup, data acquisition and analysis for Paper A was done by Kumar. The driving simulator setup was done by Kumar with dedicated people at Volvo Cars' driving simulator and VTI. The high-speed driving in the driving simulator was performed by engineers at Volvo Cars and PhD colleagues. Kumar together with Sällström build the predictive regression model. The first manuscript was written by Kumar then discussed, reviewed, and revised by all authors.

# Contents

# Part I

# Extended summary

# 1

# Introduction

This thesis brings an insight towards passenger vehicle driving stability in high-speed straight-line cruising conditions. The study focuses mainly on relating the subjective judgement of drivers to physically measurable quantities such as linear and rotational accelerations and velocity, and steering characteristics. Human perception, vehicle dynamics, and aerodynamics are the key fields coupled in this study.

Designing a vehicle is challenging as it needs to impress the customer both aesthetically and with energy efficiency. The impact of aerodynamic drag is becoming increasingly prominent, especially with the electrification of vehicles. Designing a vehicle with low aerodynamic drag might bring in susceptibility to vehicle instabilities. The pre-production vehicles are tested on-road by test drivers to subjectively assess the driving dynamics and vehicle stability in different driving scenarios. These tests take place in the later phase of development. Unsteady aerodynamics constantly influences the vehicle and is predominant at high speeds ($\geq$ 200 Km/h). The test drivers usually rate the vehicle performance from 1-10, 1-5 being unacceptable. The rating is split into different scenarios such as high-speed cornering, high-speed lane maneuvers, high-speed braking, vehicle response to gust, etc.

Nervousness is a common vehicle instability behaviour felt while driving in a straight-line. The causes for nervousness can be many. The one in focus in this study is due to aerodynamic instabilities. For drivers, such nervousness can produce subjective impressions ranging from merely inconvenient to alarmingly unacceptable behavior. Finding such behaviours during on-road tests is not desirable as it is already in the later phase of development. In this work, several studies are conducted to find ways to improve the prediction of such subjective evaluations from test drivers and relate them to objective measurable quantities in the early phase of development. Simulation tools such as CFD, wind tunnels, vehicle dynamics simulations, and driving simulators can help in developing an improved stable design. The focus of this study is developing a predictive model for drivers' ability to feel external disturbances and investigate the relationship between subjective perception and measurable objective quantities.

## 1.1 Project objectives

The first half of this research aimed to study and contribute to answering the following main questions and sub-questions:

1. *For a given phenomena, how can objective quantities such as steering response, linear and rotational accelerations be related to subjective judgement?* Find out how the driver's judgement is relatable to the measured objective quantities. How can one blind-folded point out the difference in subjective judgements between two cases from objective quantities? Can we use any add-ons to use for such comparison?

2. *Is it possible to predict a driver's ability in identifying an induced disturbance in an early design phase?* Can one predict the probability of drivers being able to identify an induced disturbance from the available objective quantities? Can the influence of the type of drivers be understood?

3. *Which quantities have a significant influence on drivers' perception towards driving instabilities?* Which quantities dominate the drivers' perception of stability over the others?

## 1.2 Limitations

This study is limited to straight line driving under a near gust-free environment. Only a set of speeds were considered in this study: paper A at 230 and 250 km/h and paper B at 200 km/h. The influence of acoustic and visual inputs on a driver's stability perception is not investigated in this study.

In on-road study (paper A), the test vehicle was a mid-size, front wheel driven and front weight biased sedan. The test was conducted using only one type of tire. For the driving simulator test (paper B), the test vehicle model was a compact sports utility vehicle (SUV). The vehicle dynamics model used for the clinical test such as tires and steering was more generic. Since both tests were done on a single type of vehicle, more tests involving different types of vehicles are needed to provide a more general outline.

Resources such as time and services limit the sample size, number of drivers, and the types of disturbances and combinations that can be studied. Furthermore, fatigue and mind saturation were also factors limiting the duration of the tests.

## 1.3 Thesis outline

Chapter 1 provides the purpose behind this project, objectives, and limitations faced during the tests. Chapter 2 narrates the necessary background, mathematical tools used for the study of the two papers. Chapter 3 explains the on-road test setups, methodology, result analysis and findings. This resulted in the first paper. Chapter 4 explains the Driving Simulator test setups, methodology, result analysis, and findings. This resulted in the second paper. Chapter 5 provides the final conclusions and plan for future investigations. Chapter 6 attaches to the resulting papers.

# 2

# Background

A vehicle behaviour under the influence of external disturbances during high speed driving provides an understanding of its stability. The key players influencing stability are aerodynamics, vehicle dynamics, driver, and environment.

In this study, the focus is on high-speed straight-line driving maneuvers. A flow diagram of the system is shown in Figure 2.1. The figure shows a simplified driver-vehicle flow design including the most important relations such as aerodynamic flow conditions and vertical road indentations. A background on high-speed straight-line test driving on-road and basic subjective relations are described in this chapter. Thereafter, the basic working principle of driving simulator is explained, followed by a brief discussion on the driver perception and subjective judgement characteristics.

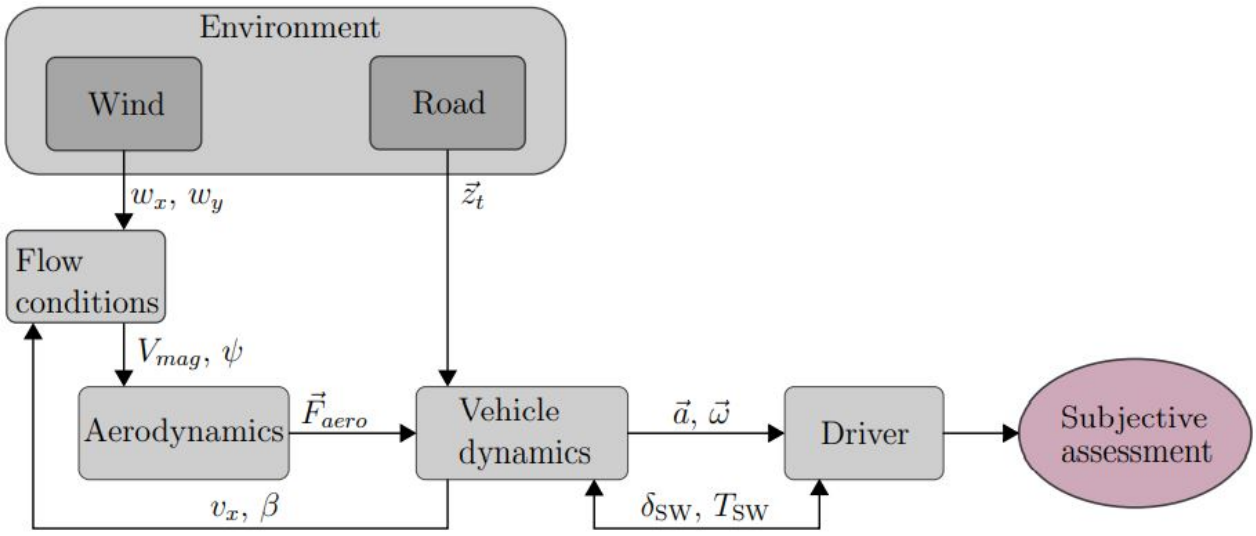


**Figure 2.1:** *A flow diagram on driver-vehicle-disturbance interactiony. Courtesy of A. Brandt [3]*

## 2.1 Testing environment

On-road testing and driving simulator testing are available to investigate the influence of unsteady aerodynamics on vehicle stability. The background on the methods used in this study is explained in the succeeding sections. In this work, on-road was used for the first experiment

resulting in paper A and the driving simulator for the second experiment resulting in paper B.

### 2.1.1 On-road test

On-road tests are still used by automobile manufacturers in the final phase of the development for final tuning and evaluation of the vehicle performance. It has many advantages over simulations. On-road tests simulate more realistic driving conditions. The drivers are more involved, they do not have the false sense of safety they have in the driving simulator. The experience felt by drivers and their resulting responses from simulated crosswinds in a wind tunnel or driving simulator are different from the ones under a natural stochastic crosswinds felt during on-road tests. On the other hand, the external environment and influences are not completely repeatable. A lot more testing is required for achieving the same uncertainty when implementing a standardized driving test under potentially high random noise. Typically, it is not realistic to do as much testing as is necessary. Moreover, certain on-road maneuvers might be hazardous and ethically challenging.

The aerodynamic disturbances affecting vehicle stability can be either due to external excitations such as impacts of wind gusts or vehicle heave or pitch due to road indentation [4–9] or as a result of complex flow structures due to the shape of the vehicle, as in studies by Okada et al. [10–12]. Okada et al. used on-road tests and CFD (Computational Fluid Dynamics) to show the influence of the rear lift fluctuations and A-pillar vortex relation on straight-line instabilities. Another study was done by Kawakami et al. [12] on improving vehicle performance by reducing the aerodynamic load fluctuations on a hatchback. The study was done using CFD, followed by a scale model wind tunnel test. Vortex generators proved to improve the subjective rating during on-road tests. The preliminary study, using CFD and wind tunnel tests showed how these vortex generators suppressed the yaw and roll moment fluctuations by creating a more distinct separation region.

An on-road study by Howell et al. [13] investigated the influence of front axle lift coefficient $C_{lf}$ and rear axle lift coefficient $C_{lr}$ on straight-line and lane change stability for several kinds of passenger vehicles. The lift coefficients were obtained from wind tunnel tests. The results provided an initial design criteria of $C_{lf} + C_{lr} \leq 0.2$ and $|C_{lf} - C_{lr}| \leq 0.1$ while designing the vehicle. Buchheim et al. [14] investigated the influence of aerodynamic parameters on vehicle stability at high-speed straight-line, braking, and crosswind conditions. The test was done on-road. Both these studies provide insight into preliminary stability criteria. Low overall lift forces and positive pitching moment is desirable for an improved high-speed straight-line driving scenario. This is the motivation towards modifying the rear of the vehicle for the on-road test in paper A. The chosen aerodynamic devices increased the lift force of the test object. Through reduced traction between tires and road surfaces, straight-line driving standards were reduced, favouring the test requirement.

Studies contributing to how on-road subjective vehicle nervousness correlates with measurable quantities such as acceleration or steering during straight-line driving are limited. On-road tests were performed in this study to contribute answers to this question and the main results are presented in Chapter 3 and paper A.

### 2.1.2 Driving simulator test

Virtual simulation of on-road driving scenarios can be conducted in driving simulators with good repeatability and controlled environment conditions. Current computational power can incorporate the full vehicle characteristics to conduct maneuvers such as high-speed stability, crosswind, and primary ride, even in early vehicle development. Analysis from such early tests can lead to sooner design decision making, resulting in better product performance and reduced development costs through fewer prototypes [15].

In a driving simulator, a realistic driving impression plays a significant role for the driver to absorb the virtual reality [16]. In order to replicate the exact vehicle motions as real on-road for a given maneuver in full scope, the motion envelope should be the same as a real on-road environment. Such a motion is ideal but not practical. The motion envelope of a simulator is limited due to boundaries such as power, computing resources, actuator stroke length, etc. A motion cueing algorithm (MCA) is used to recreate the sensation of real on-road maneuvers within these boundaries. This algorithm balances the actuated degrees of freedom (DOFs) according to the type of experiment and expectations.

#### Motion platform

The driving simulator operated in this study uses the hexapod system, which is a very commonly used hardware platform [17]. It consists of six independently controlled prismatic actuators with the ability to transfer the load within 6 DOFs [18]. They are:

- Surge: Translation along x axis (linear motion)
- Sway: Translation along y axis (linear motion)
- Heave: Translation along z axis (linear motion)
- Roll: Turning along x axis (rotation motion)
- Pitch: Turning along y axis (rotation motion)
- Yaw: Turning along z axis (rotation motion)

The hexapod system has the limitations of stroke length, as explained above, and that all DOFs are mechanically connected. As a result, the use of one DOF limits the stroke potential of the others. In the driving simulator used in this study, the whole platform is combined with an XY-sled which adds two more DOFs, shown in Figure 4.1 [19].

#### Driving cues

Certain cues play a key role for perceived realism when simulating a real on-road maneuvers. They are:

- Visual cue: The computing delays between the driver's input and the visual display of the resulting motion in the simulator should be minimal. According to Blissing et al. [20] the maximum thresholds for visual latency ranges from 50 to 150 ms. Exceeding this threshold showed effects on driver's behaviour such as lane keeping and steering wheel reversal. Motion sickness and stress were other effects found at higher visual latency. The positioning of the observer in the platform should also be accurate enough to represent the desired visual sensation.

- Steering torque feedback: The driver's haptic feedback is important. The steering wheel feedback provides the driver with an understanding of coupled interactions between the front axle tires and the road.
- Motion cue: Boundaries in the range of accelerations and rotations in the simulator necessitate developing different motion cueing strategies that control the motion platform to reproduce realistic vehicle motion. Together with the utilization of the human kinaesthetic sense and vestibular system, the simulated vehicle motions are mapped to relatable platform feedback for the driver. The motion cueing algorithm incorporates motion cueing strategies and will be explained in the next subsection.

### Motion cueing algorithm

A motion cue algorithm maps the simulated vehicle motions to simulator motions. The type of motion cue algorithms that will be explained here are the classical algorithm and washout algorithms.

The classical motion cueing algorithm uses a frequency split approach as shown in Figure 2.2. The typical acceleration (or velocity) inputs from the simulated vehicle dynamics model to motion algorithm are:

- linear accelerations: longitudinal $\ddot{x}_{vh}$, lateral $\ddot{y}_{vh}$ and vertical $\ddot{z}_{vh}$
- rotational velocity (or accelerations): roll $\dot{\phi}_{vh}$, pitch $\dot{\theta}_{vh}$, yaw $\dot{\psi}_{vh}$

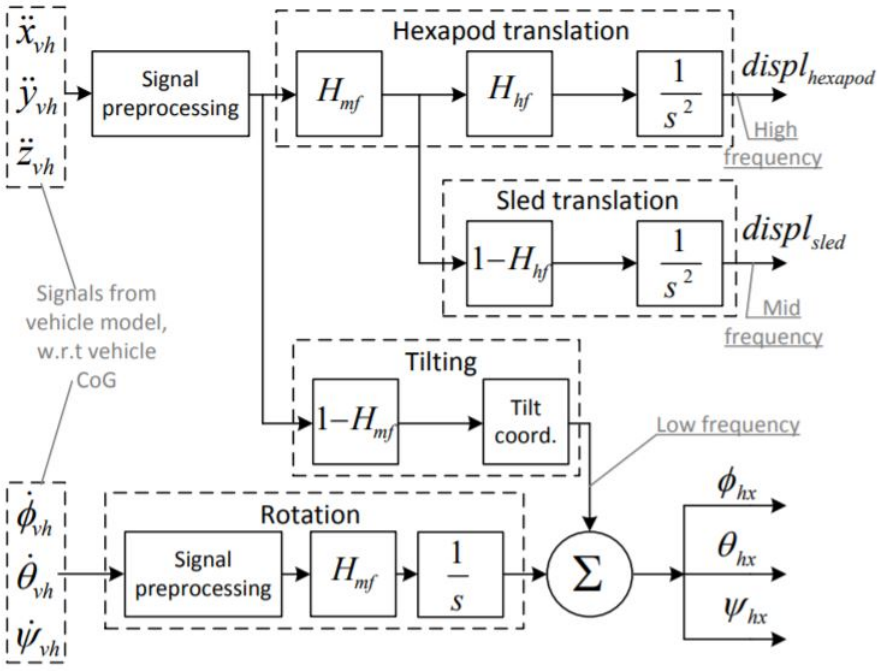


**Figure 2.2:** *Scheme of motion cue algorithm. Courtesy of A. Kusachov [18]*

The obtained accelerations (or velocities) are distributed to the hexapod and sled systems based on the frequency range. The linear accelerations are divided between translation motion and tilt coordination. The sled system takes the middle frequency linear accelerations and the hexapod takes the high frequency linear accelerations. Low frequency linear accelerations

are achieved by tilt coordination. Hexapod rotations will take this responsibility along with rotational acceleration.

The washout algorithm comes into play because during the test there can be scenarios where the simulator reaches its physical boundaries [21]. Washout is performed to prevent these conditions by bringing the platform slowly back towards its initial position. It should ideally be performed in stealth, otherwise the driver perceives false motions. A study by E. Groen et al. [22] found the rotational perception threshold as $3^\circ\ /s$.

Several studies have assessed a driver's reaction to external disturbances using driving simulators. Krantz et al. [23] investigated the crosswind influence on vehicle dynamics using a driving simulator. The unsteady aerodynamic coefficients relating to crosswind behavior of two different vehicles from wind tunnel tests were added to a single track model. The results of driving simulator tests were used to study and compare the yaw and lateral response with those of on-road tests. The drivers were asked to keep the vehicle in a straight-line. The investigated crosswind had a transient profile with a power spectral density peaking around 2 Hz. The study provided insight into the application of driving simulators in unsteady aerodynamics in the early development phase.

A paper by Huemer et al. [24] presented the influence of multidimensional vehicle response due to crosswind on driver perception also using a driving simulator. In their work the multidimensional vehicle response consists of roll velocity, yaw velocity, and lateral acceleration. The impact of amplitude changes and phase delay of crosswinds on the vehicle response was also investigated. Yaw moment disturbance showed the highest influence on driving stability, subsequently side force, and roll moment. Wagner et al. [25] studied the drivers' reactions and judgement on the vehicle behaviors due to the crosswind conditions, discussed later in Section 2.3.

Nguyen et al. [26] investigated a cornering scenario on the German autobahn with vertical disturbances simulating road unevenness and road bumps. The vehicle response was subjectively evaluated and the results included a threshold of sensitivity between pitch, roll, and lateral disturbance impulses over varying road noise intensities. In addition, the paper studied the subjective impression in the case of coupled yaw and roll motion with different phase delays and amplitudes.

In this work, a driving simulator was used with the purpose of building a regression model that can predict the probability of a driver to identify an induced disturbance with the help of the measured quantities such as vehicle and driver behaviours. The main results of the study are presented in Chapter 4 and paper B.

## 2.2 Analysis tool

Vector plotting, ride diagram and logistic regression are used for the study. These are explained in the following sections.

### 2.2.1 Vector plotting

Vector plotting is used as an objective indicator for subjective vehicle drivability, where vector lines join from one configuration to another. Vector lines that trend toward the origin implies improved drivability. The mean and standard deviation values of desired objective quantities such as steering torque or yaw rate are used to develop vector plots.

**Mean value**

The mean is calculated for a quantity $x$ according to the equation:

$$\bar{x} = \frac{1}{N}\sum_{i=1}^{N} x_i \tag{2.1}$$

where $N$ is the number of samples.

**Standard deviation**

The number of independent samples, $m$, of each signal is found using the auto-correlation function [27]. This function calculates the correlation between $x_i$ and $x_{i+k}$, where lag $k = 1, 2, 3, ...K$. According to Box et al. [28] the auto-correlation for $k$ is

$$r_k = \frac{c_k}{c_0} \tag{2.2}$$

where $c_0$ is the sample variance of the time series.

$$c_k = \frac{1}{N}\sum_{i=1}^{N-k}(x_i - \bar{x})(x_{i+k} - \bar{x}). \tag{2.3}$$

where $N$ is the total number of observations. The auto-correlation time, $\tau$, is

$$\tau = 1 + 2\sum_{k=1}^{K} r_k \tag{2.4}$$

The effective sample size is

$$m = \frac{N}{\tau}. \tag{2.5}$$

The variance of the signals are:

$$\sigma_x^2 = \frac{1}{N}\sum_{i=1}^{N}(x_i - \bar{x})^2 \tag{2.6}$$

The mean uncertainty with a coverage factor of 2, which corresponds to a coverage probability of approximately 95%, is:

$$\Delta\bar{x} = 2\frac{1}{\sqrt{m}}\sigma_x \tag{2.7}$$

### 2.2.2 Ride diagram

The ride diagram is another objective indicator used to relate potential influence of objective quantities of transient nature on subjective drivability. The method for ride diagram is done in three steps, defined by Strandemar et al. [29, 30]. The signal is divided into segments at the sign changes of the signal derivatives as shown in Equation 2.8.

$$\Omega = \{n \mid x(n-1) > x(n) < x(n+1) \text{ or } x(n-1) < x(n) > x(n+1)\} \tag{2.8}$$

Thus the $k$th segment will be expressed as:

$$y_k = \{x(n)\}_{n=n_k}^{n=n_{k+1}} \tag{2.9}$$

Where $k = 1, 2, ..., N_{k-1}$ and $N_k$ is the total number of peaks. The peak-to-peak value of $k^{th}$ segment is:

$$Ptp(k) = |\max(y_k) - \min(y_k)| \tag{2.10}$$

The segments can now be categorized as transient or stationary according to:

$$y_{trans}^k = \begin{cases} \{x(n)\}_{n_k}^{n_{k+1}} & Ptp(k) > T_{limit} \ \& \ Ptp(k-1) \leqslant T_{limit} \\ \{x(n)\}_{n_k+1}^{n_{k+1}} & Ptp(k) > T_{limit} \ \& \ Ptp(k-1) > T_{limit} \\ 0 & \text{otherwise} \end{cases} \tag{2.11}$$

where $Ptp(0) = 0,\ k = 1, 2, ..., N_k - 1$ and $N_k - 1$ is the number of segments. Figure 2.3 a shows an example of a random signal. As referred in Strandemar et al. [29], $T_{limit} = 2\sqrt{2}\ RMS(x)$ is the limit of transients also know as the signals energy equivalent amplitude.

The Mean Squared Values (MS) of transient and stationary (remaining) signals are related as shown in Equation 2.12.

$$MS_{transient} = \frac{1}{N} \sum_{k}^{N_k-1} \sum_{n} |y_{trans}^k|^2 \tag{2.12}$$

$$MS_{stationary} = \frac{1}{N} \sum_{n=1}^{N} x(n)^2 - MS_{transient} \tag{2.13}$$

For a given situation Figure 2.3 b shows the general idea of how to read the ride diagram with respect to drivability standards.

This method has some practical issues when the signals have small spikes in them. These spikes can be located in between an otherwise high peak-to-peak value as shown in Figure 2.4, as from time 26 to 27 s. when separating the signals with the $T_{limit}$ criterion, the algorithm only checks for the exact peak-to-peak values between these spikes. So the possibility is high for a peak-to-peak value, which would otherwise be eligible for being filtered as a transient segment, to not be filtered because of spikes. This can be reduced by downsampling the signals but this does not completely eliminate the problem. The method was originaly used by Strandemar et

al. [29] for relatively simple signals for testing in a driving simulator. Hence it needs further development for more realistic signals.

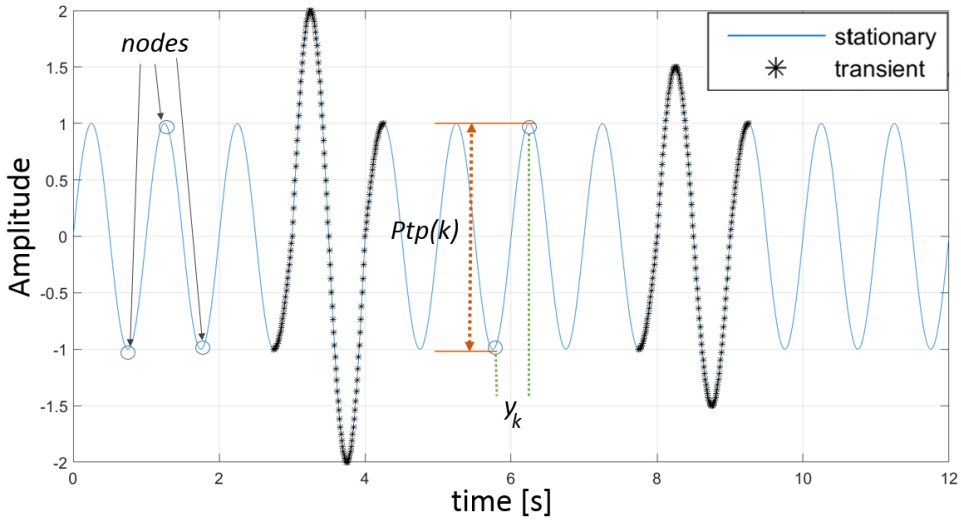


(a)

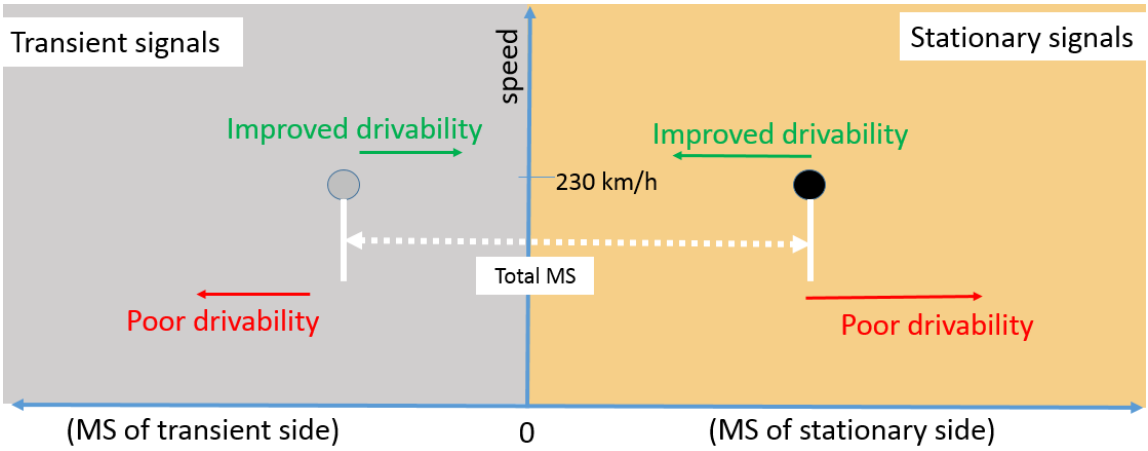


(b)

**Figure 2.3:** *Differentiation of Stationary-Transient Signal [29]: (**a**) A signal divided into segments, where Peak-to-Peak distance is marked and the dotted line segments are sorted as transient. (**b**) Simple representation of how to read the ride diagrams. Left side represents Mean Squared Value (MS) of transient part and right side represents Mean Squared Value (MS) of stationary part.*

### 2.2.3 Logistic regression

Logistic regression is used here as a binomial classification technique, [31, 32]. It is used to predict the driver's subjective response from the governing measured vehicle and driver reactions. Consider the number of observations as $n$. $R_i$ is the response, $x_i$ are the independent variables called predictors and $k$ is the number of predictors. In this case, $R_i$ consists of binary

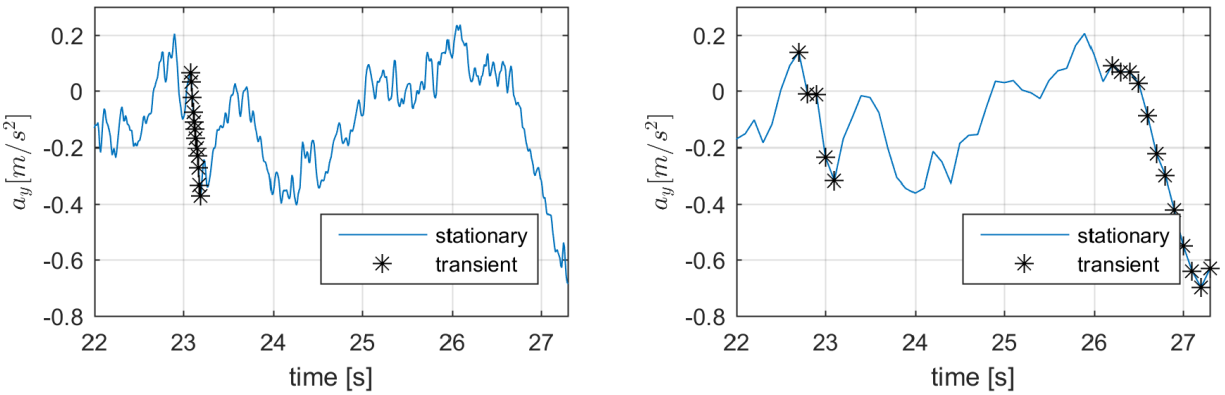


**Figure 2.4:** *Comparison of the ability to separate transient segments in different sample rates:* ***(a)*** *Lateral acceleration $a_y$ vs time with a sample rate of* 100 *Hz.* ***(b)*** *Lateral acceleration $a_y$ vs time after downsampling to* 10 *Hz.*

responses from the drivers (0 or 1). The objective of this approach is to create a response model that can predict the likelihood of each response $R_i$ for given predictors on each observation.

Logistic regression is used to obtain the model coefficients needed to estimate the log-odds $z$ of the driver response being 1, in the linear function:

$$z = \beta_0 + \beta_1 x_1 + \beta_2 x_2 + .... + \beta_k x_k \tag{2.14}$$

where, $\beta_0$ is y-intercept and $\beta_{i=1,2,3..}$ are model coefficients of respective independent variables (predictors) $x_{i=1,2,3..}$

A desired predictive model is established in the form of a logistic regression function $p(z) = 1/(1+\exp(-z))$. $p(z)$ is a sigmoid function and the value is the predicted probability of the response being 1 for a given observation. The logit model, $p(z)$, is a non-linear function resulting in local minima. Finding the global minima using the cost function further tunes the regression. This helps in selecting the best suited predictors. Here, the maximum likelihood estimate, $MLE = \sum_i (R_i \log(p(x_i)) + (1 - R_i)\log(1 - p(x_i)))$, is used. The resulting prediction accuracy can be classified as:

- Generic accuracy: The number of correct predictions over the total number of observations.
- True positive accuracy: The number of correctly predicted ones over the total number of observed ones.
- True negative accuracy: The number of correctly predicted zeros over the total number of observed zeros.

## 2.3 Subjective perception

Difficulty or inability in keeping the vehicle in lane due to frequent steering corrections or presence of undesired vehicle oscillations due to unsteady aerodynamics results in an

unacceptable vehicle dynamics behaviour. When it comes to subjective evaluation of vehicle performance, drivers' reaction to such vehicle dynamic behaviour is important [23, 25]. The importance of driver-vehicle system interdependence on the subjective evaluation of vehicle drivability is significant.

Wagner et al. [25] found difference in drivers' reactions and judgements on the vehicle behaviors depending on the crosswind conditions. At frequency range 0.5 - 1.5 H$z$ the driver's steering intensity was quite high. This resulted in intensified vehicle responses. At crosswind conditions less than 0.5 H$z$ the drivers were capable in correcting the vehicle behaviour, however, above 2 H$z$ the changes were too fast for the drivers to respond. For cross wind conditions, it is seen that yaw velocity and lateral acceleration have a strong correlation with subjective perception on stability [3]. Study by Huemer et al. [24] showed that the influence of crosswind on yaw motion was the most sensitive. In the investigation by Nguyen et al. [26], the drivers were found to have a difference in subjective impression with varying phase delays and amplitude ratio between roll and yaw moments.

Presence of jerk in the induced disturbance was found to get more attention of the driver than periodic disturbances [33, 34]. The use of ride diagrams for analysis of ride comfort came from such an observation. These studies were the motivation for implementing a similar approach to lateral behaviour in paper A.

Both the tests in this study investigates a high-speed straight-line driving condition, during which the impact of driver fatigue is crucial for subjective response and limits the duration of each test session. Driver fatigue can be a state of deterioration of mental alertness, or the transient state between sleep and awake, or psychological and physiological behaviour which when left undisturbed results in poor driver response to a given task [35–37]. Awareness decreases and sleepiness increases with prolonged monotonous driving [38, 39]. In this study, the psychological and physiological impacts on the drivers' subjective perception, such as the time of the test and frame of mind at the time of the test, could not be completely eliminated. Furthermore, the preceding signal stimuli could also influence how the driver responds to a given stimulus.

# 3

# On-road study

This chapter covers the experimental setup and outcomes of the first study resulting in paper A. An on-road study was conducted to investigate the relationship between the subjective judgement of the drivability of a vehicle and measurable variables.

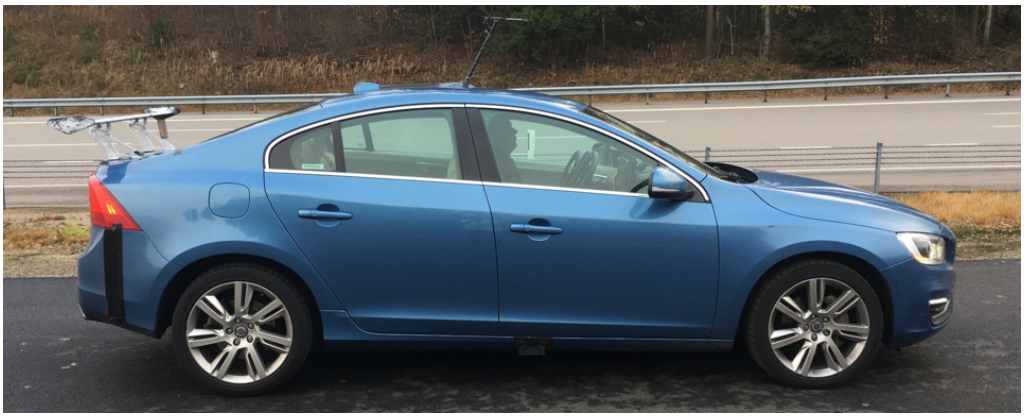

**Figure 3.1:** *Test vehicle*

## 3.1 Experimental set-up

The test object used in this study was a mid-size, front wheel drive sedan, Figure 3.1. The front wheel driven version has a more forward load distribution, compared to a four wheel driven version, hence enhancing the sensitivity in the rear due to lower traction on the rear tires.

### 3.1.1 Instrumentation

Different variables were recorded through sensors to capture the vehicle behaviour. The added sensors are shown in Figure 3.2 and listed below:

- Steering wheel clip-on sensor [SW]: This sensor measured the steering angle, steering rate and steering torque. It was placed on the steering wheel. The sensor has an uncertainty of ±0.01 deg. Details are shown in [40].
- Aeroprobe and pressure sensors [AP]: Measured headwind conditions such as yaw angle, roll angle, and angle of attack with a range of ±70 deg and an accuracy of ±1 deg. It was positioned 360 mm vertically above the center of the vehicle roof, in line with Reference

[41].

- Lazer sensors measuring ride height [RH1, RH2, RH3, RH4]: Measured ride heights of the test vehicle. RH1 and RH2 were placed on the underside of the front and rear bumpers flush with the exterior surface. The remaining two sensors were placed to the sides at the middle of the wheelbase. The measurement of uncertainty for the sensor was ±0.6 mm.
- Inertia Measurement Unit [IMU]: It was placed in the center of gravity of the vehicle except vertically (due to structural hindrances). However, the IMU can translate the readings of any reference point on the input, irrespective of the position of IMU itself. GPS was integrated into this system with the positioning of antennas, as recommended by DEWESoft [42].
- Draw-wire displacement sensors [FL, FR, RL, RR]: Four sensors were co-aligned with the spring of each wheel measuring the displacement of the suspensions with an uncertainty below ±0.3 mm.
- CAN signal: Signals from the vehicle's built-in sensors were also recorded. The absolute steering wheel angle data considered in this research during post-processing and plots were recorded from the CAN bus. The accuracy of these sensors was ±0.1 deg.
- Dewesoft Module: All sensors were connected to a Sirius Dewesoft data acquisition system. The Dewesoft X software was used for data acquisition and some post-processing.

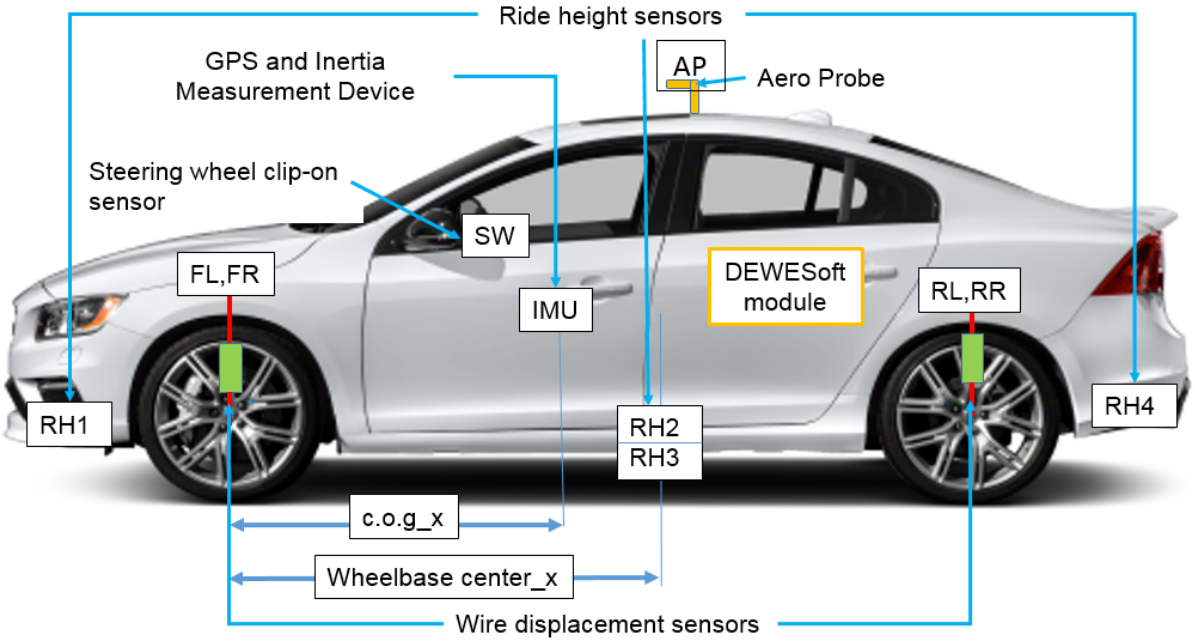


**Figure 3.2:** *Test vehicle instrument setup.*

### 3.1.2 Aerodynamic configurations

As mentioned in Section 2.1.1, the test was designed to create substandard drivability using sets of add-ons to the test vehicle. The test driver was asked to respond if he sensed any stimuli induced through different aerodynamic devices and their combinations. Three paired configurations were selected for this study. The add-ons, which can be seen in Figure 3.3, are

the following

- Anti-diffuser [a]: Designed with the intention to guide the flow downwards and partially restrict the flow along the diffuser region. The device was supposed to promote a wake downwash, resulting in a rear lift.
- Inverted wing [w]: A rear wing attached to act like aircraft wings, set to increase rear lift.
- Inverted wing with fin [w-f]: A fin placed 90° to the flow upstream as an addition on the left side of the inverted wing to generate asymmetric forces and moments.
- Side-kicks [s]: Additional aerodynamic devices shaped as slightly spiked separation edges on both sides of the rear bumper, creating an outwash while separating the flow at defined locations. This add-on was used as a pairing device for the three previous add-ons, i.e., wing [w], wing with fin [w-f], and anti-diffuser [a].

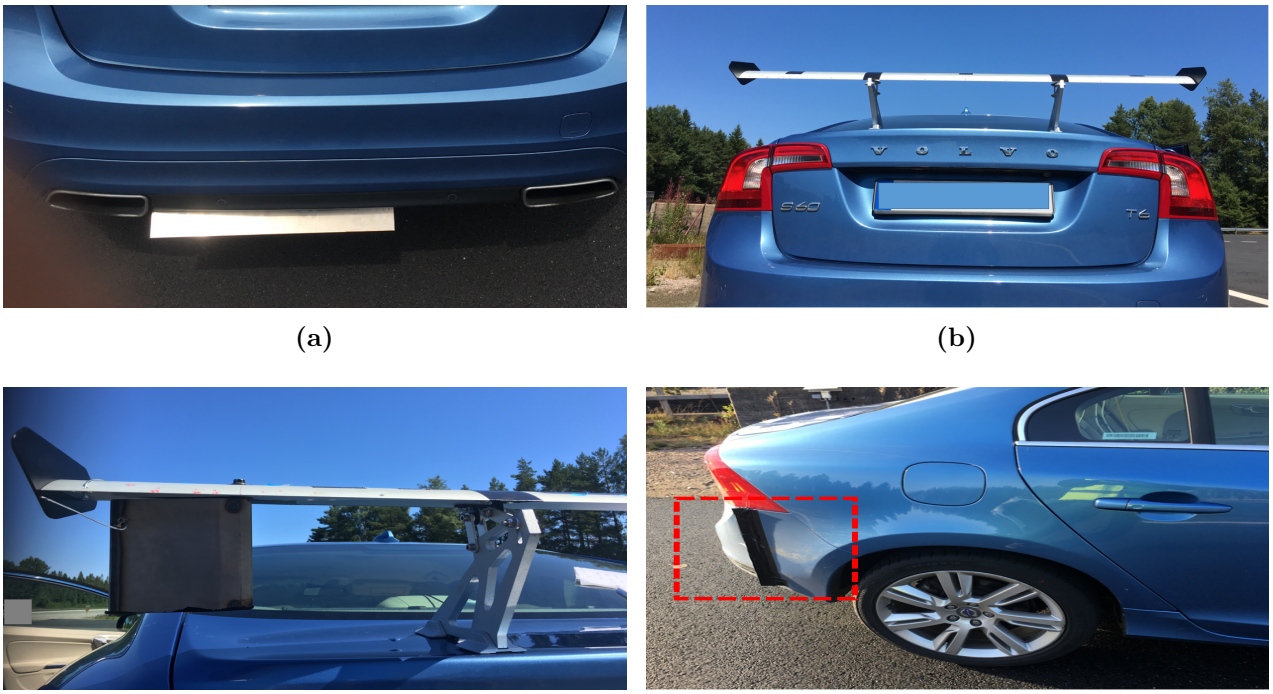


**(a)** **(b)**

**(c)** **(d)**

**Figure 3.3:** *Aerodynamic devices: (**a**) Anti- diffuser [a]. (**b**) Inverted wing [w]. (**c**) Inverted wing with fin [w-f]. (**d**) Side-kicks [s].*

Despite extreme modifications on the test vehicle, no alarming instabilities were sensed by the test drivers, which was the prior intention. Wind tunnel tests were later conducted to obtain the aerodynamic coefficients of each configuration and combination of configurations. The aerodynamic coefficients of front and rear lifts are shown in Table 3.1. The addition of a side kick did not make a significant difference to the front or rear lift coefficients in any of the cases with respect to the uncertainty of the wind tunnel measurements.

**Table 3.1:** *The change in mean aerodynamic lift coefficients of each configuration compared to the base car.*

| Configuration | ($\Delta$ = Configuration - base car value) front lift coefficient $\Delta C_{lf}$ | rear lift coefficient $\Delta C_{lr}$ |
|---|---|---|
| Anti-diffuser [a] | −0.001 | 0.005 |
| Anti-diffuser [a] + Side-kicks [s] | 0.000 | 0.004 |
| Inverted wing [w] | −0.016 | 0.096 |
| Inverted wing [w] + Side-kicks [s] | −0.016 | 0.093 |
| Inverted wing with fin [w-f] | −0.012 | 0.072 |
| Inverted wing with fin [w-f] + Side-kicks [s] | −0.012 | 0.070 |

### 3.1.3 Test track and test procedure

The test track was Volvo Cars Hällered Proving Ground. It is an oval track with two straight lines of 1.1 km, as sketched in Figure 3.4. In this study, the data analysis only considered measurements along the two straight lines.

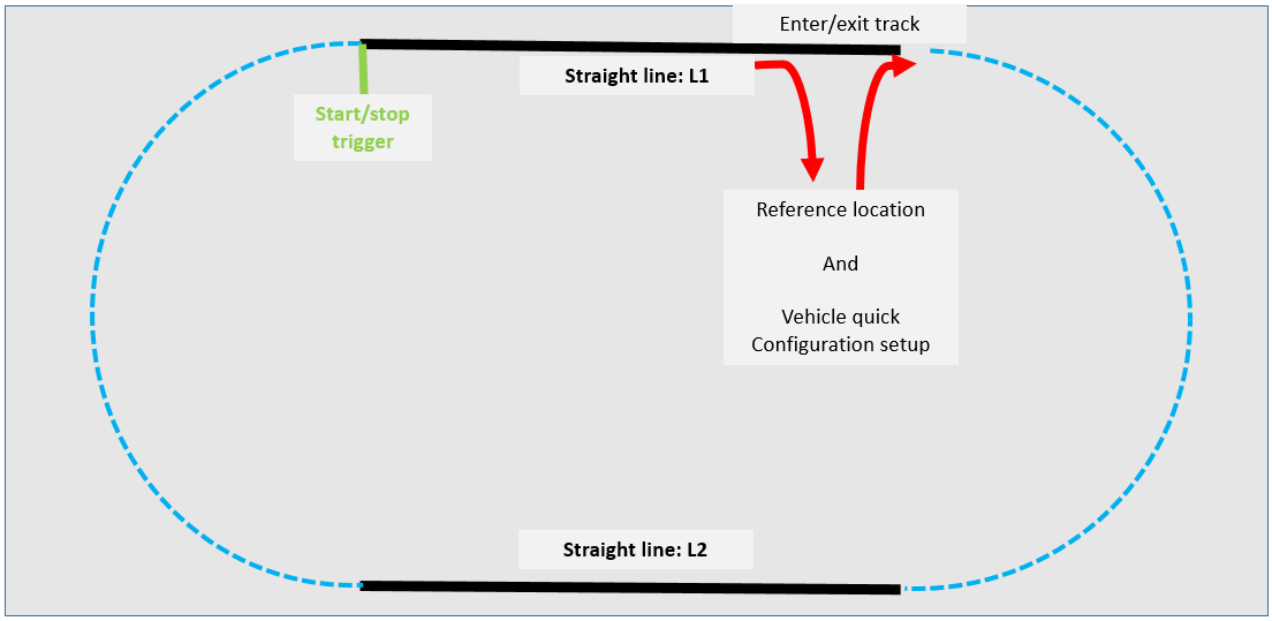


**Figure 3.4:** *Test track at Volvo Cars Hällered Proving Ground.*

During the trial runs, the subjective judgement of all three selected configuration pairs was taken from three test drivers. The analysis presented in this paper is from the recorded data of one driver. The reference location on the track, shown in Figure 3.4, was used to tare all sensors for each test with the desired configuration. It was also the starting and stopping point of these tests. The driver was asked to drive around the track following a selected fast lane. Once the desired conditions such as required speed and minimal wind speeds were achieved, the Dewesoft Module data acquisition starts as it crosses the beginning of the first straight line L1.

The trigger to record data was set at the start of L1 and stopped automatically after three full laps. Once the recording was complete, the vehicle was driven to the reference location where the next configuration was fixed and the sensors were tared. This procedure was repeated throughout all the planned configurations. The tire pressure was periodically monitored for consistency and safety. The test driver was unaware of the configurations and their impact on the test object. Such a blind test is important for an unbiased judgement.

For the analysis, out of the few tested cruising speeds, only speeds of 230 and 250 km/h were used due to their noticeable difference in vehicle behaviour. With three full laps consisting of two straight lines (L1 & L2) and two cruising speeds, a total of 12 readings were considered. Variables considered in this study to relate the subjective feel of the test driver to measurable quantities are lateral acceleration $a_y$, yaw velocity $\omega_z$, steering angle $\delta_{sw}$ and steering torque $\tau_{sw}$. The influence of heave and roll rates in this driving condition were negligible, hence, they are not further discussed. The data received from the test sensors were filtered with a low-pass filter with a 20 Hz cutoff frequency and down-sampled to 10 Hz before analysis.

## 3.2 Discussion and results

The subjective rating of the tests on three selected configurations paired as with and without side-kicks is shown in chart Figure 3.5.

| Notations | Configuration | Drivability good | Drivability poor |
|---|---|---|---|
| a | Anti- diffuser | | x |
| a-s | Anti- diffuser + side-kicks | o | |
| w | Wing | | x |
| w-s | Wing + side-kicks | o | |
| w-f | Wing + fin | | x |
| w-f-s | Wing+ fin + side-kicks | o | |

**Figure 3.5:** *Subjective judgement between paired configurations, where 'good' or 'poor' drivability is relative to the other configuration in each pair*

### 3.2.1 Analysis

The vehicle behaviours felt by drivers with the attachment of the three configurations:

- The anti-diffuser showed a more high frequency yaw behavior compared to the other configurations.
- The inverted wing gave low frequency sway behaviour with the impression that the source of excitation was from the rear end of the test object.

- The inverted wing with fin resulted in a similar behaviour similar to that with just the inverted wing, but in addition, there was a slight leftward yaw.

The use of side-kicks improved the drive quality and notably dampened the above-mentioned behaviours of the respective configurations.

Pairwise comparisons of all configurations were conducted using the available post-processed data.

### Wire sensors measurement

The RMS of the change in lift forces on each wheel for each configuration compared to the reference test object is shown in Figure 3.6. In all configurations, an asymmetric suspension expansion between the rear left and right was also notable in this bar graph. This could be due to a difference in unsprung weight. The configurations with wing (w and w-s) provided the highest lift in the rear, followed by wing with fin (w-f and w-f-s). As a result, the load was being transferred more to the front of the test object, causing compression on the front suspension. The influence of anti-diffuser (a and a-s) on rear lift was less compared to the reference, creating a positive pitch.

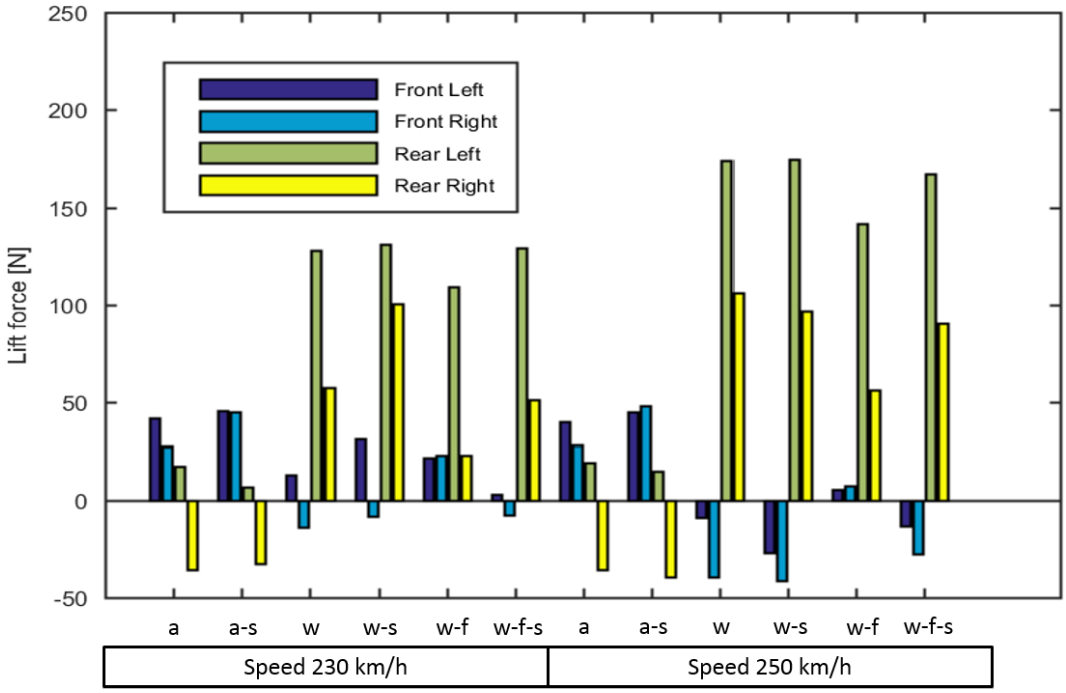


**Figure 3.6:** *RMS of relative suspension displacement for different configurations and speeds of each of the four wheels.*

### Mean and standard deviation vector plots

The vector lines represented in Figure 3.7 show each configuration pair, connecting from the configuration without to with side-kicks. The method is described in detail in Section 2.2.1.

Since the study scenario was a straight-line drive, the mean values of lateral acceleration $a_y$

and yaw velocity $\omega_z$ will be negligible. In the case of $\delta_{sw}$ and $\tau_{sw}$, the mean value depicted the excess averaged steering input required by the driver in response to exterior disturbances while keeping the test object following the straight line. Lower need for $\delta_{sw}$ and $\tau_{sw}$ response shows characteristics of good drivability which is presented in Figure 3.7a. This implies that the vector plots point towards the origin. These vector plots fall in line with the subjective judgement of all configurations with and without side-kicks except for the anti-diffuser. However, the standard deviation vector line patterns of $\delta_{sw}$ vs $\tau_{sw}$ coincides with subjective judgement for all configurations with and without side-kicks, as shown in Figure 3.7b. A similar pattern is also found for lateral acceleration $a_y$ and yaw velocity $\omega_z$. This suggests that side-kicks dampen the unsteady vehicle behaviour, resulting in better driving in a straight line.

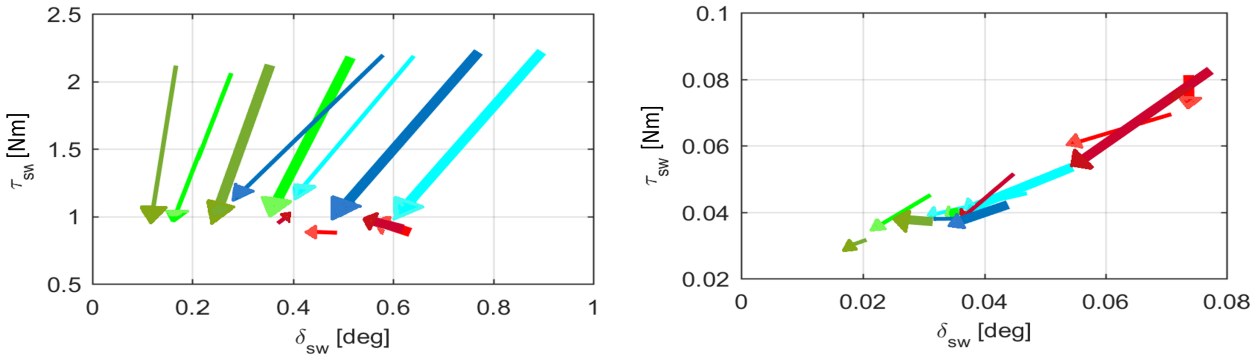


**(a)** *mean values* **(b)** *Standard deviations*

| Configurations [Without to with side-kicks(s)] | Straight line | Speed [Km/h] |
|---|---|---|
| a to a-s | L1 | 230 |
| w to w-s | L1 | 230 |
| w-f to w-f-s | L1 | 230 |
| a to a-s | L1 | 250 |
| w to w-s | L1 | 250 |
| w-f to w-f-s | L1 | 250 |
| a to a-s | L2 | 230 |
| w to w-s | L2 | 230 |
| w-f to w-f-s | L2 | 230 |
| a to a-s | L2 | 250 |
| w to w-s | L2 | 250 |
| w-f to w-f-s | L2 | 250 |

**Figure 3.7:** *Vector plots of mean values and standard deviations of steering torque $\tau_{sw}$ vs steering angle $\delta_{sw}$ of each straight line L1 and L2 for the different configurations and speeds.*

### Ride diagram method

The plots in Figure 3.8 show the mean squared values (MS) values of the transient part of the signals to the left and the MS values of the remaining stationary part of signals to the right, explained in detail in Section 2.2.2. Unfilled markers represent respective configurations without side-kicks and filled markers represent configurations with side-kicks. The sum of MS values of transient and stationary gives the total MS value of the signal. The further the MS

value is from the origin on the x axis, the lower the standard of drivability. The ride diagrams interpreted this way agree with subjective judgement of all configurations, Figure 3.8.

On the transient side in Figure 3.8a, the transient nature of the signal is larger in the configuration with anti-diffuser compared to other configurations at 250 km/h. At 230 km/h the transient side of the configuration pair with anti-diffuser is not predominant and the trend is opposite to the subjective judgment by a small margin. However, on the stationary side, the configuration with anti-diffuser, a, is mainly showing a worse trend than the configuration with anti-diffuser and side-kick, a-s. The steering characteristics such as $\tau_{sw}$, Figure 3.8b, show a larger contribution on the stationary side for wing and wing with fin configurations. The transient contribution in all configurations is negligible in comparison. This shows the inability to respond to unknown transient behaviours.

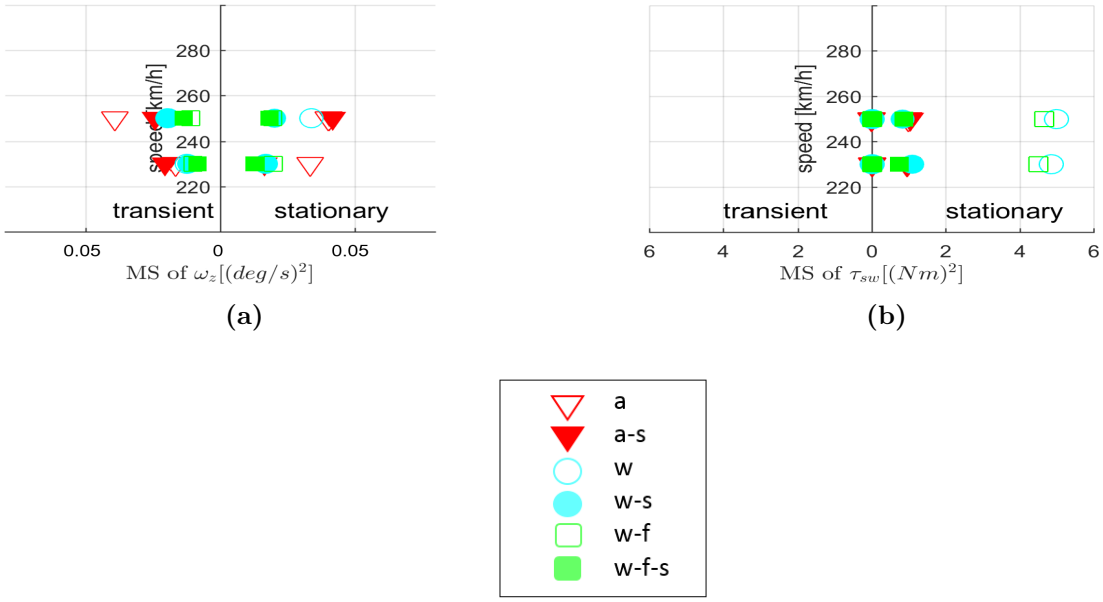


**Figure 3.8:** *Ride diagram of all configurations and selected speeds: (**a**) Yaw velocity $\omega_z$. (**b**) Steering torque $\tau_{sw}$.*

### 3.2.2 Statistical analysis

The use of mean and variance vector plots and ride diagram matches the driver's subjective judgment on drive quality. However, the measurements fall in the error region of for accelerometers and gyroscope. This brings the certainity of observations from the above plots to a grey area especially for lateral acceleration $a_y$ and yaw velocity $\omega_z$.

The statistical test is a quantitative analysis. Due to the consistent vector patterns, usually pointing towards the origin, a statistical analysis can support the qualitative evaluation. Cumulative Binomial distribution is used to assess the probability of random creation of such

a pattern. The probability that the outcome $X$ of at least $x$ successes in $n$ trials is:

$$p(x \geqslant X) = 1 - \sum_{i=0}^{x} \binom{n}{i} P^i (1-P)^{n-i} \tag{3.1}$$

In this case, the null hypothesis is that there is no difference between the configurations, depending on if they have side-kicks or not and that gives the assumption $P = 0.5$. The number of trials $n$ is twelve. With these values taken into account, the binomial distributions of the success of each of the four variables at $n$ trials are calculated as shown in Table 3.2. This shows that the probability for the random vector plots to show similar pattern as that of the results is quite low. In comparison with the variables considered the probability of such a case in $\omega_z$ is the highest with $p_x = 12\%$ which is low but still notable. The null hypothesis can be rejected for $\delta_{sw}$ and $\tau_{sw}$.

**Table 3.2:** *Cumulative Binomial distribution of random success of all variables.*

| **Variable** | $x$ | **Probability of Atleast $x$ Success for n Trials** |
|---|---|---|
| $a_y$ | 9 | 0.054 |
| $\omega_z$ | 8 | 0.12 |
| $\delta_{sw}$ | 11 | 0.003 |
| $\tau_{sw}$ | 11 | 0.003 |

# 4

# Driving simulator study

This chapter covers the experimental setup and outcomes of the paper B. The objective was to investigate drivers' ability to recognize induced external disturbances and build a regression model to predict their judgment based on measured quantitative variables.

## 4.1 Experimental set-up

This section explains the set-up and test plan for the driving simulator tests conducted at the Volvo Cars Driving Simulator and at the Swedish National Road and Transport Research Institute (VTI).

### 4.1.1 Driving simulator and vehicle model

In this study, multiple drivers drove at high speed in a straight line while experiencing realistic vertical noise simulating road unevenness. The simulated vehicle was then exposed to induced disturbances. The objective was to find at what levels and frequency ranges drivers could either detect or experience disturbances as dangerous. Logistic regression is used with the observations to create a model that can predict the likelyhood of drivers detecting given disturbance. The experiment was planned as a two step process:

**Phase I**

Conducted with three average skilled drivers (common drivers) at Volvo Cars Driving Simulator, shown in Figure 4.1a.

*System:* The simulator is a VI-Grade 075 and works with CarRealtime for vehicle dynamics modeling and simulation [43]. The vehicle dynamics model used was built to match the test vehicle.

*Test:* The drivers were asked to drive in a straight line simulating a 200 km/h long cruise driving condition on a 3-lane straight road. Before the test, they were informed about the existence of background road noise. The drivers responded 'felt' or 'felt dangerous' when they experienced a disturbance and when they didn't respond, it was categorized as 'didn't feel'. In this phase, the disturbance inputs were either yaw moments or side forces at the center of gravity of the vehicle. Depending on the drivers' response to a disturbance input, the test leader modulated the frequencies and amplitudes of the disturbance input and fed it to the

simulator. The results gave a rough estimation of the desired region of interest in terms of amplitudes and frequencies to be used in the phase II test.


**Figure 4.1:** *(a) Phase I test using Volvo Cars Driving Simulator [44] (b) Phase II test using VTI SimIV (Photo: Hejdlösa Bilder AB) [19].*

### Phase II

The clinical test was performed at VTI's (Swedish National Road and Transport Research Institute) driving simulator, which can be seen in Figure 4.1b [19]. It has a longer platform envelop for the area of interest stretching to frequencies as low as 0.25 Hz.

*System:* The simulator cabin is mounted on a hexapod, which itself rests on a movable platform through which the system provides the driver with motion feedback. Details of this simulator are described by Jansson et al. [45] and in Section 2.1.2. Details of the vehicle dynamics model can be found in [46, 47]. To have a similar vehicle dynamics behaviour to that of phase I, a few selected vehicle maneuvers were simulated using CarRealtime at the Volvo Cars Driving Simulator. The vehicle responses from those simulations were used to tune the vehicle dynamics model at VTI. The input disturbances were roll and yaw moments.

*Test:* During the test, the drivers were instructed to loosely follow a straight line, simulating a 200 km/h long cruise driving condition on a straight flat road. The drivers were given awareness of the existence of road noise applied to the vehicle. After each disturbance, the drivers were asked to provide their impressions by pressing either of the three buttons on the steering wheel as shown in Figure 4.2. Each of which represents feedback as below:

- 0 - I felt nothing
- 1 - I felt the disturbance
- 2 - I felt the disturbance and I can see it's potential of causing straight line instability

Coefficients for aerodynamic forces and moments were taken from wind tunnel tests performed earlier and translated to the centre of gravity of the vehicle. Noise was added to the experience to create a feeling of road inundations and was derived from the Inertia Measurement Unit (IMU) readings of the on-road test in the first paper. White noise was filtered to get the desired frequency spectra that matched the accelerations from the on-road data. For simplicity, only the vertical and pitch accelerations were used in this test. Feeding the disturbances on each wheel independently is more realistic. However, the available setup and time constraints resulted alternately to feed them at the center of gravity of the vehicle.


**Figure 4.2:** *Drivers were provided with step-by-step instructions on the screen, visible from cockpit, to ease adaptability.*

Due to motion cueing, the actual motion characteristics felt in the cockpit vary from the simulated vehicle dynamics response output. It is important to record the actual motion signals such as the linear and rotational accelerations and velocities in the cockpit for relating to drivers' subjective perception. In order to record these signals, the IMU was mounted on the platform of the cockpit along with the DEWEsoft Module, [42]. The drivers' impressions and steering responses were the other inputs recorded by the simulator.

Before analysis, the signals were first low pass filtered with an upper cutoff of 10 Hz and down-sampled to 100 Hz before analysis. During analysis of each disturbance, the outputs examined were split into two categories: outputs received 8 seconds to the start of the disturbance signal is considered as 'before the disturbance' and 8 seconds from the start of the disturbance signal are considered as 'during the disturbance'.

### 4.1.2 Disturbances of interest and signals sequencing

One of the profiles studied by Brandt et al. [48] is used to create a base disturbance profile of interest. This signal profile has shown a potential to have substantial instability behaviour.

The developed base disturbance was an impulse signal that ramps up from zero and instantly switches to the opposite sign and ramps back to zero, as shown in Figure 4.3. The mathematical representation of the base disturbance is:

$$y(t) = \text{sgn}\left(\frac{T}{2} - t\right) \cdot \left(1 - \cos\left(\frac{2\pi}{T} \cdot t\right)\right) \text{ for } t \in [0, 10] \tag{4.1}$$

where, $y$ is the amplitude at a given time $t$ and $T = 10$ is total signal time.

The disturbances of interest were obtained through the following steps:

1. The base disturbance was passed through an $8^{th}$ order Butterworth bandpass filter for achieving disturbances consisting of frequency ranges 0.25 - 0.5 Hz (F1), 0.5 - 1.0 Hz (F2), 1.0 - 2.0 Hz (F3), and 2.0 - 4.0 Hz (F4).

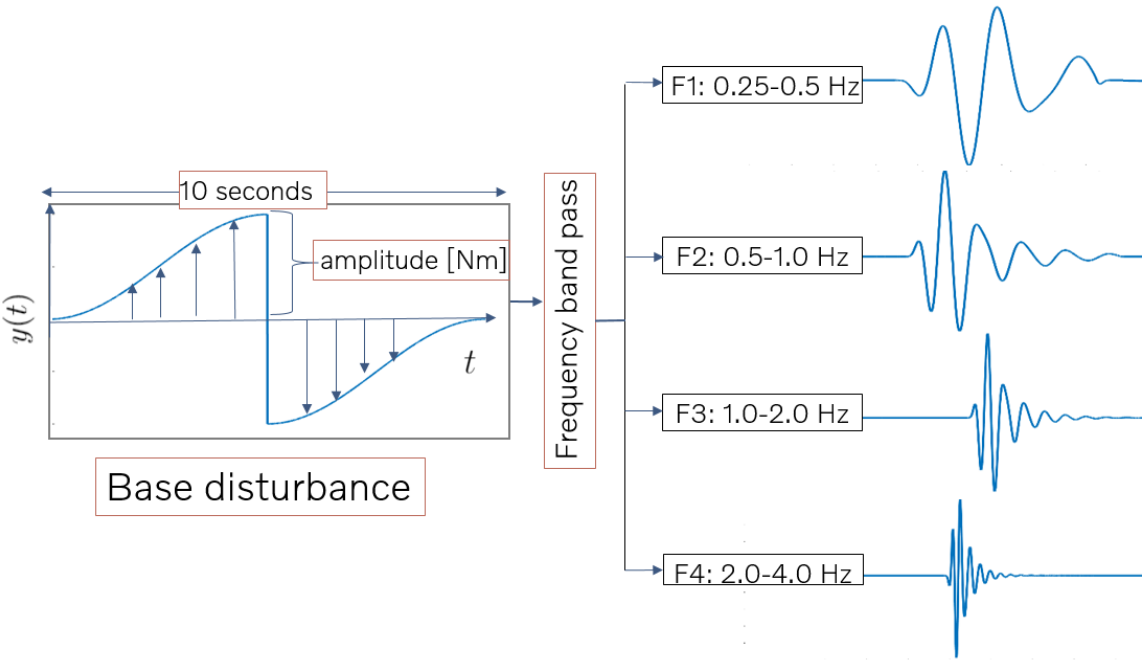


**Figure 4.3:** *The preparation of desired aerodynamic excitation signals of interest from the base disturbance using $8^{th}$ order Butterworth bandpass filters.*

2. They were amplified to the four selected amplitudes in terms of moments: 150 Nm (A1), 175 Nm (A2), 225 Nm (A3), and 325 Nm (A4).
3. This resulted in 16 distinct signals: 4 frequency range × 4 amplitudes. They were fed as yaw or roll disturbance inputs.
4. These signals were randomly sequenced uniquely for each driver.
5. In addition, the initial signal was repeated once, and two other selected signals were repeated for all the drivers to investigate repeatability.

This base disturbance being symmetric will help in minimizing the wash-out filter usage by the simulator, especially since the disturbances of interest were of low frequencies.

### 4.1.3 Clinical driving test

The clinical driving test consisted of 23 drivers in total: 13 common drivers and 10 experienced test drivers. While planning the driving span for each driver, it was important to consider driver fatigue as discussed in Section 2.3. From the summary of the studies stated above, a driving duration of 15 minutes per driver was chosen as an acceptable duration for an effective subjective judgement from the drivers. Even though the number of drivers is too small to obtain an accurate and statistically representative distribution of responses for each disturbance, other conclusions can be drawn with high statistical significance from the collected data.

Using two repeated disturbances for all drivers, a $\chi^2$ test is used to test the independence of responses from the same driver [49]. The null hypothesis is that the first and second responses

to the same disturbance from the same driver is independent. The p-value, 0.59, is higher than 0.05. As a result, one cannot reject the null hypothesis, which indicates that the responses are not strongly dependent.

## 4.2 Predictive model

Logistic regression is used to create a model for predicting the probability of driver responses to induced disturbances, as discussed in Section 2.2.3. The resulting logistic regression function equation is shown in Equation 4.2. For the model development, the values of objective variables measured in the cockpit are used. Steering angle $\delta_{sw}$, yaw velocity $\omega_z$ and roll velocity $\omega_x$ along with the respective driver's response were chosen from the available variables as they provided the most accurate predictions. Standard deviations calculated from the time period from the beginning of each disturbance and 8 seconds onwards of each of these variables are used in Equation 4.2.

Through a logistic regression model, a relation is built between dependent and independent variables [31, 32]. The independent variables (predictors) are all the above-mentioned objective variables together with the category of the drivers, named $c_{DT}$. The dependent variable is the driver's response in binary format, i.e., 0 for 'did not feel' (driver responded by pressing 0) and 1 for 'at least felt' (driver responded by pressing 1 or 2). The resulting logit function represents a linear relationship between the independent variables and the log-odds. A maximum likelihood estimate is used to estimate weights so that the prediction is as close to the actual response as possible. The model is optimized by removing independent variables that obtain high p-values (above 0.01).

$$\begin{aligned} p(x) &= \frac{1}{1+\exp(-z(\vec{x}))} \\ z(\vec{x}) &= \beta_0 + \beta_1 x_1 + \beta_2 x_2 + \beta_3 x_3 + \beta_4 x_4 \\ \vec{x} &= \begin{bmatrix} x_1 & x_2 & x_3 & x_4 \end{bmatrix} \\ &= \begin{bmatrix} \omega_{x,std} & \omega_{z,std} & \delta_{sw,std} & c_{DT} \end{bmatrix} \end{aligned} \tag{4.2}$$

where

$p(x)$ is the logistic model that predicts the probability, $p$, of achieving an output equal to 1 for a given set of independent variables $x_{i=1,2,3..}$.
$\beta_0$ is $y$-intercept,
$\beta_{i=1,2,3..}$ are model parameters for respective independent variables (predictors) $x_{i=1,2,3..}$

## 4.3 Discussion and results

The results and discussion of the two test phases are presented here, followed by the drivers' experience and predictive model. In the following sections, peak-to-peak values of variables are considered. Peak-to-peak is defined as the difference between the maximum and minimum value of the variable within the chosen time segment.

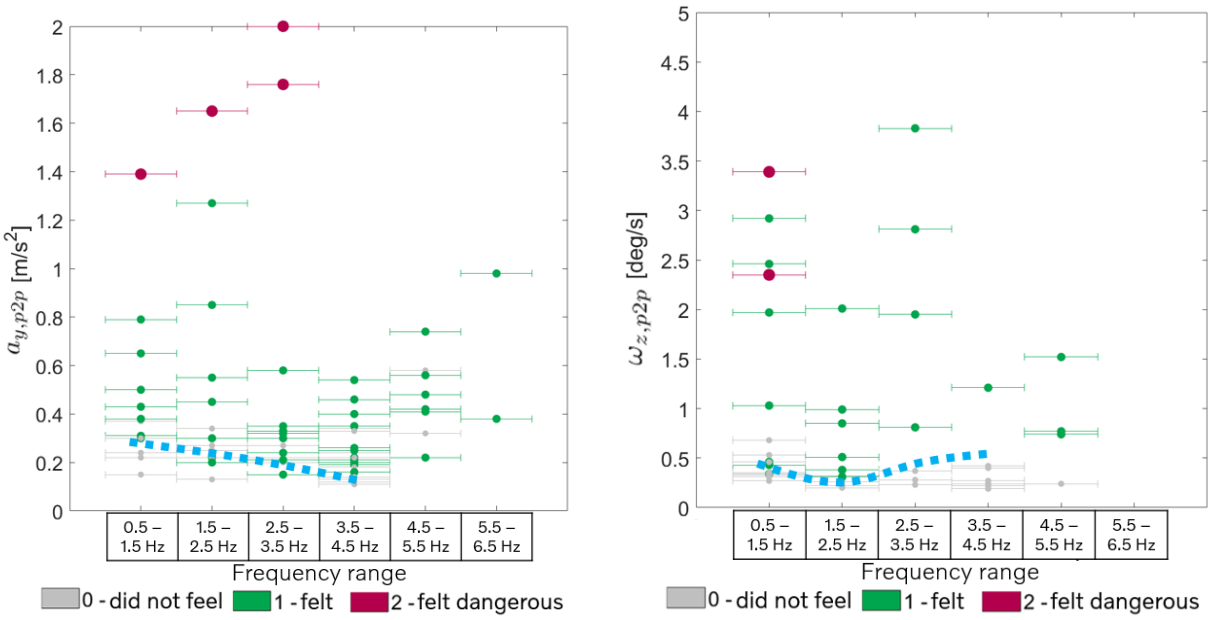


**(a)** *Lateral acceleration (peak-to-peak), $a_{y,p2p}$, over frequency range.*

**(b)** *Yaw velocity (peak-to-peak), $\omega_{z,p2p}$, over frequency range.*

**Figure 4.4:** *Drawn rough blue line indicating amplitudes where the drivers start to feel from some phase I tests analysis at the Volvo Cars Driving Simulator.*

### 4.3.1 Phase I analysis

From the phase I tests data, the resulting peak-to-peak lateral acceleration, $a_{y,p2p}$ and yaw velocity $\omega_{z,p2p}$, felt in the cockpit for all trials of yaw and side disturbances of varying frequency range and amplitudes were plotted. Two of them, Figures 4.4a and 4.4b, are shown here. From these figures, blue dashed lines representing the rough transition line between 'felt' and 'did not feel' can be observed over each frequency range. The sample sizes are relatively small in certain frequency ranges. This is because the drivers provided consistent responses of either 'felt' or 'did not feel' to an induced disturbance for the given amplitudes within the first few trials. For lateral acceleration, Figure 4.4a, the blue dashed line passes through 0.3 m/s$^2$ at 0.5 - 1.5 Hz and decreases as the frequency range increases. For yaw velocity $\omega_z$, Figure 4.4b, the line starts from 0.5 deg/s at 0.5 - 1.5 Hz and after a minimum at 1.5 - 2.5 Hz, it rises as the frequency range increases.

### 4.3.2 Phase II analysis

From the phase I study, the driver sensitivity seems to decline for yaw motion with the increase in frequency. Moreover, the losses in the output from the simulator tend to increase significantly with the increase in frequency due to limitations of the system. As a result, the frequency range of interest in phase II is limited at the upper end to 4 Hz.

#### Driver response to various disturbance amplitudes and frequency ranges

The analysis in this section is strictly based on the drivers' responses to disturbance amplitudes and frequency ranges. The influence of road noise, vehicle reactions to the drivers' actions,

drivers' steering intensity and the vehicle response to disturbances affect the subjective judgements of drivers. The vehicle response to a given input disturbance and how it was felt in the cockpit is not linear over frequencies and amplitudes. As a result, depending on the vehicle models, some can be more sensitive compared to others for the same disturbance.

Drivers' responses to yaw disturbance input over selected amplitude and frequency ranges are shown in Figure 4.5a. The main observations are:

- The test drivers have a broader frequency span of ability to identify disturbances and lower tolerance towards disturbance amplitude compared to common drivers.
- Transition from 1 ('felt') to 2 ('felt the potential towards instability') is seen for test drivers between the frequency range of 0.25 and 2 Hz with an increase in amplitude.
- Transition from 0 ('did not feel') to 1 ('felt') is seen for common drivers throughout the frequency range with an increase in amplitude.
- The number of drivers that could observe the yaw disturbances at frequency range 2 to 4 Hz is considerably low for both test and common drivers.

Drivers' responses to roll disturbance input over selected amplitude and frequency ranges are shown in Figure 4.5b. The main observations are:

- Only transition from 0 ('did not feel') to 1 ('felt') is seen for both types of drivers, which increases with higher amplitude and higher frequency range.
- Fischer's exact test indicates that the test drivers are only significantly more sensitive to disturbances in the frequency range 0.25 to 0.5 Hz when compared to common drivers, with a p-value of 0.023.

The plot in Figure 4.5 does not include the repeated signals, so the number of sample points at each frequency range and amplitude is 13 for common drivers and 10 for test drivers.

**Driver response depending on measured variables**

In this section, the selected objective variables from those measured in the cockpit are peak-to-peak values of steering torque $\tau_{sw}$, steering rate $\dot{\delta}_{sw}$, yaw velocity $\omega_z$ and roll velocity $\omega_x$. Swarm plotting is used to provide a better understanding of the relationship between quantitative measurements and subjective judgement patterns of the drivers.

*Response to yaw moment input*

Figure 4.6 shows peak-to-peak yaw velocity, $\omega_{z,p2p}$, and driver responses of the vehicle over the investigated frequency ranges and amplitudes of yaw moment disturbance input. Similar to the observation from Phase I, the peak-to-peak yaw velocity, $\omega_{z,p2p}$, transition line between 'felt' and 'did not feel' is clustered around 0.5 deg/s at lower frequency range for common drivers. The $\omega_{z,p2p}$ response for the same amplitude disturbance increases with increased frequency up to $1-2$ Hz but is then damped significantly by the chassis at $2-4$ Hz.

Figure 4.6 shows that a selected disturbance with a given amplitude results in a distribution

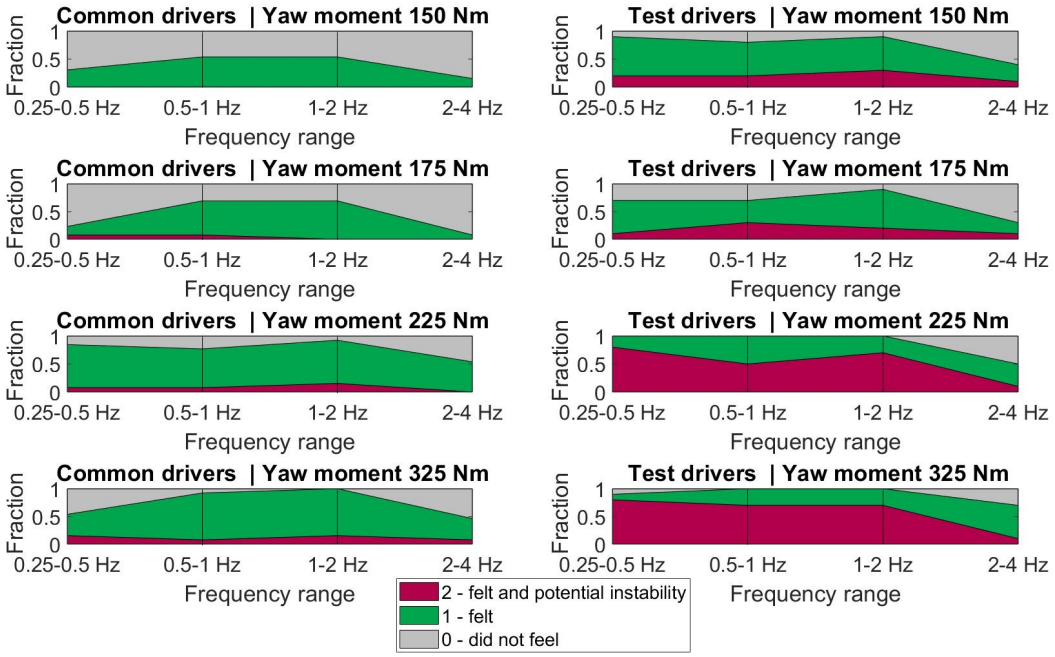


**(a)** *Yaw disturbance input.*

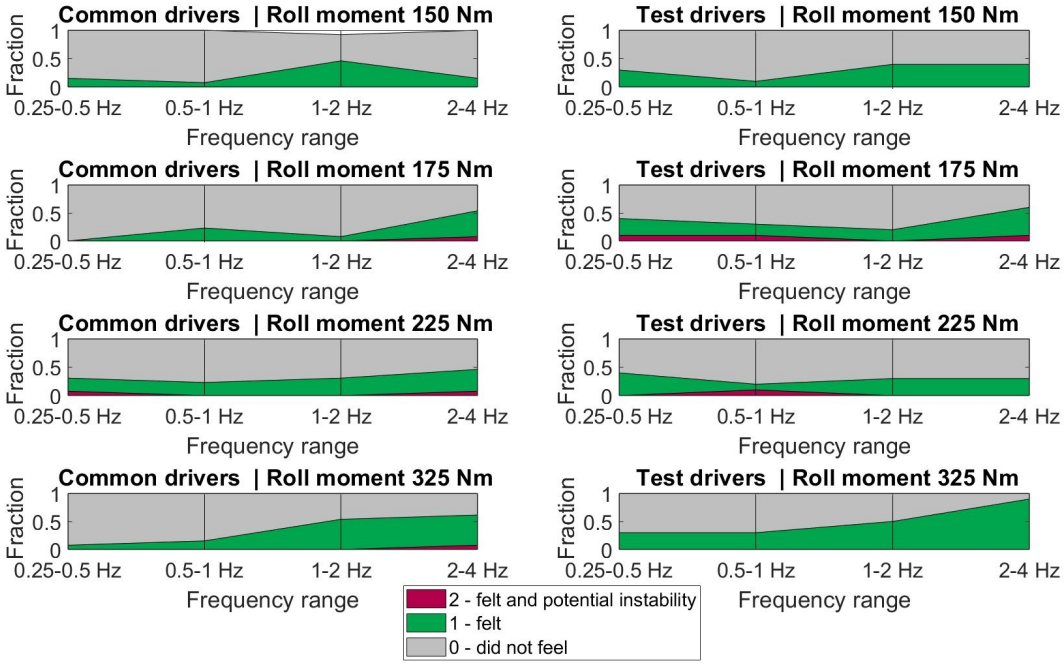


**(b)** *Roll disturbance input.*

**Figure 4.5:** *Stacked fraction of Phase II driver responses for yaw and roll moment disturbance input at different amplitudes and frequency ranges.*

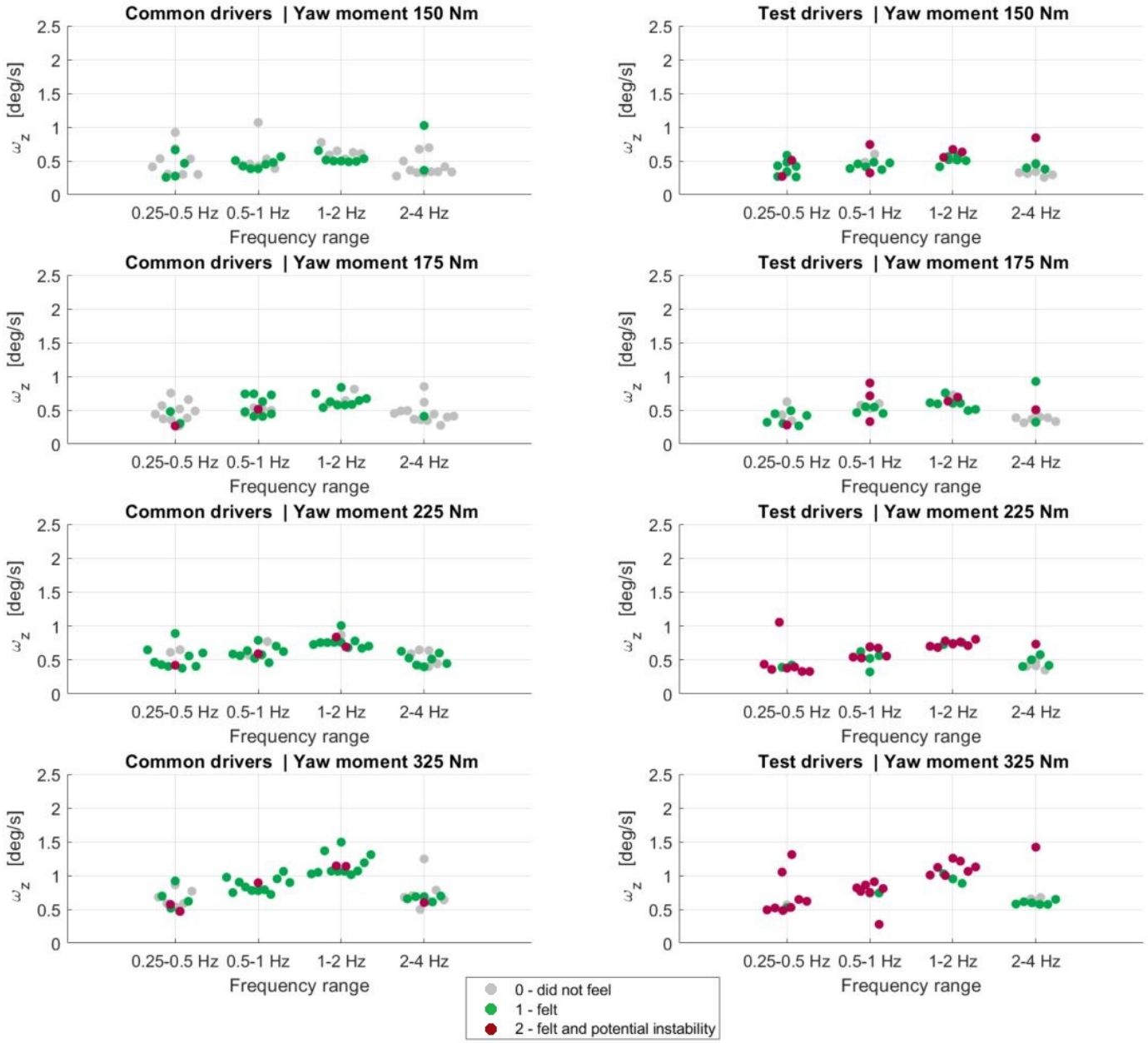


**Figure 4.6:** *Swarm plot of frequency range vs. peak-to-peak yaw velocity $\omega_{z,p2p}$ vs. driver response for different driver type and yaw moment disturbance amplitudes.*

in amplitude for $\omega_{z,p2p}$. Hence, because of road noise, driver input and vehicle dynamics, the condition under which every sample are taken is unique. There is an overlap in the measured amplitudes of yaw velocity between different amplitudes of disturbance. This can help explain why there are different responses given to the same input. No explanation relating to the difference in driver response can be deduced when considering only peak-to-peak or standard deviation of yaw velocity, $\omega_z$. Since there is a distribution of measured amplitudes from the IMU, rather than distinct points, doing a regression is a suitable method.

*Response to roll moment input*

Input of the vertical road indentations on each suspension masks the induced roll disturbances. According to a study by Nguyen et al. [26], this is one reason for the poor ability to differentiate between roll disturbance and road disturbances. In this test, road indentations are fed to the centre of gravity of the vehicle. In this way, road noise cannot mask the roll disturbance response, making it more likely for the drivers to notice the roll disturbances. However, the results suggest that drivers are still much less likely to observe the roll disturbance than yaw disturbance, which is in line with Huemer et al [24] and Nguyen et al. [26].

The peak-to-peak roll velocity, $\omega_{x,p2p}$, is about 0.35 deg/s at the lowest frequency range, $0.25-0.5$ Hz, regardless of driver type and amplitude as shown in Figure 4.7. At higher frequencies the $\omega_x$ response increases and amplitudes get higher in response to higher disturbance amplitude. The influence of damping of roll moment input by the vehicle dynamics plays a significant role in interpreting and reading the results. The vehicle is more sensitive in the $2-4$ Hz range which contains the eigenfrequency of the vehicle chassis. When comparing other frequency ranges, same input amplitude results in higher measured $\omega_{x,p2p}$.

*Steering characteristics to disturbance input*

In the case of both yaw and roll disturbances, the steering intensities right before and during the disturbances are not significantly different, regardless of the driver type. However, the steering input is significantly lower for test drivers than for common drivers while driving on a straight line. An example of the yaw disturbance steering characteristics is shown in Table 4.1.

The steering feedback and vehicle dynamics are coupled, which will be shown using logistic regression in Section 4.3.3. For the common drivers, the higher inputs from steering might create an anticipated vehicle behaviour, making them less sensitive to induced disturbances. This could be one possible explanation for their lower ability to identify the induced external disturbances, especially at low amplitudes.

### 4.3.3 Predictive model analysis

The model uses the standard deviations of the objective variables measured in the cockpit from the beginning of the disturbance and 8 seconds onwards. The predictive model is developed from both roll and yaw moment disturbance output. The relevant independent variables

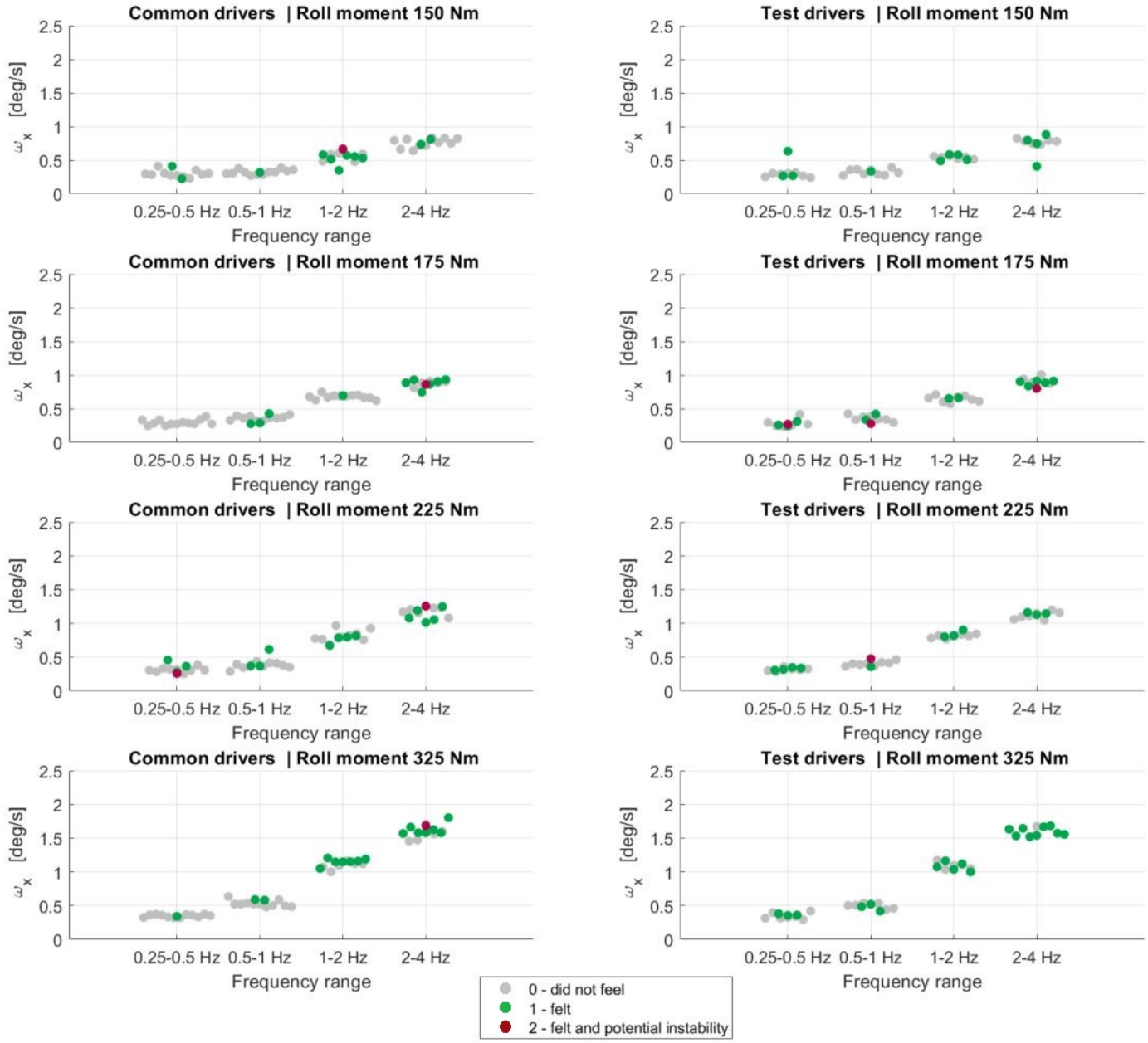


**Figure 4.7:** *Swarm plot of driver response to roll moment disturbance input. Peak-to-peak roll velocity $\omega_{x,p2p}$ deg/s vs frequency diagrams.*

**Table 4.1:** *Paired sample t-test used for analysing the influence of driver type and the presence of induced yaw disturbance on $\tau_{sw,p2p}$.*

| | | Common drivers | Test drivers | p-value |
|---|---|---|---|---|
| | no. of observations | 241 | 148 | |
| Before disturbance | mean value | 1.623 | 1.316 | |
| | standard deviation | 0.609 | 0.424 | $1.29 \cdot 10^{-7}$ |
| During disturbance | mean value | 1.692 | 1.377 | |
| | standard deviation | 0.581 | 0.373 | $7.81 \cdot 10^{-9}$ |
| p-value | | 0.20 | 0.19 | |

**Note:**
**Case 1 Null hypothesis:** The steering behaviour doesn't have association with the type of driver irrespective of the presence of any yaw moment disturbance.
*Result:* p-values lower than 0.02 imply that there is significant difference in steering feedback between test drivers and common drivers
**Case 2 Null hypothesis:** The steering behaviour during disturbance doesn't have association with before and during the yaw moment disturbance for both types of drivers.
*Result:* p-values higher than 0.02 imply that the test fails to reject null hypothesis.

(predictors) with significant influence, p-values $< 0.001$, are chosen. $c_{DT}$ is an independent variable with values 1 and 2 assigned to represent common drivers and test drivers, respectively. The resulting logit function $z$ is:

$$z = \beta_0 + \beta_1\ \omega_{x,std} + \beta_2\ \omega_{z,std} + \beta_3\ \delta_{sw,std} + \beta_4\ c_{DT} \tag{4.3}$$

**Table 4.2:** *Resulting properties of model parameters*

| | values | unit | 95% confidence interval | | | p-value |
|---|---|---|---|---|---|---|
| $\beta_0$ | -3.71 | [-] | -4.70 | to | -2.71 | $0.23 \cdot 10^{-12}$ |
| $\beta_1$ | 9.86 | [s/deg] | 3.99 | to | 15.72 | $0.98 \cdot 10^{-3}$ |
| $\beta_2$ | 58.26 | [s/deg] | 47.19 | to | 69.34 | $0.61 \cdot 10^{-24}$ |
| $\beta_3$ | -419.42 | [1/deg] | -508.88 | to | -329.96 | $0.39 \cdot 10^{-19}$ |
| $\beta_4$ | 0.93 | [-] | 0.55 | to | 1.31 | $0.14 \cdot 10^{-5}$ |

The black dotted line in Figure 4.8 represents the predicted probability for 'at least felt' outcome for a given $z$ and properties of the model parameters are shown in Table 4.2. It has 71% accuracy with 60% accuracy to predict 'at least felt' and 81% accuracy to predict 'did not feel'. The statistical significance can be improved with more tests and resulting data.

To understand the influence of each independent variable (predictor) on predicting 'at least felt', the chosen independent variable (predictor) is varied between two standard deviations from its mean of standard deviation value and the remaining predictors are kept at their mean standard deviation values from all observations. The outcome is compared between the test and common drivers, shown in Figure 4.9.

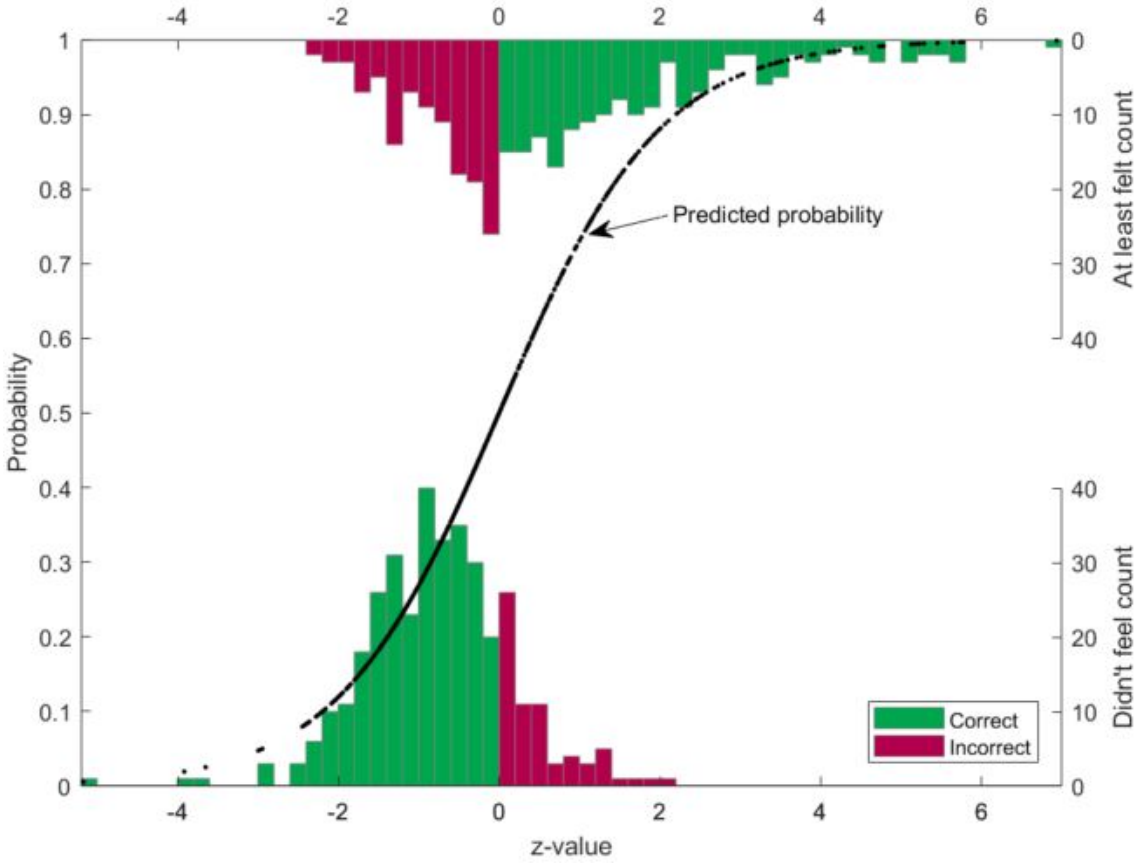


**Figure 4.8:** *Logistic regression plot over $z$. Histogram plot represents the count of 'at least felt' and 'did not feel'.*

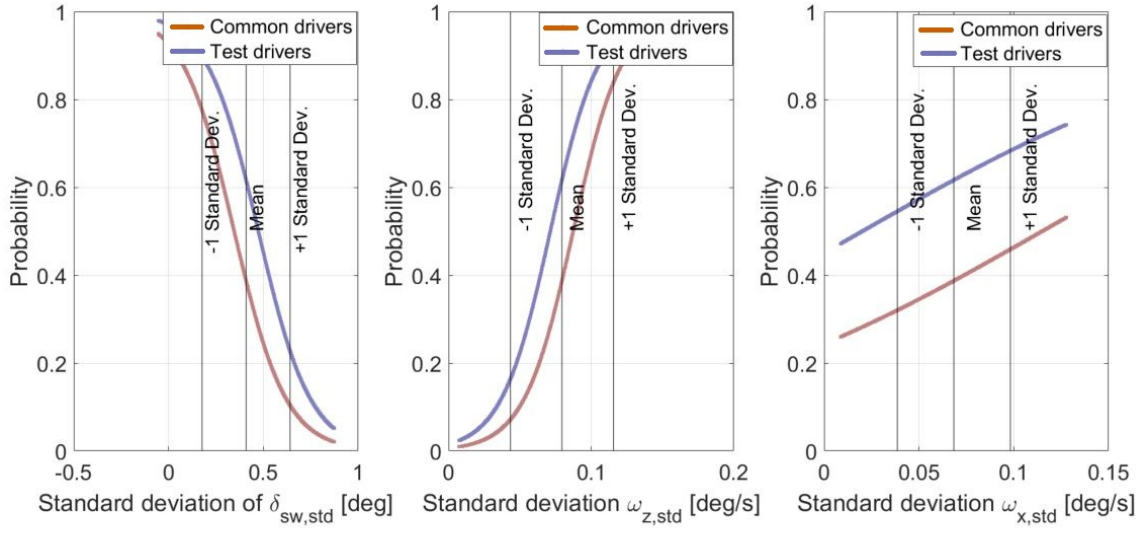


**Figure 4.9:** *Influence of one independent variable on prediction while remaining variables are kept constant at their mean of standard deviation values from all observations.*

The results indicate that:

- The test drivers are more sensitive to disturbances than common drivers, which shows up in the $c_{DT}$ constant, even after accounting for the increased sensitivity test drivers have because they steer less.
- Roll velocity fluctuations, $\omega_{x,std}$ are the least sensitive, provided $\delta_{sw,std}$ and $\omega_{z,std}$ are fixed.
- The model predicts the driver to be about 6 times more sensitive to yaw than roll disturbances.

# 5

# Concluding remarks and future work

The findings so far provided insight into the relationship between subjective judgement and objective quantities under external disturbances such as unsteady aerodynamics and its impact on vehicle behavior on straight-line high-speed drive. The outcomes of this study can be used to improve early phase development prediction of a more aerodynamically stable vehicle.

The on-road experiment was aimed at finding a co-relation between the subjective judgement of drivability and measurable quantities such as steering responses, and linear and rotational motions. Several aerodynamic configurations were used to excite varying forces and moments: An inverted wing, an inverted wing with fin, and an anti-diffuser. They were paired as with and without sidekicks. The paired comparisons showed that the presence of side-kicks improved straight-line drivability compared to without for any given configuration pair. The vector plots of mean and standard deviation pointed toward the origin when plotting pairs from without sidekick to with sidekick. This implies that the vehicle response and steering effort to aerodynamic disturbances were reduced with side-kicks, depicting the improved subjective assessment of drivability. The study suggests that a smaller standard deviation of steering angle, steering torque, yaw velocity, and lateral acceleration is related to a better subjective assessment of drivability at high-speed straight-line driving. The Ride diagram helped to differentiate the influence of transient and stationary behaviour. The accuracy of sensors was a limitation resulting in the outcome being a qualitative analysis reinforced with the help of statistical assessment. To quantify drivability in a robust way, more accurate sensors are needed along with more configurations showing even worse drivability and instability conditions.

Driving simulators were used to obtain data for a regression model to predict which disturbances drivers can feel in relation to given objective quantities. The model quantifies the difference in sensitivity between driver types and the difference in sensitivity to yaw and roll disturbances. The model can also be used to identify which signals can be ignored when searching for problematic disturbances. The study supports that drivers are more sensitive to yaw disturbances than roll. Professional drivers were more sensitive to yaw moment disturbances at all tested frequency ranges. Unlike test drivers, common drivers were less sensitive to the lowest frequency ranges. The impact of steering input affects the sensitivity to externally induced disturbances. Professional test drivers steered less than common drivers. This partially explains the higher sensitivity of test drivers.

The results obtained from the on-road and driver simulator tests provide a reference for assessing and investigating flow behaviors that could result in disturbances in the form of

vehicle instabilities or nervousness for the driver. Moreover, the results can be used for analyzing data from wind tunnel and on-road tests to identify potentially problematic unstable aerodynamic behavior.

# Future work

The configuration setup found in the on-road study, Chapter 3 (Paper A), and the related aerodynamic flow nature will not be found in a production design. A more realistic test vehicle profile with instabilities on road will be proposed along with few configurations designed and ready for testing. Sensors set-up similar to the ones used in the on-road study will be installed to record the vehicle behavior. A clinical test will be conducted in order to understand and develop a regression predictive model with more realistic environmental influences. The resutling model will be compared with the model derived in Paper B.

The study in Chapter 4 (Paper B) showed the influence of steering on the sensitivity of the drivers. In the case of both yaw and roll disturbances, the steering intensities right before and during the disturbances were not significantly different, regardless of the driver type. However, increased steering intensity was related to a decrease in sensitivity to induced disturbances. Hence, predicting output to any given disturbance input isn't straight forward because the involvement of driver interaction created uncertainty when predicting output. As a result, an in-depth study relating the drivers' responses with the uncertain movement of the vehicle will be undertaken. Driving simulator tests that includes both yaw moment, side forces and combinations of the two as well as a wider range of amplitudes compared to the test done in this paper would be of interest.

# 6

# Summary of papers

## 6.1 Paper A

*Analysis of Subjective Qualitative Judgement of Passenger Vehicle High Speed Drivability due to Aerodynamics*

This paper focused on building a relation between the vehicle motion and subjective perception of high-speed straight-line drivability. The test was performed on a front-load biased compact sedan at the Volvo Cars Hällered Proving Ground. Different aerodynamic devices were used for generating higher lift and asymmetric aerodynamic forces resulting in substandard straight-line drivability on-road. The resulting poor drivability of the test vehicle with the aerodynamic devices was improved with the help of side-kicks. The paper investigated the trend of drivability of configurations with and without side-kicks in relation to vector plots of mean and standard deviation. The ride diagram was used to separate the presence of transient behaviour and study its impact on subjective judgement. The qualitative assessment of the resulting trends agrees well with the subjective judgement of the driver.

## 6.2 Paper B

*Prediction of Driver's Subjective Perception and Vehicle Reaction under Aerodynamic Excitations*

This paper further investigates the subjective perception and responses of drivers to aerodynamic excitations in high-speed straight-line driving condition. Clinical tests involving both common and experienced test drivers were conducted using driving simulators at Volvo Cars and VTI. The results provided an insight towards the disturbance frequencies and amplitudes of interest. The paper presents a model from the test data that can predict the drivers' subjective perception after experiencing induced aerodynamic excitations. The drivers were more sensitive to yaw disturbances than roll disturbances. The impact of drivers' steering actions on their subjective perceptions towards these disturbances is also shown in this paper.

# References


[1] Kumar, A. et al. "Analysis of Subjective Qualitative Judgement of Passenger Vehicle High Speed Drivability due to Aerodynamics". *Energies* **12**.14 (2019). DOI: 10.3390/en12142839.

[2] Kumar, A. et al. "Prediction of Driver's Subjective Perception and Vehicle Reaction under Aerodynamic Excitations". *Submitted to Vehicle System Dynamics* (2021).

[3] Brandt, A. "Driving stability of passenger vehicles under crosswinds". *Licentiate thesis, Department of Mechanics and Maritime Sciences Chalmers University of Technology* (2021).

[4] Baker, C. J. and Reynolds, S. "Wind-induced accidents of road vehicles". *Accident Analysis & Prevention* **24**.6 (1992), 559–575. DOI: 10.1016/0001-4575(92)90009-8.

[5] Macadam, C. C. et al. "Crosswind Sensitivity of Passenger Cars and the Influence of Chassis and Aerodynamic Properties on Driver Preferences". *Vehicle System Dynamics* **19**.4 (1990), 201–236. DOI: 10.1080/00423119008968942.

[6] Howell, J. and Panigrahi, S. "Aerodynamic Side Forces on Passenger Cars at Yaw". *SAE World Congress and Exhibition* (2016). DOI: 10.4271/2016-01-1620.

[7] Theissen, P. "Unsteady Vehicle Aerodynamics in Gusty Crosswind". *PhD thesis, Technical University of Munich* (2012). URL: http://mediatum.ub.tum.de/doc/1096026/520174.pdf.

[8] Hucho, W. H. "Aerodynamics of Road Vehicles". *SAE International* (1998).

[9] Willumeit, H. P. et al. "Method to correlate vehicular behaviour and driver's judgment under side wind disturbance". *Vehicle System Dynamics* **17** (1988), 508–524. DOI: 10.1080/00423118808969292.

[10] Yoshihiro, O. et al. "Flow Structures above the Trunk Deck of Sedan-Type Vehicles and Their Influence on High-Speed Vehicle Stability 1st Report: On-Road and Wind-Tunnel Studies on Unsteady Flow Characteristics that Stabilize Vehicle Behavior". *SAE International Journal of Passenger Cars - Mechanical Systems* (2009), 138–156. DOI: 10.4271/2009-01-0004.

[11] Takuji, N. et al. "Flow Structures above the Trunk Deck of Sedan-Type Vehicles and Their Influence on High-Speed Vehicle Stability 2nd Report: Numerical Investigation on Simplified Vehicle Models using Large-Eddy Simulation". *SAE International Journal of Passenger Cars - Mechanical Systems* (2009), 157–167. DOI: 10.4271/2009-01-0006.

[12] Kawakami, M., Murata, O., and Maeda, K. "Improvement in Vehicle Motion Performance by Suppression of Aerodynamic Load Fluctuations". *SAE International Journal of Passenger Cars - Mechanical Systems* (2015), 205–216. DOI: 10.4271/2015-01-1537.

[13] Howell, J. and Good, G. L. "The Influence of Aerodynamic Lift on High Speed Stability". *SAE Technical Paper Series Technial 01.0651* (1999). DOI: 10.4271/1999-01-0651.

[14] Buchheim, R., Maretzke, J., and Piatek, R. "The Control of Aerodynamic Parameters Influencing Vehicle Dynamics". *SAE Paper, 850279–850279* (1985). DOI: 10.4271/850279.

[15] Heiderich, M., Friedrich, T., and Nguyen, M. T. "New approach for improvement of vehicle performance by using a simulation-based optimization and evaluation method".

$7^{th}$ *International Munich Chassis Symposium, ATZ, Munich* (2016). DOI: https://10.1007/978-3-658-14219-3-21.

[16] Fainello, M., Ferrari SpA-Diego Minen, and VI-grade. "Active vehicle ride and handling development by using integrated SIL / HIL techniques in a high performance driving simulator". *5th International Munich Chassis Symposium* (2014). DOI: 10.1007/978-3-658-14219-321.

[17] Stewart, D. "A Platform with Six Degrees of Freedom". *Proceedings of the Institution of Mechanical Engineers* **180** (1965), 371–386.

[18] Kuschov, A. "Motion Perception and Tire Models for Winter Conditions in Driving Simulators". *Licentiate thesis, Department of Mechanics and Maritime Sciences Chalmers University of Technology* (2016).

[19] VTI (accessed on 20 April 2021). URL: https://www.vti.se/en/research/vehicle-technology-and-driving-simulation/driving-simulation/simulator-facilities.

[20] Blissing, B., Bruzelius, F., and Eriksson, O. "Effects of Visual Latency on Vehicle Driving Behavior". *ACM Transactions on Applied Perception* **14**.1 (2016), 1–12. DOI: 10.1145/2971320.

[21] Grant, P. R. and Reid, L. D. "Motion Washout Filter Tuning: Rules and Requirements". *Journal of Aircraft* **34**.2 (1997), 145–151. DOI: 10.2514/2.2158.

[22] Groen, E. and Bles, W. "How to use body tilt for the simulation of linear". *Journal of Vestibular Research* **14**.5 (2004), 375–385.

[23] Krantz, W. et al. "Simulation des Fahrens unter instationärem Seitenwind". *Automobiltechnische Zeitschrift* **116** (2014), 64–68. DOI: 10.1007/s35148-014-0046-6.

[24] Huemer, J. et al. "Influence of unsteady aerodynamics on driving dynamics of passenger cars". *Vehicle System Dynamics* **52**.11 (2015), 1470–1488. DOI: 10.1080/00423114.2014.944191.

[25] Wagner, A. and Wiedemann, J. "Crosswind Behavior in the Driver's Perspective". *World Congress & Exhibition. SAE International* (2002). DOI: 10.4271/2002-01-0086.

[26] Nguyen, M. et al. "Subjective Perception and Evaluation of Driving Dynamics in the Virtual Test Drive". *SAE International Journal of Vehicle Dynamics, Stability, and NVH* **1**.2 (2017), 247–252. DOI: 10.1080/00423114.2014.944191.

[27] Hamilton, J. D. "Time Series Analysis". *Princeton University Press: Princeton, USA* **4** (2013).

[28] Box, G. E. P., Jenkins, G. M., and Reinsel, G. C. "Time Series Analysis: Forecasting and Control". *John Wiley & Sons, New Jersey, US* **3** (2008).

[29] Strandemar, K. "On Objective Measures for Ride Comfort Evaluation". *Ph.D. Thesis, Control Technology, Stockholm, Sweden* (2005).

[30] Strandemar, K. and Thorvald, B. "The Ride Diagram, A Tool for Analysis of Vehicle Suspension Settings: The Dynamics of Vehicles on Roads and on Tracks". J. Veh. Syst. Dyn. Int. J. Veh. Mech. Mobil. **44** (2006), 913–920. DOI: 10.1080/00423110600907618.

[31] Walker, S. H. and Duncan, D. B. "Estimation of the probability of an event as a function of several independent variables". *Princeton University Press: Princeton, USA* **54** (1967), 167–178. DOI: 10.2307/2333860.

[32] David, A. F. "Statistical Models: Theory and Practice". *Cambridge University Press* (2009), 128.

[33] Strandemar, K. and Thorvald, B. "Truck Characterizing Through Ride Diagram: In Vehicle Dynamics and Chassis Developments". Sae Commer. Veh. Eng. Congr. (2004), 913–920. DOI: 10.4271/2004-01-2714.

[34] Strandemar, K. and Thorvald, B. "Driver perception sensitivity to changes in vehicle behavior". Vehicle System Dynamics (2004), 272–281.

[35] Williamson, A. M., Feyer, A. M., and Friswell, R. "The impact of work practices on fatigue in long distance truck drivers". *Accid. Anal. Prev.* **26**.28 (1996), 709–719. DOI: 0.1016/s0001-4575(96)00044-9.

[36] Lal, S. K. L. and Craig, A. "A critical review of the psychophysiology of driver fatigue". *Biol. Psychol.* **55**.3 (2001), 173–194. DOI: 10.1016/s0001-4575(02)00014-3.

[37] Thiffault, P. and Bergeron, J. "Monotony of road environment and driver fatigue: A simulator study". *Accid. Anal. Prev.* **35**.6 (2003), 381–391. DOI: 10.1016/s0001-4575(02)00014-3.

[38] Ranney, T. A., Simmons, L. A., and Masalonis, A. J. "Prolonged exposure to glare and driving time: Effects on performance in a driving simulator". *Accid. Anal. Prev.* **31**.6 (1999), 601–610. DOI: 10.1016/s0001-4575(99)00016-0.

[39] Kecklund, G. and Åkerstedt, T. "Sleepiness in long distance truck driving: An ambulatory EEG study of night driving". *Ergonomics* **12**.36 (1993), 1007–1017. DOI: 10.1080/00140139308967973.

[40] PM Intrumentation (2017). DOI: \hl{accessedon15May2019}. URL: %7B%20https://pm-instrumentation.com/docpdf/Systemes/embarque-%20volant/PMI-01184-Volant-telemetrique.pdf%7D.

[41] Oettle, N. R. et al. "The Effects of Unsteady On-Road Flow Conditions on Cabin Noise". SAE Int. J. Passeng. Cars - Mech. Syst. **4** (2011), 120–130. DOI: 10.4271/2011-01-0159.

[42] DEWESoft. "Documentation on IMU and GPS". 2019. URL: https://dewesoft.com/products/interfaces-and-sensors/gps-and-imu-devices. (accessed on 20 May 2019, accessed on 20 May 2021).

[43] VI-Grade. URL: https://www.vi-grade.com/en/products/dim-dynamic-simulator/s. (accessed on 20 April 2021).

[44] Volvo Cars. URL: https://www.media.volvocars.com/se/sv-se/media/pressreleases/167927/volvo-cars-anvander-varldens-mest-avancerade-chassisimulator-for-att-utveckla-nasta-generation-bilar. (accessed on 20 April 2021).

[45] Jansson, J. et al. "Design and Performance of the VTI Sim IV". *Driving Simulation Conference Paris, September 4-5. France* (2014).

[46] Bruzelius, F., Gomez, F. J., and Augusto, B. "A Basic Vehicle Dynamics Model for Driving Simulators". *International Journal of Vehicle Systems Modelling and Testing* **8**.4 (2013), 364–385. DOI: 10.1080/00423114.2019.1566555.

[47] Obialero, E. "A Refined Vehicle Dynamic Model for Driving Simulators". *Master's Thesis. Chalmers University of Technology* (2013).

[48] Brandt, A. et al. "Quantitative High Speed Stability Assessment of a Sports Utility Vehicle and Classification of Wind Gust Profiles". *WCX SAE World Congress Experience* (2020). DOI: 10.4271/2020-01-0677.

[49] Fisher, R. A. "On the interpretation of 2 from contingency tables, and the calculation of Probability". *Journal of the Royal Statistical Society.* **85**.1 (1922), 87–94. DOI: 10.2307/2340521.

# Part II

# Appended papers

# Paper A

## Analysis of Subjective Qualitative Judgement of Passenger Vehicle High Speed Drivability due to Aerodynamics

in

Energie Journal, https://doi.org/10.4271/2020-01-0677

energies

MDPI

Article

# Analysis of Subjective Qualitative Judgement of Passenger Vehicle High Speed Drivability due to Aerodynamics

**Arun Kumar [1,2,*], Simone Sebben [1], Erik Sällström [2] and Bengt J.H. Jacobson [1] and Alexander Broniewicz [2]**

[1] Department of Mechanics and Martime Sciences, Chalmers University of Technology, Hörsalsvägen 7A, SE-412 58 Göteborg, Sweden
[2] Volvo Car Corporation, Torslanda, SE-405 31 Göteborg, Sweden
* Correspondence: arun.kumar@volvocars.com

Received: 17 June 2019; Accepted: 19 July 2019; Published: 23 July 2019


**Abstract:** The flow created by the shape of a vehicle and by environmental conditions, such as cross-winds, will influence the dynamics of a vehicle. The objective of this paper is to correlate the driver's subjective judgement of drivability with quantities which are measurable during a vehicle test. For this purpose, a sedan vehicle, fitted with different aerodynamic external devices that create disturbances in the flow field, were assessed on a test track. These configurations intend to result in substandard straight line drivability. The aerodynamic devices investigated are an inverted wing, an inverted wing with an asymmetric flat plate and an asymmetric air curtain attached under the bumper. The devices generate more lift and asymmetric forces resulting in increased vehicle sensitivity to external disturbances. Pairs of configurations with and without bumper side-kicks are also tested. The side-kicks create a defined flow separation which helps to stabilize the flow and increase drivability. Plots of mean and standard deviation and ride diagram of lateral acceleration, yaw velocity, steering angle and steering torque are used to understand vehicle behaviour for the different configurations. Ride diagrams are used to visualize vehicle excitations with transient events separated from the stationary signal. The range of the measured quantities for understanding the drivability is not predicted in advance and it turns out that the error margins of the measurements are smaller than the measurement uncertainty of the Inertia Measurement Unit. Although the outcome lacks the ability to objectively quantify subjective judgements, it provides a useful qualitative assessment of the problem as the trends agree well with the subjective judgement of the driver.

**Keywords:** drivability; ride diagram; drive quality; aerodynamics; vehicle; high speed; stability

## 1. Introduction

Subjective evaluation of a vehicle by test drivers is an important part of the final assessment of vehicle performance. In most cases, these evaluations are done on test tracks or under real world conditions like on the Autobahn. The feedback from drivers is the input for the fine tuning of vehicle dynamics [1,2]. The impact of aerodynamics also contributes to the ratings from the test drivers on ride quality and directional stability [3]. Most of the research available that is related to aerodynamics and its influence on vehicle dynamics is on the impact of cross-wind/gusts stability and vehicle response [4–9]. In these examples, the field of straight line drivability without external influences such as cross-winds/gusts are not considered. A vehicle showing low standard in straight line drivability at high speed is seldom unstable in a strict mathematical way, rather it is uncomfortable or 'nervous' to drive. According to Proton et al. [10], drivability is defined as the smoothness of vehicle operation

under all driving conditions. It determines the vehicle's ability to behave according to customers requirements. In this case, poor straight line drivability rating at high speed by the test driver can be due to poor lane keeping ability, feel of disturbance in the form of lateral acceleration or yaw acceleration or need of subtle but frequent, steering input from the driver.

Research relating objective measurements to subjective judgements is found in few papers. Klause et al. [11] studied objective evaluation of subjective judgement on secondary ride comfort; i.e, vibrations $> 4$ Hz and handling. Ten cars of different categories such a sports and luxury cars were studied. Hence, the results of handling characteristics were scattered. The results could only point out the potential of either handling or steering improvement for a given car. Their methodology did not explain on how to commonly formulate the objective rating factor for any vehicle. Chandrasekaran et al. [12] focused on comparing objective and subjective drivability on a compact SUV. They used neural networks with the help of the AVL drive software to determine objective drivability ratings. This software aids in measuring physical quantities such as vehicle speeds and accelerations via sensors and interfaces. The driving conditions are recognized with fuzzy logic. The investigation at constant speed was one among ten maneuvers of the driving cycle. The driving environment for constant speed maneuver such as, whether it is a straight road, existence of external disturbances such as road unevenness was not explained. Moreover, it is difficult to give formula or interpret relationships resulting from a neural network between physical quantity to the objective drivability.

Strandemar et al. [13,14], used ISO 2631 to show that transient disturbances play important role in subjective evaluation. They pointed out that the basic evaluation tool used in ISO 2631 is the Weighted acceleration RMS value which decreases the contribution of transient nature. ISO 2631, Evaluation of Human Exposure to Whole-body Exposure [11] is commonly used for determining the ride quality of a vehicle under a condition consisting of a consistent disturbance pattern such as road roughness. It agrees with subjective rating provided the vibrations are stationary in nature. An alternative method called the ride diagram, introduced by Strandemar et al. [15] was used to visualize vehicle excitations with transient events separated from the stationary signal. A signal is characterized as a stationary signal when, at any two time instance, any signal value is equally probable of happening with respect to any other signal value irrespective of the distance between these signal values. On the other-hand, a transient signal show presence of sudden jumps in an otherwise stationary signal. Their investigation was on vertical ride comfort and no further research on remaining variables such as lateral acceleration, pitch or yaw rate was carried out. Also the subjective tests were done on different test drivers using a motion simulator behaving as a real truck under different suspension characteristics. Tests on a real on-road test will tend to have more uncertainties than a controlled environment such as a simulator.

For this study, a sedan vehicle is considered with on-road tests done on a test track with two straight sections, each long enough to capture the influence of the aerodynamic devices added to the model. The flow around the vehicle is altered to create asymmetric flow patterns intended to result in undesired aerodynamic forces and moments on the vehicle. The purpose of these aerodynamic devices is to develop substandard driving quality at high speeds during straight line drive. Three configurations are considered in this study; an inverted wing, an inverted wing with an asymmetric flat plate and an asymmetric air curtain attached to the diffuser. All the three configurations have the primary intention to increase the lift of the vehicle. These configurations are paired with and without side-kicks. The side-kicks are additional aerodynamic devices used to create a defined flow separation line in the rear side of the vehicle intending to stabilize the rear wake. Comparison of the subjective judgement from a trained test driver are done between the pair of configurations. Combining any of the other aerodynamic devices with side-kicks results in an improved drivability. Various sensors are used to record the vehicle behaviour. This study aims to find a relationship between these measurements and subjective judgements. Objective measures would be very useful to support virtual verification/evaluation on earlier stages of vehicle development.

## 2. Experimental Set-Up

In this study, the test object is a mid-size sedan, shown in Figure 1. The car is front wheel driven giving a more forward load distribution than the four wheel driven version. This enhances the sensitivity in the rear due to lower traction on the rear tires. The instrumentation used, the configurations studied and the test track and test procedure will be discussed next.

**Figure 1.** Test Vehicle.

### *2.1. Instrumentation*

In order to capture the vehicle behaviour, different variables are recorded with the help of sensors. As shown in Figure 2, the added sensors are as listed below:

- Steering Wheel clip-on sensor (SW): This sensor measures the steering angle and the steering torque. The steering effort sensor, part of the device, is fastened on the steering wheel like an auxiliary steering wheel. the other part is attached to the windshield with the help of vacuum and is used to get the angular position. A belt drives the angular position sensor which is connected to the steering effort sensor. Analog outputs are produced from the two sensors using an analog converter [16]. The effort sensor has an uncertainty of $\pm 0.01$ deg. However, the reference positioning of the angular position sensor is not accurate and therefore neither are absolute values. SW is apt for comparing the change in steering behaviour between different conditions.
- Aeroprobe and pressure sensors (AP): The head wind condition plays an important role in the aerodynamics of the vehicle as a result it is important to track the head wind angles during the test. The aeroprobes have 7 ports at the tip measuring the respective pressures. These pressure values can later be used to calculate the slip angle, roll angle and angle of attack of the head wind. They have a range of $\pm 70$ deg and an accuracy of $\pm 1$ deg. The aeroprobe is placed over the roof of the test object at a vertical height of 360 mm from the roof, in line with Reference [17]. In the XY plane, it is placed in the intersection of the lines bisecting the wheelbase and track width. The disturbances created by cylindrical aeroprobe holder in the form of vortex shedding are minimized by using helical strakes. The pressure sensors are placed inside a small box on the roof in between the aeroprobe holder and the antenna with minimal interference to the flow.
- Ride height sensors (RH1, RH2, RH3, RH4): Attaching aerodynamic devices results in change of ride height of the test vehicle. There are four sensors attached to the test object. One placed inside the front bumper, another inside the rear bumper making the it flush with the exterior surface and remaining two sensors are placed to the sides at the middle of the wheel base. They are attached to the stiff body structure to minimize the influence of dynamic flexing of the body. Measurement of uncertainty for the sensor is $\pm 0.6$ mm.
- Inertia Measurement Unit (IMU): It is also placed in the center of gravity of the vehicle except for the z coordinate (due to structural hindrances). However the IMU can translate the readings of any reference point one inputs, irrespective of the position of IMU itself. Although the measuring acceleration closest to driver gives the best correlation between objective and subjective measure,

from previous studies the acceleration measurements vary a lot between test runs and test drivers as a result the repeatability is quite low [11]. In addition, the region of interest is the quality of vehicle drivability which is associated with rigid body and chassis dynamics; that is, frequency <4 Hz. This falls in to the primary ride comfort category. The IMU is positioned, as suggested by ISO 2631 [18], to the vehicle structure in the interest for chassis vibrations and behaviour. GPS is integrated to this system with the positioning of antennas as recommended by DEWESoft [19].

- Draw-wire displacement sensors (FL, FR, RL, RR): The displacement of suspensions shows aerodynamic and road influence on the vehicle. Four sensors are co-aligned with the spring of each wheel, each able to measure a displacement of ±120 mm with an uncertainty below ±0.3 mm.
- CAN signal: Signals from the vehicle's built-in sensors are also recorded. The steering wheel angle data considered in this research during post-processing and plots is recorded from the CAN bus. The accuracy of these sensors are ±0.1 deg.
- Dewesoft Module: All the sensors are conected to the data acqusation system called Sirius Dewesoft. Dewesoft X software is used for data acquisition and some post processing.

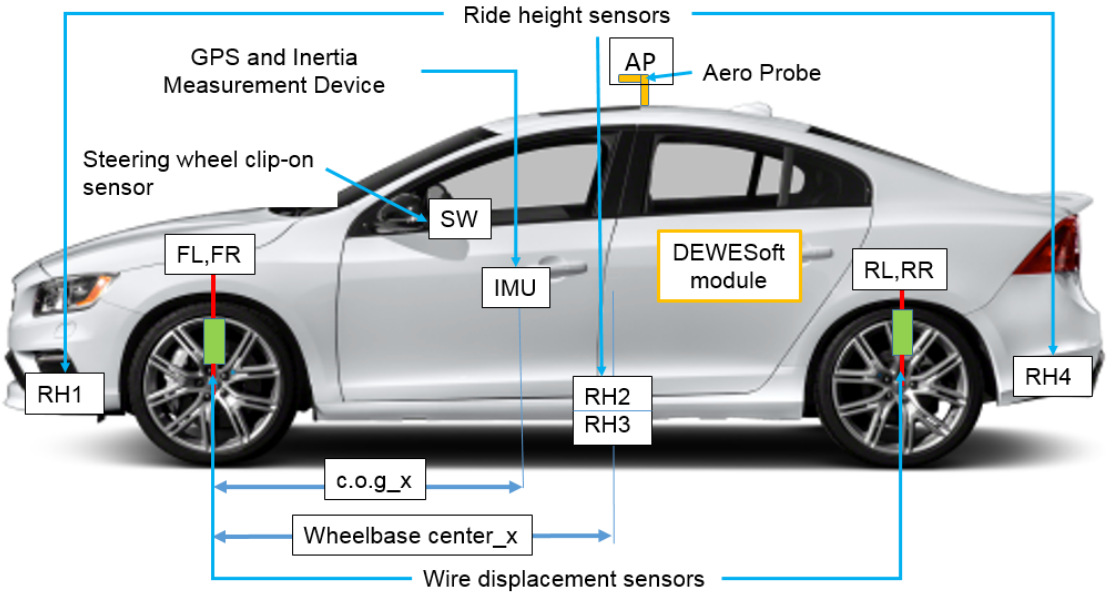


**Figure 2.** Test Vehicle Instrument Setup.

## 2.2. Aerodynamic Configurations

As mentioned, the tests involved creating intentional substandard drivability in order to observe the driver's response. One way to reduce the straight line driving standards is to reduce the traction between tires and road surface. With less traction between road and tires, the test object becomes more sensitive to undesired forces or moments. Paper by Jeff Howell et al. [20] provides a better understanding on relation between lift over lateral aerodynamic characteristics for passenger cars, providing motivation towards modifying the rear of the vehicle. The chosen aerodynamic devices increase lift forces of the test object to favour this need. Referring to Human Perception Theory by Heeger [21], stimulus of different intensities are created with different aerodynamic devices and their combinations and the test driver is asked to respond if he senses it or not. This subjectively establishes sensory absolute thresholds of the test driver. The absolute threshold is the minimum intensity required to be detected by the test driver. After test driving different combinations of a number of aerodynamic devices, three paired configurations are selected for this study. The chosen aerodynamic devices for these configurations are:

- Inverted Wing [w]: The wing is attached inverted, like on an aircraft, to the boot-lid of the vehicle, as shown in Figure 3a, in such a way that it generates more lift in the rear. The angle of attack of the wing is 22.5°. Several test runs are done with tufts on the wing to adjust to the maximum possible angle of attack before stall. The behaviour of the tufts is viewed using cameras attached to the winglet.
- Wing with fin [w-f]: The second device is a fin is placed 90° to the flow upstream on the left side of the inverted wing, as shown Figure 3b. With the addition of a fin on only one side, the wing is expected to experience asymmetric force and moment.
- Anti-diffuser [a]: Figure 3c shows the anti diffuser, which is an asymmetric air curtain placed under the rear bumper. It is positioned to guide the flow downwards and partially restrict the flow along the diffuser region. The resulting asymmetric downwash is expected to affect the vehicle base wake behaviour thus creating non-uniform and periodic forces and moments on the vehicle. This device is termed anti-diffuser as it acts opposite in functionality to a diffuser. The device is suppose to promote a downwash resulting in rear lift.
- Side-kicks [s]: Side-kicks are additional aerodynamic devices shaped as separation edges on both sides of the rear bumper, as shown in Figure 3d. They also have a slight spike to create an outwash while separating the flow at the defined locations. The objective of the side-kicks is to repair the negative effects induced by the three configurations, i.e, wing [w], wing with fin [w-f] and anti-diffuser [a].

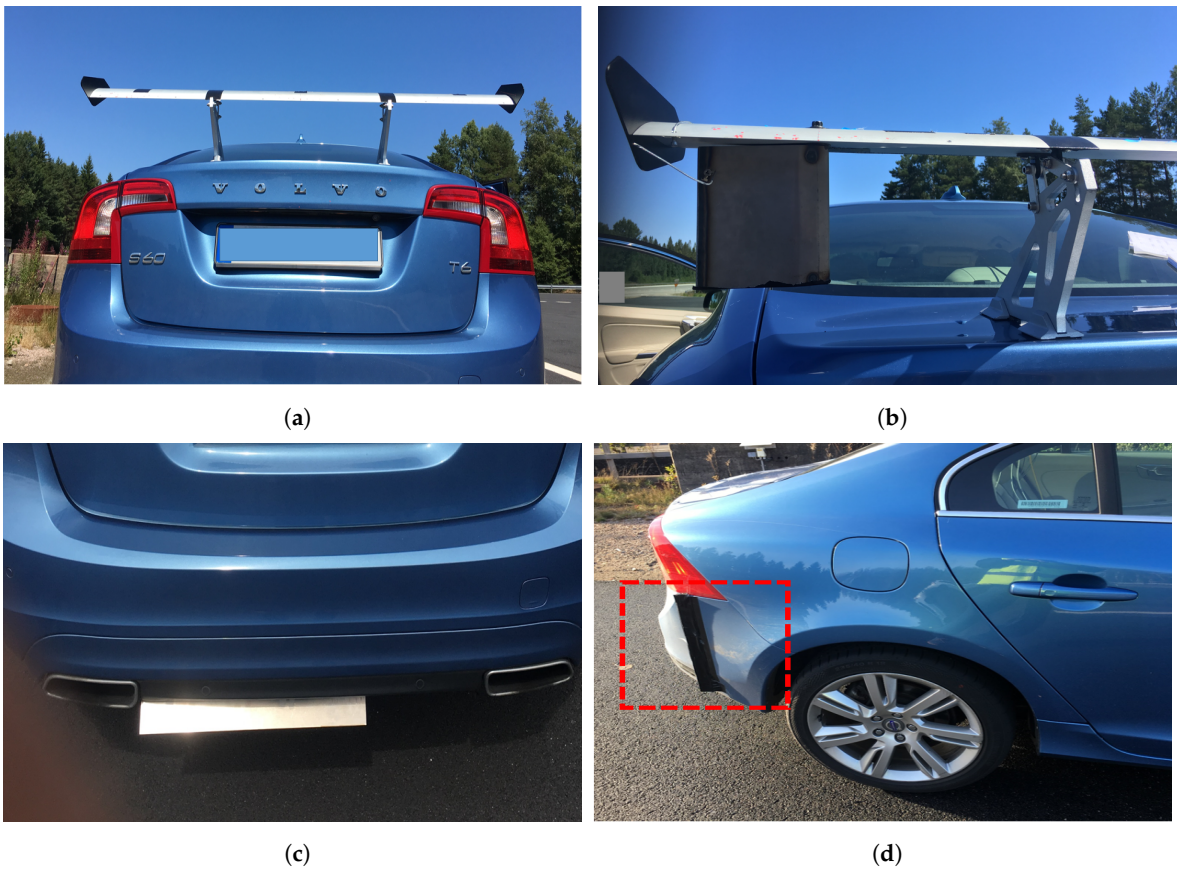


(**a**) (**b**)

(**c**) (**d**)

**Figure 3.** Aerodynamic Devices: (**a**) Inverted Wing [w]. (**b**) Inverted Wing with Fin [w-f]. (**c**) Anti-diffuser [a]. (**d**) Side-kicks [s].

### 2.3. Test Track and Test Procedure

The tests are performed at the Volvo Cars Hällered Proving Ground. The test track used for this study is an oval track with two straight lines of 1.1 km, as sketched in Figure 4. Only measurements along the two straight lines are considered.

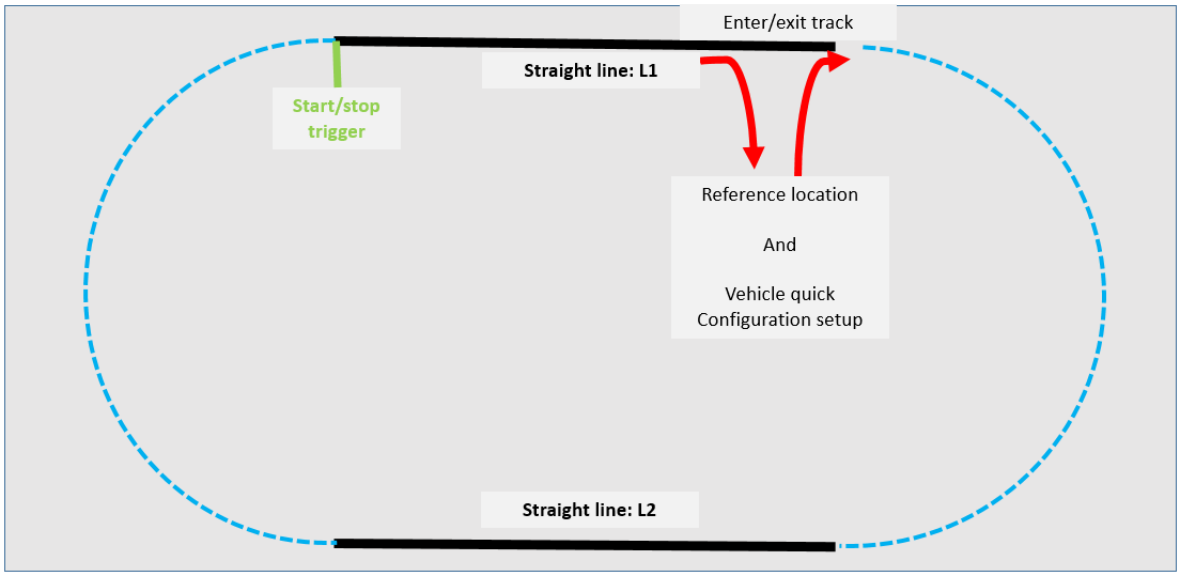


**Figure 4.** Test Track at Volvo Cars Hällered Proving Ground.

The test begins with the test object at the reference location where the sensors are tared. By doing so, the measured values are the difference from the reference position. The test object is first run at high speed to heat the tires to a temperature that remains consistent during high speed drives. The tire pressure is periodically monitored during the tests to ensure its consistency and safety After that it is set to desired configuration and parked at the reference position where a tare is performed. The test object is then driven around the track and the driver is assigned to keep the test object in a straight line. As soon as it passes the first straight line L1, provided the speed is the intended speed and consistent, the Dewesoft Module starts data acquisition. The recording of the data is triggered using coordinates at the beginning of L1 and stops after three full laps. As soon as the recording is complete the test object returns to the reference location for setting up the next configuration and the sensors are tared. This process is repeated for all planned configurations. Throughout the test, the test driver is unaware of the configurations and what to expect from them especially while attaching and detaching the side-kicks, hence providing an unbiased judgement. The tests are done for four different speeds: 140, 200, 230 and 250 km/h. Differences in vehicle behaviour are only observed at speeds of 230 and 250 km/h. Hence, these two speeds are considered in the analysis. Six readings are considered for each speed, three for straight line L1 and three for straight line L2 for speeds 230 and 250 km/h. These speeds are measured using GPS with an accuracy of $\pm 0.01$ m/s. The speed is kept constant using cruise control which an accuracy of $\pm 5$ km/h at 230 and 250 km/h. The average wind speed and direction are received from the traffic control over each test run. The test is done only when the wind speed is below 2 m/s thus minimizing the head angle. During trial runs the subjective judgements are done by three test drivers for all three configurations pairs. In addition, the first author is always present in the passenger seat in all the tests. The tests with recorded data which are presented in the paper are only for one driver. The drivers are not explained about the influences or the set-ups of the aerodynamic devices attached on the test vehicle. As a result, this can be considered as a blind test.

## 3. Drivability Analysis Methods

To understand vehicle response to an excitation, such as steering angle, the transfer function from steering angle to lateral acceleration or yaw velocity is commonly used. All aerodynamic excitations and responses are small in this test, so transfer function becomes sensitive to sensor errors. The investigated transfer functions do not show that the response is dependent on the input. The input and output coherence between the signals in the test data is fluctuating over each frequency and is weak on average over the desired frequency spectrum, So, no credible transfer functions can be found from the kind of tests done.

In an attempt to relate the subjective feel of the test driver to measurable quantities, a few basic variables are considered: lateral acceleration $a_y$, yaw velocity $\dot{\omega}_z$, steering angle $\delta_{sw}$ and steering torque $\tau_{sw}$. Roll and heave rates also contribute to subjective judgment especially in cases such as cross-wind and high speed lane change maneuvers. In this study, straight line drive, their influence is negligible hence they are not further discussed. While $a_y$ and $\dot{\omega}_z$ are feed-backs of vehicle response to aerodynamic disturbances, $\delta_{sw}$ and $\tau_{sw}$ can be either the vehicle response or the driver's response or combination of both to aerodynamic disturbances. The data received from the test consists of three laps and four speeds as mentioned in Section 2. Only the two straight lines, named L1 and L2, are considered in the analysis.

### *3.1. Mean Value Vector Plots Method*

Six mean values are considered for each speed, three for L1 and three for L2 for speeds 230 and 250 km/h. The mean is calculated for a quantity $x$ separately for each speed according to the equation:

$$\bar{x} = \frac{1}{N}\sum_{i=1}^{N} x_i \tag{1}$$

where $N$ is the number of samples. Vector lines connecting the values of the desired quantities of the configurations without side-kicks to the corresponding configurations with side-kicks are referred as vector plots.

Here, plotting mean values of $\delta_{sw}$ against $\tau_{sw}$ and connecting configurations without side-kicks to the corresponding configurations with side-kicks give respective vector plots. These vector plots show the trend of vehicle handling for each configuration pair.

### *3.2. Standard Deviation Vector Plots Method*

The number of independent samples, $m$, of each signal is found using auto-correlation function [22]. This function calculates the correlation between $x_i$ and $x_{i+k}$, where lag $k = 1, 2, 3, ...K$. According to Box et al. [23] the auto-correlation for $k$ is

$$r_k = \frac{c_k}{c_0} \tag{2}$$

where, $c_0$ is the sample variance of the time series.

$$c_k = \frac{1}{T}\sum_{i=1}^{T-k}(x_i - \bar{x})(x_{i+k} - \bar{x}). \tag{3}$$

where $T$ is the effective sample. The variance of the signals are:

$$\sigma_x^2 = \frac{1}{N}\sum_{i=1}^{N}(x_i - \bar{x})^2 \tag{4}$$

The mean uncertainty with a coverage factor of 2, which corresponds to a coverage probability of approximately 95%, is:

$$\Delta\bar{x} = 2\frac{1}{\sqrt{m}}\sigma_x \tag{5}$$

### 3.3. Ride Diagram Method

The mean and variance show an average vehicle response to different configurations but lacks the ability when it comes to understanding the presence of transient behavior. The ride diagram uses a filter to separate the transient behaviour from the remaining signal. The method for ride diagram is done in three steps, defined by Strandemar et al. [24]. The signal is divided into segments at the sign changes of the signal derivatives as shown in Equation (6).

$$nodes = \begin{cases} n & x(n-1) > x(n) < x(n+1) \\ & or\ x(n-1) < x(n) > x(n+1) \end{cases} \tag{6}$$

Thus the $k$th segment will be expressed as:

$$y_k = \{x(n)\}_{n=n_k}^{n=n_{k+1}} \tag{7}$$

where $k = 1, 2, ..., N_k$ and $N_k$ is total number of peaks. The peak-to-peak value of $k$th segment is:

$$ptp(k) = |max(y_k) - min(y_k)| \tag{8}$$

The segments can now be categorized as transient or stationary according to:

$$y_{trans}^k = \begin{cases} \{x(n)\}_{n=n_k}^{n=n_{k+1}} & ptp(k) > T_{limit}\ \&\ ptp(k-1) \leqslant T_{limit} \\ \{x(n)\}_{n=n_k+1}^{n=n_{k+1}} & ptp(k) > T_{limit}\ \&\ ptp(k-1) > T_{limit} \\ 0 & \text{otherwise} \end{cases} \tag{9}$$

where $ptp(0) = 0$, $k = 1, 2, ..., N_k - 1$ and $N_k - 1$ is the number of segments. Figure 5a shows an example of a random signal. As referred in Strandemar et al. [24], $T_{limit} = 2\sqrt{2}\, rms(x)$ is the limit of transients also know as the signals energy equivalent amplitude. The Mean Squared Values (MS) of transient and stationary (remaining) signals are related as shown in Equation (10).

$$MS_{transient} = \frac{1}{N}\sum_{k}^{N_k-1}\sum_{n}|y_{trans}^k|^2 \tag{10}$$

$$MS_{stationary} = \frac{1}{N}\sum_{1}^{N}x(t)^2 - MS_{transient} \tag{11}$$

For a given situation Figure 5b shows a general idea of reading the ride diagram with respect to drivability standards.

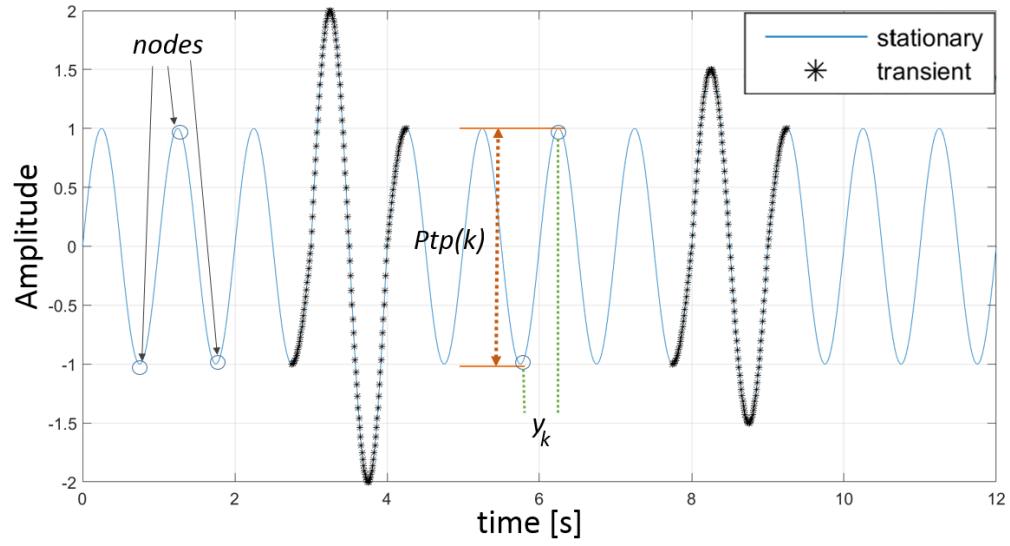


(**a**)

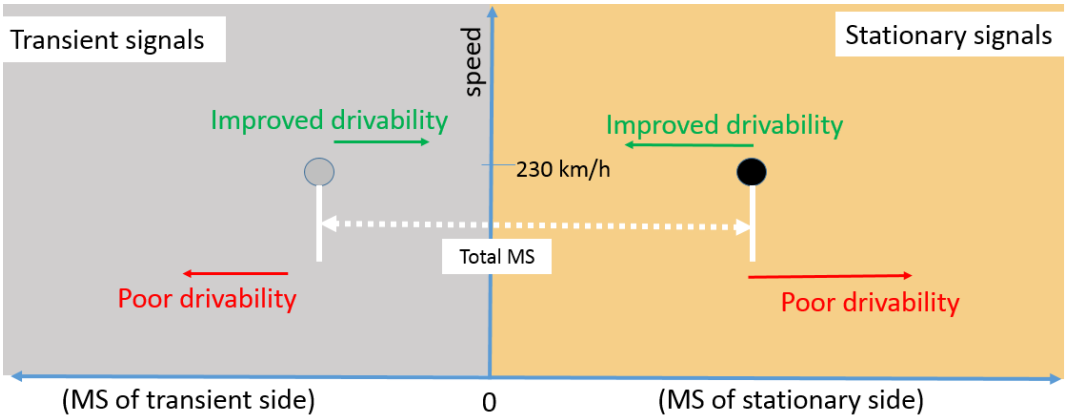


(**b**)

**Figure 5.** Differentiation of Stationary-Transient Signal [24]: (**a**) A signal divided into segments, where Peak-to-Peak distance is marked and the dotted line segments are sorted as transient. (**b**) Simple representation of how to read the ride diagrams. Left side represents Mean Squared Value (MS) of transient part and right side represents Mean Squared Value (MS) of stationary part.

## 4. Discussion and Results

Three configurations that give subjective substandard drivability are selected. Side-kicks are then added to improve drivability. The subjective rating of the tests are shown in chart Figure 6.

The different configurations gives the following behaviours:

- The inverted wing gives low frequency sway, believe to be excited from the rear end of the test object.
- The inverted wing with fin shows similar behaviour as just the inverted wing but in addition there is a slight leftward yaw.
- The anti-diffuser shows a more high frequency yaw behavior compared to the other configurations.

The use of side-kicks improves drive quality and notably dampens the above mentioned behaviours of the respective configurations.

| Notations | Configuration | Drivability good | Drivability poor |
|---|---|---|---|
| a | Anti- diffuser | | x |
| a-s | Anti- diffuser + side-kicks | o | |
| w | Wing | | x |
| w-s | Wing + side-kicks | o | |
| w-f | Wing + fin | | x |
| w-f-s | Wing+ fin + side-kicks | o | |

**Figure 6.** Subjective Judgement.

### *4.1. Limitations*

In this work the significance of subjective judgement is based on statistics. Higher the number of test drivers and test runs, the better the significance of the judgement. However, time taken for testing all these configurations by each driver along with the desired weather conditions are some limitations to be considered. In this test three test drivers are used for subjective evaluation during trial runs and the recorded data presented is of only one test driver. This collection of subjective evaluation along with six runs each should be statistically significant.

Despite major changes to the test object with the intention to increase the lift, the subjective feel for disturbances is still subtle. No alarming instability issue could be sensed by the test drivers which was the prior intention. The relative effect; i.e, comparison with all configurations against each other, was difficult due to time constrains. In addition, when the behaviour is subtle, it is difficult to keep subjective judgement in mind of all configuration tests and rate them against each other. Mind saturation and exhaustion plays a significant role in subjective rating. Since the feel is subtle, the energy and concentration required for the evaluation is significant.

The presence of uncertainty for some measurements is also a challenge which is solved using statistical support as later discussed in Section 4.3.

### *4.2. Analysis*

The data received from the test sensors are filtered with low pass filter with a 20 Hz cutoff frequency and the feedback from the test drivers is expected to be due to effects below 2 Hz. This falls in the primary ride quality which is related to vehicle chassis behaviour, as mention in Section 3.

Wire displacement sensors are used to determine the lift forces of all the configurations which are compared with the reference test object, that is, the test object without any configurations. The RMS of the change in lift forces on each wheel for each configuration compared to the reference test object is shown in Figure 7. It is interesting to observe that the configuration with anti-diffuser (a and a-s) creates less lift distribution on rear right wheel compared to the reference. The rear right suspension receives a lower lift force where the anti-diffuser is not restricting the flow along the diffuser and the rear left has higher lift where the anti-diffuser restricts the flow along the diffuser. The configurations with anti-diffuser provide the lowest lift forces of all the configurations independent of speed. For the wing (w and w-s) and wing with fin (w-f and w-f-s) configurations, the increase in speed from 230 to 250 km/h results in higher rear lift. As a result the load is being redistributed more to the front of the test object. This causes the front suspension to compress and the test object to pitch down. When comparing the configuration pairs in Figure 7, it is hard to make any conclusive statement on the side-kicks' contribution to lift. The asymmetric suspension expansion between rear left and right is also notable in this bar graph. This could be due to a difference in unsprung weight.

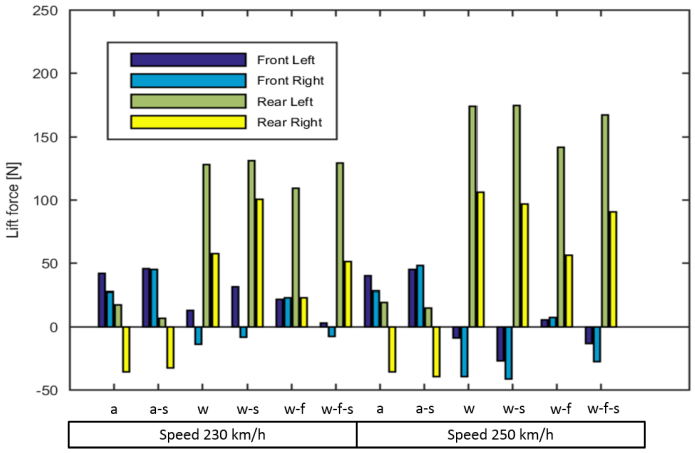


**Figure 7.** RMS of relative suspension displacement for different configurations and speeds.

#### 4.2.1. Comparison Using Mean Values

Figure 8 depicts the effect on mean steering behaviour of the test object with vector plot of steering angle $\delta_{sw}$ in x axis and steering torque $\tau_{sw}$ in y axis. Since the car follows a straight line, the mean values of lateral acceleration $a_y$ and yaw velocity $\dot{\omega}_z$ are close to zero as the lateral displacement an rotation of the test object from start to end of a straight line are negligible. In the case of $\delta_{sw}$ and $\tau_{sw}$, the mean value depicts the excess averaged steering input required by the driver in response to exterior disturbances while keeping the test object following the straight line. It is intuitive to interpret that low $a_y$ and $\dot{\omega}_z$ together with lower need for $\delta_{sw}$ and $\tau_{sw}$ response shows the characteristics of good drivability. This characteristics is shown by arrow pointing towards the origin. Figure 8 shows the improvement in drivability for configurations with side-kicks as they require lower $\delta_{sw}$ and $\tau_{sw}$ compared to ones without side-kicks. Although the subjective judgement of the configuration with anti-diffuser (red arrows) suggests an improvement in drivability due to side-kicks, the results are not as clear as for the other configurations (wing and wing with fin). The vector plots suggests that unlike the other configurations the driver requires similar mean steering response within the pair. Except for the configuration pair with anti-diffuser, the steering characteristics have marked their importance when it comes to high speed straight line drive subjective judgement.

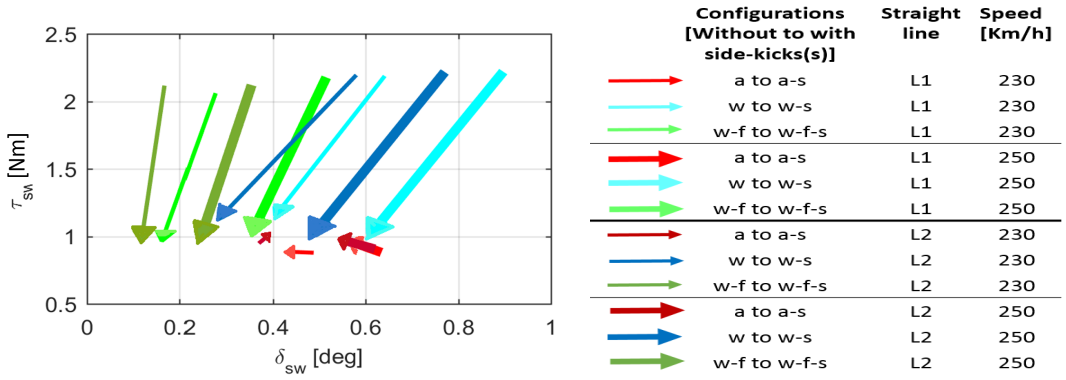


**Figure 8.** Mean vector plot steering torque $\tau_{sw}$ vs steering angle $\delta_{sw}$ of each straight line L1 & L2 for the different configurations and speeds.

#### 4.2.2. Comparison Using Standard Deviations

The standard deviation comparison is of major interest as it shows unsteady behaviours of a vehicle. The vector plots in Figure 9 show the change in standard deviation for all configurations with and without side-kicks. The configuration pair with anti-diffuser (a to a-s) shows a notable behaviour change between with and without side-kicks, unlike in the mean vector plots. This suggests

that side-kicks dampen the unsteady vehicle behaviour resulting in better driving on a straight line. Similar behaviour is seen in the configurations with wing and wing with fin. It is interesting to note that in Figure 9 the configuration with anti-diffuser at 250 km/h have only steering torque $\tau_{sw}$ improvement with side-kicks at straight line L1. Similarly, the wing with fin configuration (w-f to w-f-s) has no influences with respect to vehicle response, i.e, lateral acceleration $a_y$ and yaw velocity $\dot{\omega}_z$ at 250 km/h. However, in general the vector plot pattern of configurations without side-kicks to with side-kicks is towards the origin of the graph, showing a reduction in magnitude of all the variables investigated. This is inline with the subjective judgement of an improved drivability.

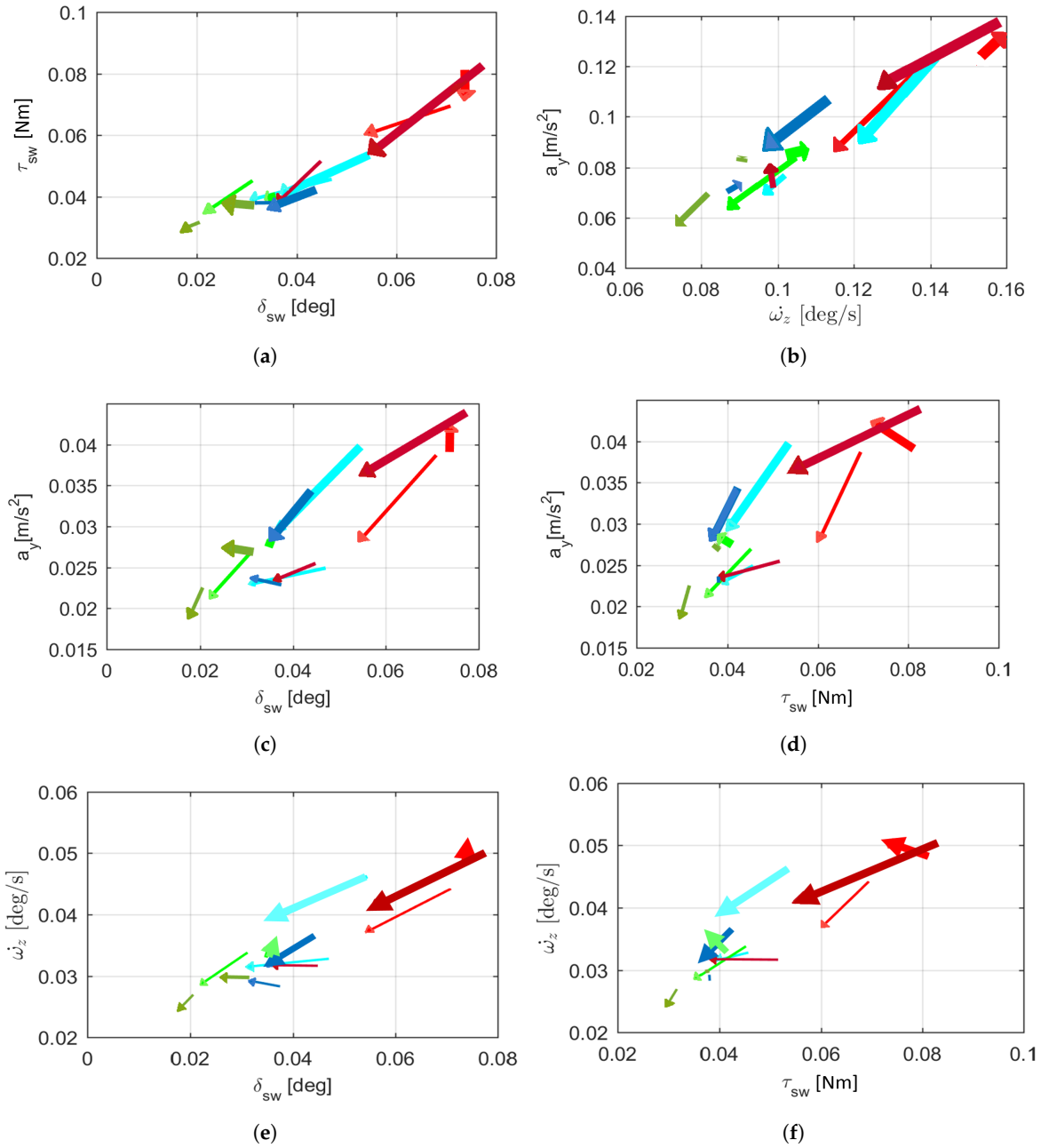


**Figure 9.** Standard deviation vector plots of each straight line L1 & L2 for the different configurations and speeds: (**a**) Steering torque $\tau_{sw}$ vs steering angle $\delta_{sw}$. (**b**) Lateral acceleration $a_y$ vs yaw velocity $\dot{\omega}_z$. (**c**) Lateral acceleration $a_y$ vs steering angle $\delta_{sw}$. (**d**) Lateral acceleration $a_y$ vs steering torque $\tau_{sw}$. (**e**) Yaw velocity $\dot{\omega}_z$ vs steering angle $\delta_{sw}$. (**f**) Yaw velocity $\dot{\omega}_z$ vs steering torque $\tau_{sw}$. Legend same as Figure 8.

#### 4.2.3. Comparison Using Ride Diagram

Figure 10 shows ride diagrams of all configurations using all four variables considered. The graph plots the MS values of the transient part of the signal to the left and the MS values of remaining (stationary) signals to the right. Unfilled markers represent respective configurations without side-kicks and filled markers represent configurations with side-kicks. The sum of MS values of transient and stationary gives the total MS value of the signal. Figure 10a,b show that the contribution of transient nature is larger in the configuration with anti-diffuser compared to other configurations. The steering characteristics, as seen in Figure 10c,d show a larger contribution on the stationary side, especially for wing and wing with fin configurations and the transient contribution is negligible in comparison. This shows the inability to respond to unknown transient behaviours. This is clearer while comparing the steering characteristic, $\tau_{sw}$, of all the configurations in Figure 10d where the wing and wing with fin configurations have significant $\tau_{sw}$ difference between with side-kicks and without side-kicks. Figure 10 showing the simple representation of how the ride diagram is looked into, portraits that the further the MS value is from the origin on the x axis, the lower the standard of drivabilty. The ride diagrams interpreted this way agree with subjective judgement of all configurations.

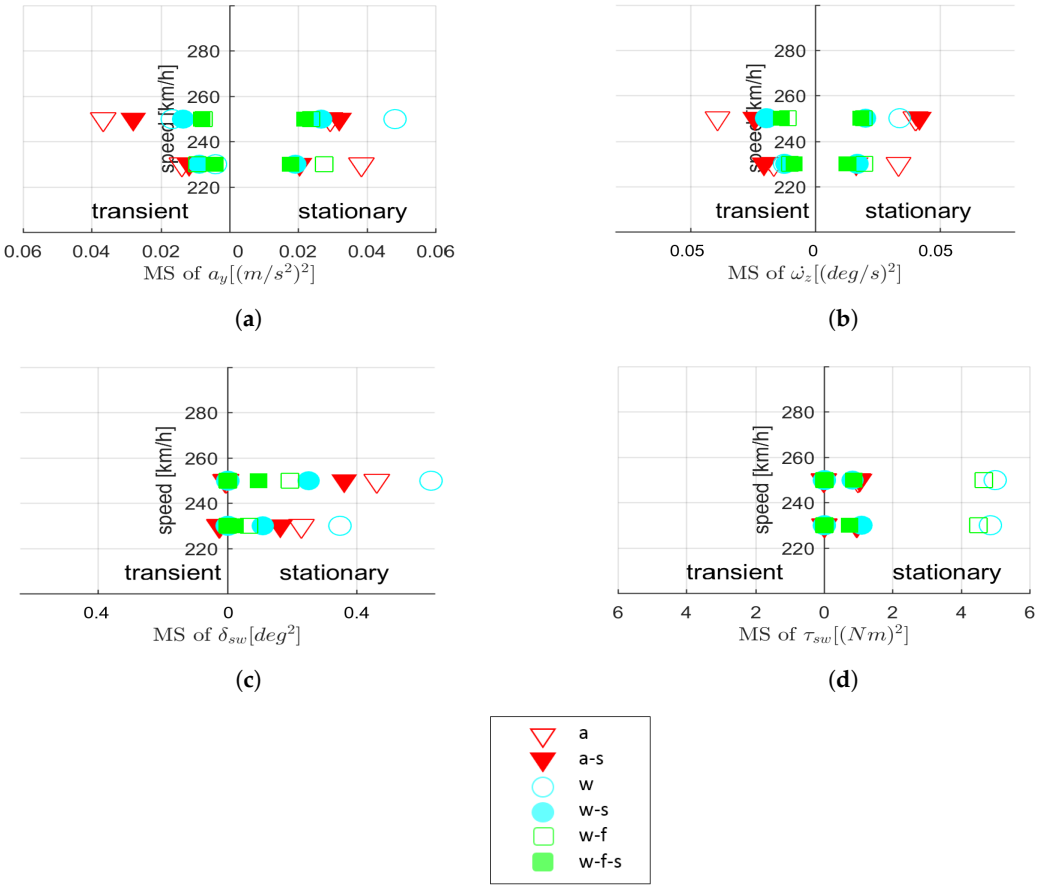


**Figure 10.** Ride diagram of all configurations and selected speeds: (**a**) Lateral acceleration $a_y$. (**b**) Yaw velocity $\dot{\omega}_z$. (**c**) Steering angle $\delta_{sw}$. (**d**) Steering torque $\tau_{sw}$.

This method has some practical issues when the signals have small spikes in them. These spikes can be located in between an otherwise high peak-to-peak value as shown in Figure 11, as from time 26 to 27 s. As a result while separating the signals with the $T_{limit}$ criterion, it only checks for the exact peak-to-peak values between these spike as set by the filtering mechanism. So the possibility is high for a peak-to-peak value, which would otherwise be eligible for being filtered as a transient segment, to not be filtered because of spikes. This can be reduced by downsampling the signals but this does not completely eliminate the problem. The method was originaly used by Strandemar et al. [24] for relatively simple signals for testing in a driving simulator. Hence it needs further development for more realistic signals.

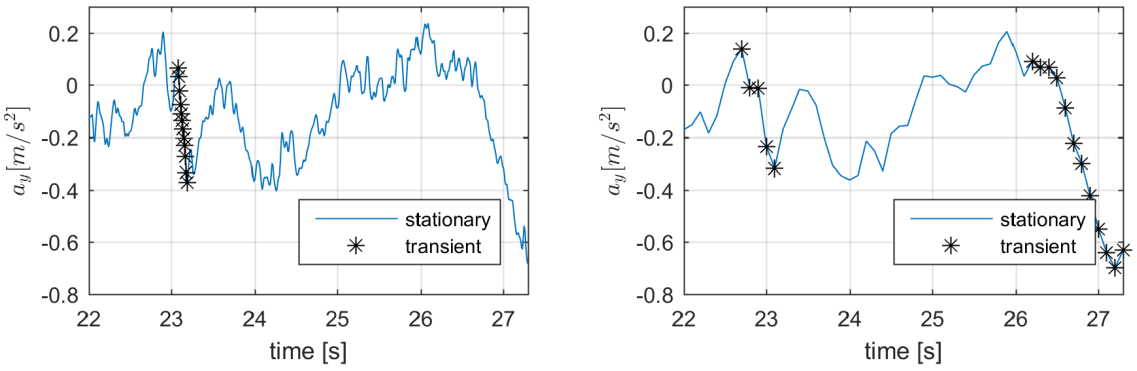


**Figure 11.** Comparison of the ability to separate transient segments in different sample rates: (**a**) Lateral acceleration $a_y$ vs time with a sample rate of 100 Hz. (**b**) Lateral acceleration $a_y$ vs time after downsampling to 10 Hz.

### *4.3. Statistical Analysis*

It has been shown that the use of mean and variance vector plots and Ride diagram matches the driver's subjective judgment on drive quality. But the measurements fall in the error region of for accelerometers and gyroscope. This brings the certainity of observations from the above plots to a grey area especially for lateral acceleration $a_y$ and yaw velocity $\dot{\omega}_z$. This eliminates the possibility of a quantitative analysis. Due to the consistent vector patterns, usually pointing towards the origin, a statistical analysis can support the qualitative evaluation. Cumulative Binomial distribution is used to assess the probability of random creation of such a pattern. The probability of atleast $x$ successes in $n$ trials:

$$p(\geqslant x) = 1 - \sum_{i=0}^{x} \binom{n}{i} P^i (1-P)^{n-i} \tag{12}$$

In this case the null hypothesis is that there is no difference between the configurations, depending on if they have side-kicks or not and that gives the assumption $P = 0.5$. The number of trials $n$ is twelve. With these values taken into account the binomial distribution of the success of each of the four variables at $n$ trials are calculated as shown in Table 1. This shows that the probability for the random vector plots to show similar pattern as that of the results is quite low. In comparison to all the variables considered the probability of such a case in $\dot{\omega}_z$ is the highest with $p_x = 12\%$ which is low but still notable. The null hypothesis can be rejected for $a_y$, $\delta_{sw}$ and $\tau_{sw}$.

**Table 1.** Cumulative Binomial distribution of random success of all variables.

| Variable | $x$ | Probability of Atleast $x$ Success for n Trials |
|---|---|---|
| $a_y$ | 9 | 0.054 |
| $\dot{\omega}_z$ | 8 | 0.12 |
| $\delta_{sw}$ | 11 | 0.003 |
| $\tau_{sw}$ | 11 | 0.003 |

## 5. Conclusions

The objective of this test is to correlate the driver's subjective judgement of drivability with measurable quantities. In this study several aerodynamic configurations are used to create undesired forces and moments: Inverted wing, inverted wing with fin and anti-diffuser. These configurations are tested in pairs with and without side-kicks. The test driver is asked for a subjective evaluation of the test object at high speed straight line driving with these configurations. The main conclusions of this test are the following:

- The configurations with side-kicks show an improvement in straight line drivability compared to the respective ones without side-kicks and it is believed that the reason for this is because of a better defined flow separation with sidekicks. The analysis models presented in this study show a trend that agrees with the subjective judgement of the test driver.
- The vector plots of mean and standard deviation point toward the origin. This implies that the vehicle response and steering efforts to aerodynamic disturbances are reduced with side-kicks, depicting the improved subjective assessment of drivability.
- The study suggests that smaller standard deviation of steering angle, steering torque, yaw velocity and lateral acceleration gives better subjective assessment of drivability at high speed straight-line driving.
- The Ride diagrams show the contribution of transient nature, if any, in these configurations along with the ability to differentiate the pairs on substandard drivability.
- The Ride diagram methodology needs to be further developed in order to capture real signals having spikes which deceive the current filtering mechanism in considering potential transient segments as non-transient.
- The limitation of the accuracy of the sensors used makes it a qualitative analysis with the help of a statistical assessment. In order to quantify drivability in a robust way, more accurate sensors are needed along with more configurations showing even worse drivability and instability conditions.
- Analysis of suspension displacements of all four wheels suggests that the side-kicks achieved improved straight line drivability without notable lift changes within the pair.
- The side-kicks can be used as an aerodynamic device for subjective evaluation while comparing different configurations. To accept side-kicks as a production solution, its influence on drag needs to be investigated using computational fluid dynamic simulations or wind tunnel tests.

**Author Contributions:** Contribution of the authors are as follows: Conceptualization, formal analysis, data curation, investigation and writing—original draft preparation is done by A.K. Methodology is done by A.K. with the support from B.J.H.J. Software: Matlab is used for data analysis by A.K. with the support from E.S. Validation is done by A.K. and E.S. Resources are provided by A.B. and E.S. Writing—review, editing and visualization is done together with S.S., E.S., B.J.H.J. and A.K. Supervision done by S.S., E.S. and A.B. Project administration managed by A.B.

**Funding:** This research was funded by the Swedish Energy Agency and the Strategic Vehicle Research and Innovation Programme (FFI).

**Acknowledgments:** The authors would like to thanks Mats Jonasson from Chalmers University for his help and valuable comments. The authors are also very grateful to the Volvo Cars Hällered Proving Ground, mechanics and instrument support. The author is also grateful to Volvo cars and Hällered Proving Ground vehicle test engineers for their contribution.

**Conflicts of Interest:** The authors declare no conflict of interest. The funders had no role in the design of the study; in the collection, analyses, or interpretation of data; in the writing of the manuscript, or in the decision to publish the results.

## Abbreviations

The following abbreviations are used in this manuscript:

| | |
|---|---|
| IMU | Inertia Measurement Unit |
| MS | Mean Square Value |
| RMS | Root Mean Square Value |
| CAN | Controller Area Network |

## References


1. Park, S.J.; Lee,Y.S.; Nahm, Y.E.; Lee, Y.W.; Kim, J.S. *Seating Physical Characteristics and Subjective Comfort: Design Considerations*; SAE Technical Paper, SAE International: Detroit, MI, USA, 1998.
2. Qunan, H.; Huiyi, W. *Fundamental Study of Jerk: Evaluation of Shift Quality and Ride Comfort*; SAE International Detroit, MI, USA, 2004.
3. Hucho, W.H.; Warrendale, P.A. *Aerodynamics of Road Vehicles*, 4th ed.; Butterworth-Heinemann: Oxford, UK, 2013; ISBN 978-0-7506-1267-8.
4. Huemer, J.; Stickel, T.; Sagan, E.; Schwarz, M.; Wolfgang A.W. Influence of unsteady aerodynamics on driving dynamics of passenger cars. *J. Veh. Syst. Dyn. Int. J. Veh. Mech. Mobil.* **2014**, *52*, 1470–1488. [CrossRef]
5. Carbonne, L.; Winkler, N.; Efraimsson, G. Use of Full Coupling of Aerodynamics and Vehicle Dynamics for Numerical Simulation of the Crosswind Stability of Ground Vehicles. *SAE Int. J. Commer. Veh.* **2016**, *9*, 359–370. [CrossRef]
6. Forbes, D.; Page, G.; Passmore, M.; Gaylard, A. A Fully Coupled, 6 Degree-of-Freedom, Aerodynamic and Vehicle Handling Crosswind Simulation using the DrivAer Model. *SAE Int. J. Passeng. Cars - Mech. Syst.* **2016**, *9*, 710–722. [CrossRef]
7. Juhlin, M. Directional stability of buses under influence of crosswind gusts. *J. Veh. Syst. Dyn. Int. J. Veh. Mech. Mobil.* **2007**, *46*, 827–835. [CrossRef]
8. Fukagawa, T.; Shimokawa, S.; Itakura, E.; Nakatani, H.; Kitahama, K. Modeling of Transient Aerodynamic Forces based on Crosswind Test. *SAE Int. J. Passeng. Cars Mech. Syst.* **2016**, *9*, 572–582. [CrossRef]
9. Schroeck, D.; Krantz, W.; Widdecke, N.; Wiedemann, J. Unsteady Aerodynamic Properties of a Vehicle Model and their Effect on Driver and Vehicle under Side Wind Conditions. *SAE Int. J. Passeng. Cars Mech. Syst.* **2011**, *4*, 108–119. [CrossRef]
10. Isa, I.Y.A.M.; Abidin, M.A.Z.; Mansor, S. Objective Driveability: Integration of Vehicle Behavior and Subjective Feeling into Objective Assessments. *JMES* **2014**, *6*, 782–792. [CrossRef]
11. Klaus, W.; Hoppermans, J.; Kraaijeveld, R. Objective Evaluation of Subjective Driving Impressions. *Soc. Automot. Eng. Jpn.* **2008**.
12. Chandrasekaran, K.; Rao, N.; Palraj, S.; Kurella, C.; Lebbai, M.N. Objective Drivability Evaluation on Compact SUV and Comparison with Subjective Drivability. *Symp. Int. Automot. Technol.* **2017**. [CrossRef]
13. Strandemar, K.; Thorvald, B. The Ride Diagram, A Tool for Analysis of Vehicle Suspension Settings: The Dynamics of Vehicles on Roads and on Tracks. *J. Veh. Syst. Dyn. Int. J. Veh. Mech. Mobil.* **2006**, *44*, 913–920. [CrossRef]
14. Strandemar, K.; Thorvald, B. Driver perception sensitivity to changes in vehicle behavior. *Veh. Syst. Dyn.* **2004**, 272–281.
15. Strandemar, K.; Thorvald, B. Truck Characterizing Through Ride Diagram: In Vehicle Dynamics and Chassis Developments. *Sae Commer. Veh. Eng. Congr.* **2004**. [CrossRef]
16. PM Intrumentation. 2017. Available online: https://pm-instrumentation.com/docpdf/Systemes/embarque-volant/PMI-01184-Volant-telemetrique.pdf (accessed on 15 May 2019).
17. Oettle, N.R.; Sims-Williams, D.; Dominy, R.; Darlington, C.; Freeman, C.; Tindall, P. The Effects of Unsteady On-Road Flow Conditions on Cabin Noise. *SAE Int. J. Passeng. Cars Mech. Syst.* **2011**, *4*, 120–130. [CrossRef]
18. ISO. Mechanical Vibration and Shock: Evaluation of Human Exposure to Whole-Body Vibration. 1997. Available online: https://www.iso.org/standard/7612.html (accessed on 19 May 2019).

19. DEWESoft. Documentation on IMU and GPS. 2019. Available online: https://dewesoft.com/products/interfaces-and-sensors/gps-and-imu-devices (accessed on 20 May 2019).
20. Howell, J.P.; Fuller, J.B. *A Relationship between Lift and Lateral Aerodynamic Characteristics for Passenger Cars*; SAE Technical Paper;SAE International: Detroit, MI, USA, 2010.
21. Heeger, D. Course Notes for Introduction to Perception. Available online: https://www.coursehero.com/sitemap/schools/17-Stanford-University/courses/2113753-PSYCH30/ (accessed on 12 December 2018).
22. Hamilton, J.D. *Time Series Analysis*, 4th ed.; Princeton University Press: Princeton, NJ, USA, 2013; ISBN 978-0-6910-4289-3.
23. Box, G.E.P.; Jenkins, G.M.; Reinsel, G.C. *Time Series Analysis: Forecasting and Control*, 3rd ed.; John Wiley & Sons: New Jersey, NJ, USA, 2008; ISBN 978-1-118-67502-1.
24. Strandemar, K. On Objective Measures for Ride Comfort Evaluation. Ph.D. Thesis, KTH Royal Institute of Technology, Stockholm, Sweden, 2005.

# Paper B

## Prediction of Driver's Subjective Perception and Vehicle Reaction under Aerodynamic Excitations

under review in

Vehicle System Dynamics (since 2021-09-13)

# Prediction of Drivers' Subjective Perception and Vehicle Reaction under Aerodynamic Excitations

Arun Kumar[a,b], Erik Sällström[b], Kaveh Amiri[b], Bengt Jacobson[a] and Simone Sebben[a]

[a]Department of Mechanics and Martime Sciences, Chalmers University of Technology, 412 96 Göteborg, Sweden.
[b]Volvo Cars Corporation, Torslanda SE-405 31 Göteborg, Sweden.

**ARTICLE HISTORY**
Compiled September 10, 2021

**ABSTRACT**
How drivers react to a vehicle's dynamic performance is important to auto manufacturers. Test engineers and test drivers perform several on-road assessments to evaluate the vehicle's dynamic performance before sign-off for production. One such test is a straight-line, high-speed stability test. The presence of external disturbances such as aerodynamic forces and moments created by the flow of air around the vehicle play a significant role in the overall vehicle assessment. As a result, it is important to understand the relation between the subjective experience of the drivers and these external disturbances acting on the vehicle. In this study, a sequence of external disturbances from yaw and roll moments varying in amplitudes and frequencies is added to a straight-line high-speed stability simulation test in the Driving Simulator at the Swedish National Road and Transport Research Institute. The object is to learn which quantities are of importance to measure when studying vehicle stability. The tests are performed with both common and professional test drivers, and their responses to these external disturbances are recorded. The sampled data from these tests are used to generate a regression model predicting the drivers' subjective perception after experiencing induced external disturbances. The outcome also shows a relationship between steering input and driver's sensitivity towards the external disturbances in a straight line drive.

**KEYWORDS**
Subjective Judgement; Stability; Driver vehicle-environment; Driving Simulator; Human vehicle interaction; Drivability; Unsteady aerodynamics; Vehicle stability; Prediction model; Chassis development; Driver perception

## 1. Introduction

Drivers have a bandwidth of sense where they subjectively can rate the vehicle behavior between excellent and unacceptable under different driving scenarios. The impact of external aerodynamic forces and moments on the vehicle during straight line driving is one such scenario. In this scenario, the test engineers can rate the vehicle behavior unacceptable for either of the following reasons; (i), the case of direct instability during certain maneuvers, such as high speed lane changes or high speed braking, or due to

CONTACT Arun Kumar. Email: arun.kumar@volvocars.com

external excitations such as impacts of wind gusts, vehicle heave or pitch due to road indentation [1–6]; (ii), the inability of the vehicle to provide confidence to the driver, such as lack of feel of road contact through steering or unpredictable subtle nervousness induced on the vehicle due to similar excitations as previously discussed [7]. These behaviors are prominent at high speeds as the aerodynamic forces increase with the square of the velocity. In addition, some subtle nervous behavior might or might not affect confidence but causes discomfort over a long driving period as studied by Kumar et al. [7] and Brandt et al. [8]. The impact of complex flow structures on vehicle stability is always challenging as it is not easy to answer how and why they cause instabilities. Okada et al. [9,10] for example, found a coupling of rear lift fluctuations and A-pillar vortex created straight line instabilities.

Several studies have assessed a driver's reaction to external disturbances using driving simulators. Krantz et al. [11] investigated crosswind influence on vehicle dynamics using a driving simulator. The unsteady aerodynamic coefficients relating to crosswind behavior of two different vehicles from wind tunnel tests were added to a single track model. The results of driving simulator tests were used to study and compare the yaw and lateral response with that of on-road tests. The drivers were asked to keep the vehicle in straight line. The crosswind investigated was a transient profile with power spectral density peaking around 2 Hz. The study provided an insight towards the application of a driving simulators in unsteady aerodynamics in early development phase. A paper by Huemer et al. [12] presented the influence of multidimensional vehicle response due to crosswind on driver perception also using a driving simulator. In their work the multidimensional vehicle response consisted of roll velocity, yaw velocity and lateral acceleration. The impact of amplitude changes and phase delays of crosswinds on the vehicle response was also investigated. Aerodynamic yaw moment disturbance showed the highest influence in driving stability followed by side force and roll moment.

Wagner et al. [13] studied the drivers' reactions and judgements on the vehicle behaviors due to the crosswind conditions. The study proposed a criterion called intensification factor (I-factor) that can be used to evaluate the vehicle-driver interaction for random crosswind conditions. It was found that the driver's steering intensity was quite high from 0.5 - 1.5 Hz resulting in intensified vehicle responses, while the driver's ability to compensate for crosswind conditions less than 0.5 Hz was good and above 2 Hz the changes were too fast to respond. Such a conclusion provided an insight in terms of frequency range and driver's response characteristics.

Nguyen et al. [14] investigated a cornering scenario on the German autobahn with vertical disturbances simulating road unevenness and road bumps. The vehicle response was subjectively evaluated and the results included a threshold of sensitivity between impulsive pitch, roll and lateral disturbance over varying road noise intensities. The threshold of yaw acceleration was found to be most sensitive. The road disturbances influenced the sensitivity towards rolling motion. In addition, while coupling yaw and roll vehicle motion, the paper also shows the difference in subjective impression with varying phase delays and amplitude ratio.

The above-mentioned studies provide a background for the present investigation where excitations at varying amplitudes and frequencies are related to subjective judgement of drivers, with the main purpose of understanding what aerodynamic disturbances are of importance. The objective is to create a model from the data recorded from the cockpit that can predict subjective vehicle stability in early vehicle development. This will be achieved through logistic regression with subjective driver response as the dependent variable and independent variables based on linear and rotational

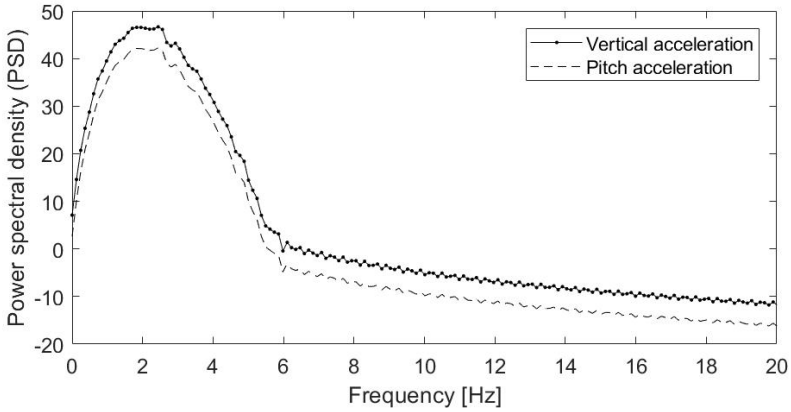


Figure 1. The vertical and pitch road noise frequency spectra simulating the indentations on the road.

accelerations and velocities, and steering behaviour.

## 2. Experimental set-up

### *2.1. Driving simulator and vehicle model*

Driving simulators are effective tools to incorporate the full vehicle characteristics for analysis of combined longitudinal and lateral dynamics such as high-speed stability, crosswind, and primary ride even in early vehicle development [15]. Quality of road and vehicle model, graphics, sound quality and effective motion cueing are the key parameters in providing a realistic driving impression [16].

In the present test, the visual presentation of the driving environment was kept relatively simple. No road indentations were visible. The noise from road indentations was feed as variation of vertical force and pitch moments at the centre of gravity of the vehicle, shown in Figure 1. They were reproduced through vertical and pitch accelerations from Inertia Measurement Unit (IMU) readings from a previous on-road study by Kumar et al. [7]. The vertical noise was generated by filtering a continuous white noise signal to get frequency spectra that matched the vertical and pitch accelerations from on-road data. It was not possible to feed the disturbances on each wheel centre with the available setup and time constrains. Noises in lateral or roll direction were also not considered as incorporating these noises would have been challenging and time consuming. A major challenge would be the ability to co-relate the visual road indentations to the respective vehicle lateral and roll behaviour and drivers' feel to this virtual driving scenario. The coefficients for aerodynamic forces and moments were taken from wind tunnel tests performed earlier and translated to the centre of gravity of the vehicle. The test plan was split into two phases.

#### *2.1.1. Phase I test*

Phase I was a pre-study test conducted with three drivers of average driving skills (termed common drivers) at the Volvo Cars Driving Simulator, Figure 2a. The simulator is a VI-Grade 075 and works with CarRealtime for vehicle dynamics modeling and simulation [17]. The vehicle dynamics model used was built to match with the test

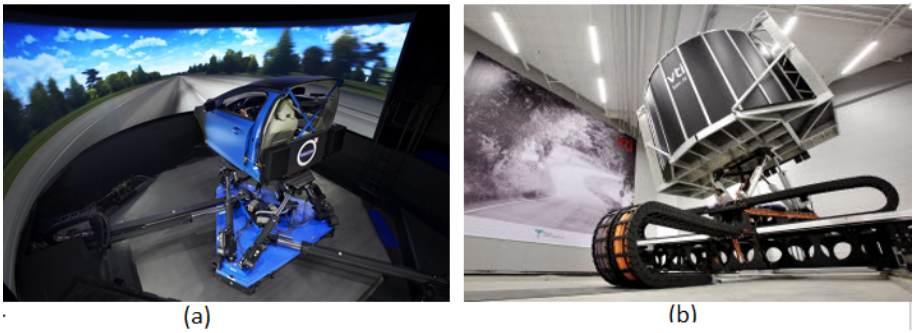


Figure 2. (a) Phase I test using Volvo Cars Driving Simulator [19] (b) Phase II test using VTI SimIV (Photo: Hejdlösa Bilder AB) [18].


Figure 3. Drivers were provided with step-by-step instructions on the screen, visible from cockpit, to ease adaptability.

vehicle. The drivers were asked to loosely keep a straight line simulating a 200 km/h long cruise driving condition on a 3-lane straight road. Before the test, they were informed about the existence of the background road noise. The drivers responded 'felt' or 'felt dangerous' when they experienced a disturbance and when they didn't respond to an induced disturbance, it was categorised as 'didn't feel'. In this phase, the disturbance inputs were either yaw moments or side forces at the centre of gravity of the vehicle. Depending on drivers' response to a disturbance input, the test leader modulated the frequencies and amplitudes of the disturbance input and fed it to the simulator. The results gave a rough estimation of the desired region of interest in terms of amplitudes and frequencies to be used in the phase II tests. Phase II of the experiment was performed in a driving simulator with a larger platform envelop as the area of interest proved to stretch to frequencies as low as 0.25 Hz.

### *2.1.2. Phase II test*

Phase II is the final clinic test of subjective judgement from drivers on the selected disturbances. The VTI (Swedish National Road and Transport Research Institute) driving simulator was used for this study, Figure 2b, [18]. The simulator cabin is mounted on a movable platform though which the system provides the driver with motion feedback. The simulated vehicle behaviour is mapped to a platform movement using a motion cueing algorithm [20]. The moving base consists of linear sled system, providing large linear strokes, and a hexapod is mounted on top of this base. Together, the system is capable of 8 degrees-of-freedom motion. Vip Core is the main software

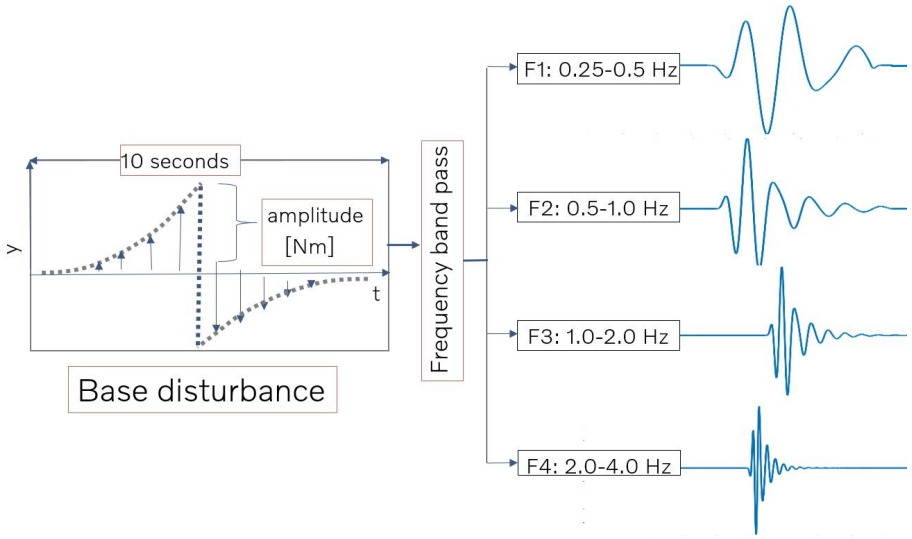


Figure 4. Creating aerodynamic excitation signals of interest from the base disturbance using $8^{th}$ order Butterworth band pass filters.

used to run the vehicle dynamics simulations. Details of the development of this simulator is described by Jansson et al. [21]. The tyre model was a brush tyre model (parabolic pressure distribution) with a carcass stiffness and damping effect appended to the model.

Since phase II tests is conducted in a different driving simulator, the software and vehicle dynamics model were also different and shown in detail in [22,23]. To have a similar vehicle dynamics behaviour to that of phase I, a few selected vehicle maneuvers were simulated using CarRealtime at the Volvo Cars Driving Simulator. The vehicle responses from those simulations were used to tune the vehicle dynamics model at VTI. The input disturbances were roll and yaw moments. The interest in roll disturbance came from some on-road tests conducted after phase I. The clinical test began with a training exercise where the drivers were asked to drive at certain fixed speeds in between cones set in slalom configurations. This was done to get a feeling for the driving simulator, steering and settle oneself comfortably with the test setup. The drivers were then instructed to loosely follow a straight line, simulating a 200 km/h long cruise driving condition on a straight flat road. The drivers were given awareness of the existence of road noise applied to the vehicle. After each disturbance, the drivers were asked to provide their impressions by pressing either of the three buttons on the steering wheel as shown in Figure 3. Each of which represents a feedback as below:

- 0 - I felt nothing
- 1 - I felt the disturbance
- 2 - I felt the disturbance and I can see it's potential of causing straight line instability

Actual motion characteristics felt by the drivers are important to relate the subjective judgements with objective variables. The actual motion felt on the cockpit varies to that found from the simulated vehicle dynamics response output due to motion cueing. As a result, the IMU was mounted on the platform of the cockpit along with the

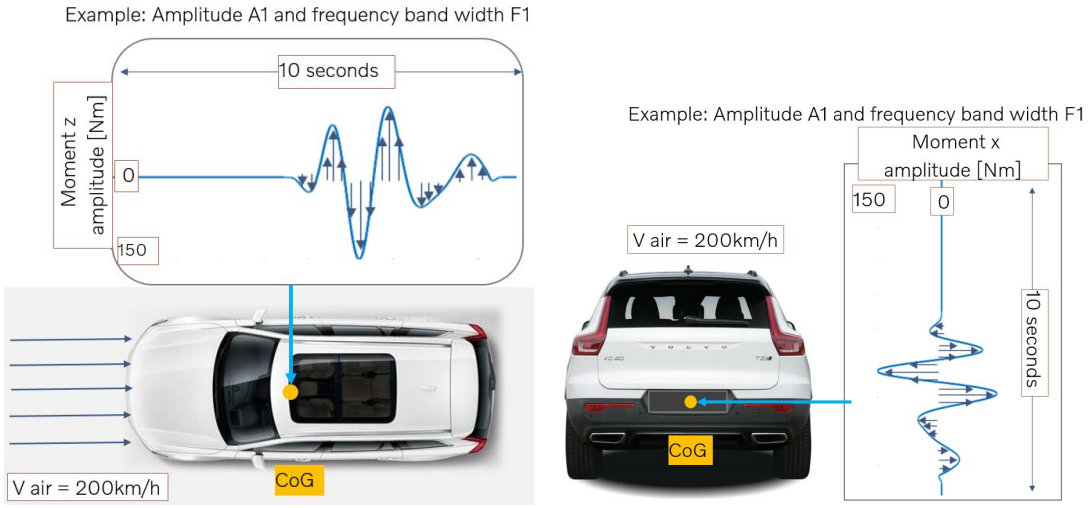


(a) Yaw input representation.

(b) Roll input representation.

Figure 5. Induced yaw or roll moment disturbance representation on a vehicle.

DEWESoft Module for data acquisition [24]. Out of many recorded signals from the IMU, the linear and rotational accelerations and velocities are of interest in this study. The other outputs examined from the simulator include drivers' impressions, steering torque, steering angle and rate of change of steering angle. While post-processing, the signals are low pass filtered with a 10 Hz cut-off frequency and down-sampled to 100 Hz. During analysis of each disturbance the outputs examined are split into two category: outputs received 8 seconds to the actual start of the disturbance signal is considered as 'before the disturbance' and 8 seconds from the actual start of the disturbance signal is considered as 'during the disturbance'.

### *2.2. Disturbances of interest and signals sequencing*

A base disturbance is used to create disturbances of interest. The developed base disturbance is an impulse signal consisting of a ramp up and a sudden switch to the opposite sign and ramping back to zero, as shown in Figure 4. This signal is similar to one of the profiles studied by Brandt et al. [8] and it was chosen because it can provide substantial instability behaviour. The mathematical representation of the base disturbance is shown in Equation 1.

$$\mathsf{y}(t) = \frac{\frac{T}{2} - t}{\left|\frac{T}{2} - t\right|} \cdot \left(1 - \cos\left(\frac{2\pi}{T} \cdot t\right)\right)^{1/2} \text{ for } t \in [0, 10] \tag{1}$$

where, $\mathsf{y}$ is the amplitude at a given time $t$ and T is total signal time.

This base disturbance was passed through $8^{th}$ order Butterworth band pass filter for achieving disturbances consisting of frequency ranges 0.25 - 0.5 Hz (F1), 0.5 - 1.0 Hz (F2), 1.0 - 2.0 Hz (F3) and 2.0 - 4.0 Hz (F4). They were amplified to the four selected peak amplitudes in terms of moments: 150 Nm (A1), 175 Nm (A2), 225 Nm (A3) and 325 Nm (A4). Thus a total of 32 distinct signals exist: 4 frequency range $\times$ 4 amplitudes $\times$ 2 input types (yaw and roll moments). These signals were randomly ordered into 23 unique sequences, so each driver receives a unique sequence. The initial

signal was repeated once, and two other selected signals are repeated for all the drivers to investigate repeatability. The disturbances act in the direction of either yaw or roll moment disturbance as intended, see 5. The symmetry of the base signal will help minimize the effect of the simulator's wash-out filter, especially since the disturbances of interest are of low frequencies. A wash-out filter is usually used by the simulator to slowly bring the platform back to centre during simulation for maximum leverage in performance. It is important to do so with minimum impact on the driver's experience.

### *2.3. Clinical driving test*

The clinical driving test consisted of 23 drivers in total: 13 common drivers and 10 experienced test drivers. Common drivers are predominantly male drivers and either engineers at Volvo Cars or PhD students working with the car industry. While planning the driving span for each driver, it was important to consider driver fatigue. Driver fatigue can be the state of deterioration of mental alertness as discussed by a study of Williamson et al. [25], the transient state between sleep and awake as shown by Lal et al. [26] or psychological and physiological behaviour which when left undisturbed results in poor driver response to a given task, presented by Thiffault et al. [27]. Since this test is a straight-line drive at high speed with the task of keeping the car in lane, the impact of driver fatigue is crucial for subjective response. Awareness decreases and sleepiness increases with prolonged monotonous driving [28,29]. From the summary of the studies stated above, it was decided that an acceptable threshold for an effective subjective judgement from the drivers was a driving period of less than 20 minutes. In this test, a period of 15 minutes per driver was chosen.

The psychological and physiological impact to the drivers' response mentioned above cannot be completely eliminated and are also affected by the time of the test such as early morning or late afternoon, before or after lunch, or frame of mind. The response to a given stimuli is also influenced by the preceding signal stimuli. These biases along with a total of 23 driver and 32 different unique disturbance signals cause difficulties when it comes to representing a small clinical sample for the entire population. Even though the number of drivers is too small to obtain an accurate and statistically representative distribution of responses for each disturbance, other conclusions can be drawn with high statistical significance from the collected data.

A $\chi^2$ test is used to test the independence of responses from the same driver [30]. The null hypothesis is that the first and second response to the same disturbance from the same driver are independent. The two disturbances that were repeated for all drivers were used for this test and the contingency table is shown in Table 1. The p-value is 0.59. Since the p-value is higher than 0.05, the null hypothesis cannot be rejected which indicates that different responses from same driver are not strongly

Table 1. $\chi^2$ test for analysing the independence of the drivers first and second response to repeated signals.

| First response / Second response | didn't feel | at least felt [responded '1' or '2'] |
|---|---|---|
| didn't feel | 15 | 10 |
| at least felt [responded '1' or '2'] | 21 | 21 |

$\chi^2$ test p-value: 0.59.

dependent.

### *2.4. Predictive model*

Logistic regression is used to create a model for predicting the probability of driver responses to induced disturbances. The resulting logistic regression function equation is shown in Equation 2. For the model development the values of objective variables measured in the cockpit are used. Steering angle $\delta_{sw}$, yaw velocity $\omega_z$ and roll velocity $\omega_x$ along with the respective driver's response were chosen from the available variable as they provided the most accurate predictions. The array of standard deviations from the beginning of each disturbance upto 8 seconds of each of these variables are used in Equation 2.

Through a logistic regression model, a relation is built between dependent and independent variables [31,32]. The independent variables (predictor) are all the above-mentioned objective variables together with the category of the drivers, named $DriverType$. The dependent variable is the driver's response in binary format, i.e. 0 for 'did not feel' (driver responded by pressing 0) and 1 for 'at least felt' (driver responded by pressing 1 or 2). The resulting logit function represents a linear relationship of the independent variables using maximum likelihood estimation. In logit, each independent variable is given the best predicted weight so that the prediction is as close to the actual response. The model is optimized by removing independent variables that obtain high p-values (above 0.01).

$$\begin{aligned} p(x) &= \frac{1}{1+\exp(-z(\vec{x}))} \\ z(\vec{x}) &= \beta_0 + \beta_1 x_1 + \beta_2 x_2 + \beta_3 x_3 + \beta_4 x_4 \\ x &= \begin{bmatrix} x_1 & x_2 & x_3 & x_4 \end{bmatrix} \\ &= \begin{bmatrix} \omega_{x,std} & \omega_{z,std} & \delta_{sw,std} & DriverType \end{bmatrix} \end{aligned} \tag{2}$$

where

$p(x)$ is the logistic model that predicts the probability, $p$, of achieving an output equal to 1 for a given set of independent variables $x_{i=1,2,3..}$.

$\beta_0$ is y-intercept,

$\beta_{i=1,2,3..}$ are model parameters of respective independent variables (predictors) $x_{i=1,2,3..}$

## 3. Results and discussion

The results and discussions the two test phases are presented in different sections. It is followed by the drivers' experience and predictive model.

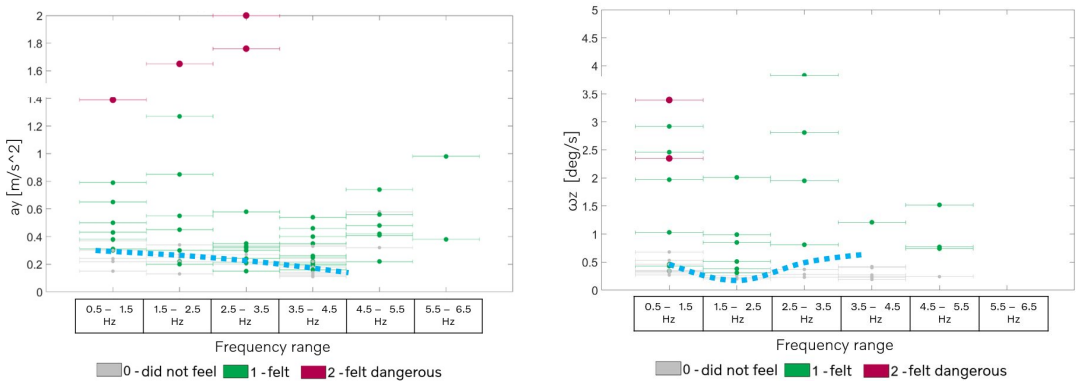


(a) Lateral acceleration (peak-to-peak), $a_{y,p2p}$, over frequency range.

(b) Yaw velocity (peak-to-peak), $\omega_{z,p2p}$, over frequency range.

Figure 6. Drawn rough blue line indicating amplitudes where the drivers start to feel from some phase I tests analysis at the Volvo Cars Driving Simulator.

### *3.1. Phase I analysis*

The data from phase I tests consist of vehicle and drivers' response to side force and yaw moment disturbances fed through trials with varying frequency range and amplitudes. All the trials are plotted in terms of resulting peak-to-peak lateral acceleration, $a_{y,p2p}$ and yaw velocity $\omega_{z,p2p}$, felt in the cockpit. Peak-to-peak is defined here as the difference between the maximum and minimum value of the variable within the chosen time segment. The results show a line of transition in response between 'felt' and 'did not feel' over each frequency range. One such investigation is shown in Figure 6. The blue dashed lines represent a rough transition region between drivers' ability to identify and not identify disturbances. The sample sizes are relatively small in certain frequency ranges; this was because the drivers provided consistent responses of either 'felt' or 'did not feel' to an induced disturbance for the given amplitudes within the first few trials. For lateral acceleration, Figure 6a, the blue dashed line passes through 0.3 m/s$^2$ at 0.5 - 1.5 Hz and decreases as the frequency range increases. While for yaw velocity $\omega_z$, Figure 6b, the line starts from 0.5 deg/s at 0.5 - 1.5 Hz and after a minimum at 1.5 - 2.5 Hz, it rises as the frequency range increases.

### *3.2. Phase II analysis*

A pre-study was done with the simulator with different amplitudes and frequencies to compare what was felt in the cockpit to what was expected to be felt from the online simulation. There were losses in the output from the simulator due to motion cueing. Moreover, from the phase I study the driver sensitivity seems to decline with the increasing frequency. As a result, frequency range of interest in phase II is limited at the upper end to 4 Hz.

#### *3.2.1. Driver response over disturbance input amplitudes and frequency ranges*

Drivers' responses to disturbance input over selected amplitude and frequency ranges are shown in Figure 7. The plot does not include the repeated signals so the number of sample points at each frequency range and amplitude is 13 for common drivers and

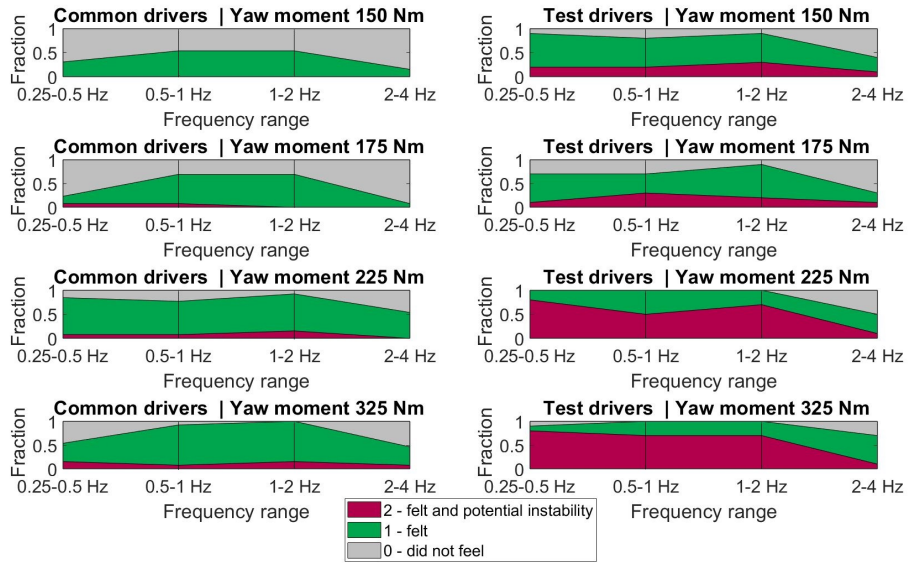


(a) Yaw disturbance input.

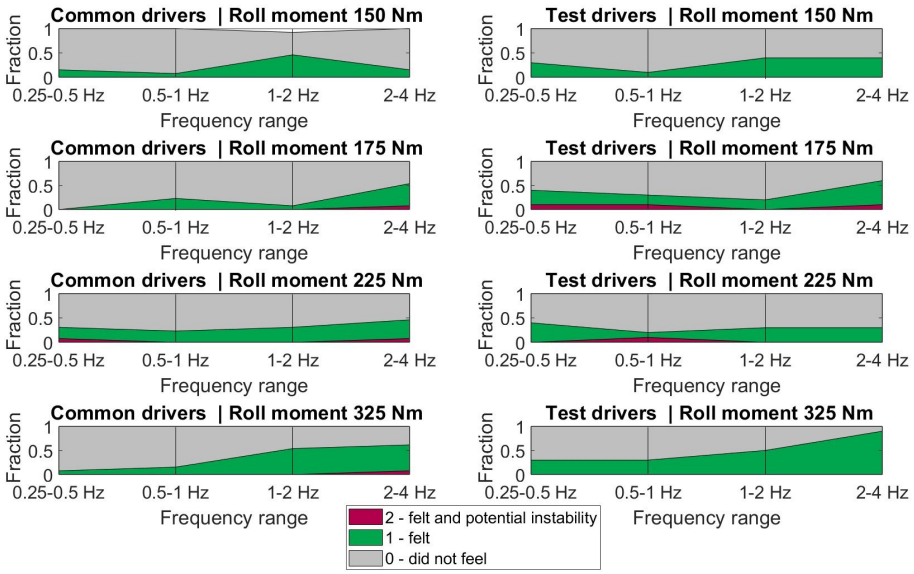


(b) Roll disturbance input.

Figure 7. Stacked fraction of Phase II driver responses for yaw and roll moment disturbance input at different amplitudes and frequency ranges.

Table 2. Fisher's exact test of the response to roll moment disturbances. Null hypothesis: Both types of drivers have same sensitivity towards the disturbance.

| Frequency | Response | Common driver | Test driver | p-value |
|---|---|---|---|---|
| 0.25-0.5 Hz | did not feel | 46 | 26 | |
| | at least felt | 7 | 14 | 0.0227 |
| 0.5-1 Hz | did not feel | 43 | 32 | |
| | at least felt | 10 | 9 | 0.7979 |
| 1-2 Hz | did not feel | 34 | 27 | |
| | at least felt | 19 | 14 | 1 |
| 2-4 Hz | did not feel | 31 | 21 | |
| | at least felt | 24 | 22 | 0.542 |

p-values are high through out the frequency range except frequency $0.25-0.5$ Hz. Null hypothesis can only be rejected in the lowest frequency range.

10 for test drivers. With the increase in amplitude of yaw moment disturbance input, shown in Figure 7a, the responses from test drivers show a clear transition from 1 ('felt') to 2 ('felt the potential towards instability') between the frequency range of 0.25 and 2 Hz. The responses from common drivers show a clear transition from 0 ('did not feel') to 1 ('felt') with increase in amplitude. The number of common drivers who responded 1 peaks between 0.5 to 2 Hz. In the case of the common drivers, the transition from 1 to 2 only trends to begin at higher amplitudes. A generic observation for both test and common drivers is that the number of drivers that were able to observe the yaw disturbances is considerably lower at frequency range 2 to 4 Hz. This frequency range shows a transition in the number of drivers observed from 0 ('did not feel') to 1 ('felt') with increase in amplitude. The figure shows explicitly that the test drivers have a broader frequency span of ability to identify disturbance and lower tolerance towards disturbance amplitude compared to common drivers.

For the roll moment disturbance input, a statistically significant difference between test drivers and common drivers can only be seen around 0.25 to 0.5 Hz while observing Table 2. For both types of drivers only the transition trend from 0 ('not felt') to 1 ('felt') is visible, which increases with higher amplitude and higher frequency range, Figure 7b. A common profile from this figure is that the highest number of drivers that sensed the roll moment disturbance is at frequency range 2 to 4 Hz. This will be further discussed in section 3.2.2.

This analysis is strictly relating the drivers' responses from the input disturbance amplitudes and frequency ranges. The influence of road noise, vehicle reactions to the drivers' actions, drivers' steering intensity and the vehicle response to disturbances affect the subjective judgements of drivers. The vehicle response to a given input disturbance and how it was felt in the cockpit is not linear over frequencies and amplitudes. As a result, depending on the vehicle models chosen, some can be more crosswind sensitive compared to others.

### *3.2.2. Driver response depending on measured variables*

The objective variables measured in the cockpit are steering torque $\tau_{sw}$, lateral acceleration $a_y$, yaw acceleration $\dot{\omega}_z$, roll acceleration $\dot{\omega}_x$, steering rate $\dot{\delta}_{sw}$, yaw velocity $\omega_z$ and roll velocity $\omega_x$. Here the peak-to-peak values and standard deviations used are over an 8 s time segment starting at the beginning of the disturbances.

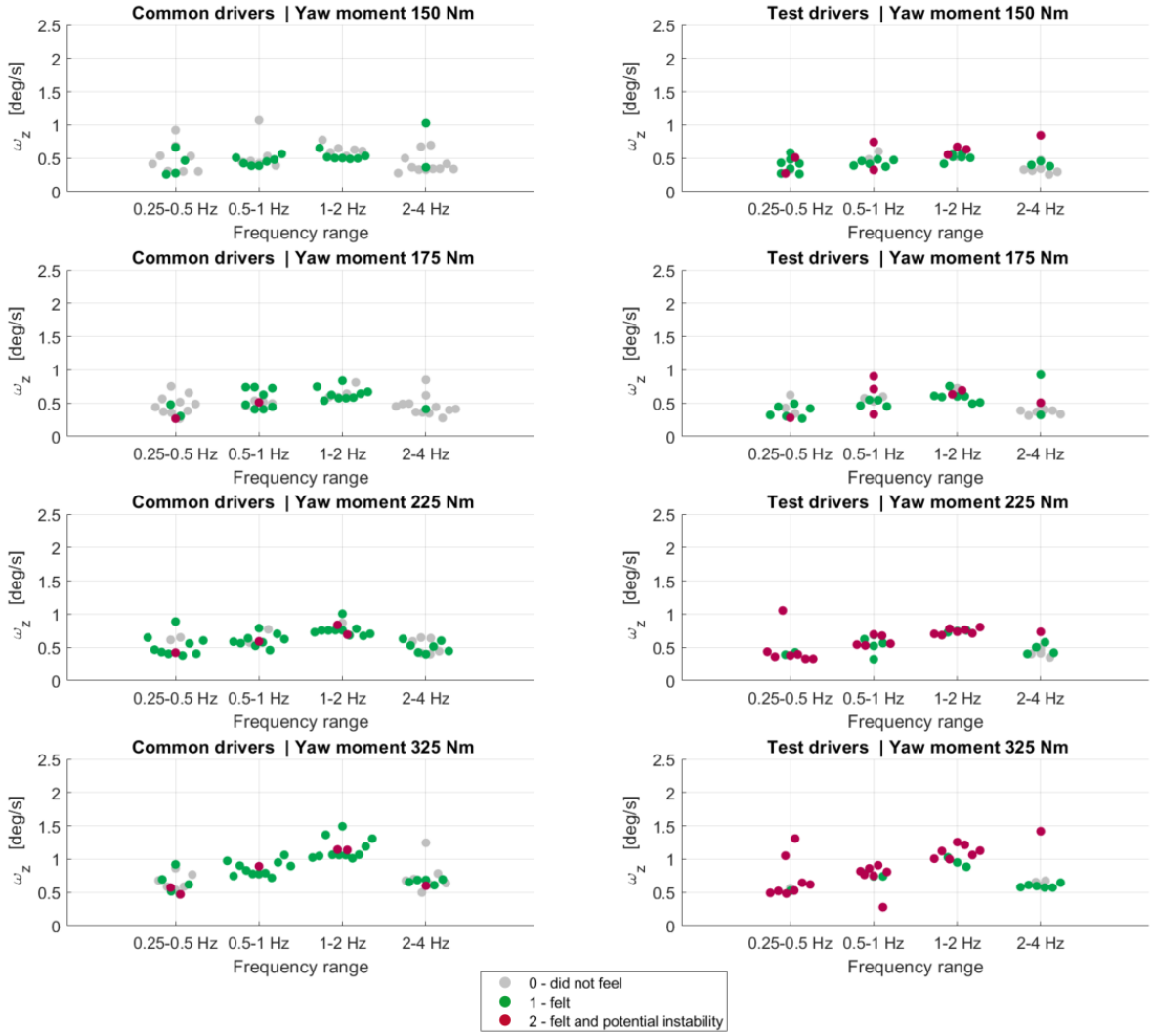


Figure 8. Swarm plot frequency range vs. peak-to-peak yaw velocity $\omega_{z,p2p}$ vs. driver response for different driver type and yaw moment disturbance amplitudes.

*Response to yaw moment input*

Figure 8 shows peak-to-peak yaw velocity, $\omega_{z,p2p}$, and driver responses of the vehicle over the investigated frequency ranges and amplitudes of yaw moment disturbance input. Swarm plotting is used to provide a better understanding of the relationship between quantitative measurements and subjective judgement patterns of the drivers. The yaw velocity responses felt in the cockpit around frequency ranges $0.25 - 0.5$ Hz and $2 - 4$ Hz remain almost unaffected to disturbance amplitude. The test drivers are sensitive across a broader frequency range and are much more likely to identify disturbances especially at the low frequencies, $0.25 - 0.5$ Hz. Their region of sensitivity threshold seems to lie lower than the tested amplitudes. The $\omega_{z,p2p}$ response for the same amplitude disturbance increases with increased frequency up to $1 - 2$ Hz but is then damped significantly by the chassis at $2 - 4$ Hz.

Figure 8 shows that a selected disturbance with a given amplitude results in a distribution in amplitude for $\omega_{z,p2p}$. Hence, because of road noise, driver input and vehicle dynamics, the conditions under which every sample is taken is unique. There is an overlap in measured amplitudes of yaw velocity between different amplitudes of disturbance. This can help explain why there are different responses given to the same input. No explanation relating to difference in driver response can be deduced when considering only peak-to-peak or standard deviation of yaw velocity, $\omega_z$. Since there is a distribution of measured amplitudes from the IMU, rather than distinct points, doing a regression is a suitable move.

Figure 9 shows the peak-to-peak steering torque, $\tau_{sw,p2p}$, feedback from the drivers before and during the yaw moment disturbances. The steering input is significantly lower for test drivers than common drivers while driving on a straight line, as shown in Table 3. However, the steering intensity right before and during the disturbances are not significantly different, regardless of driver type. As will be shown using logistic regression in Section 3.3, the steering feedback and vehicle dynamics are coupled. For the common drivers, the higher inputs from steering might create an anticipated vehicle behaviour making them less sensitive to induced disturbances. This could be one possible explanation for their lower ability to identify the induced external disturbance especially at low amplitudes. On an additional note, the pattern for peak-to-peak steering rate, $\dot{\delta}_{sw,p2p}$, feedback is similar to Figure 9.

Table 3. Paired sample $t$-test used for analysing the influence of driver type and the presence of induced yaw disturbance on $\tau_{sw,p2p}$.

| | | Common driver | Test driver | p-value |
|---|---|---|---|---|
| | no. of observations | 241 | 148 | |
| Before disturbance | mean value | 1.623 | 1.316 | |
| | standard deviation | 0.609 | 0.424 | $1.29 \cdot 10^{-7}$ |
| During disturbance | mean value | 1.692 | 1.377 | |
| | standard deviation | 0.581 | 0.373 | $7.81 \cdot 10^{-9}$ |
| p-value | | 0.20 | 0.19 | |

Case 1 Null hypothesis: the steering behaviour doesn't have association with the type of driver irrespective of the presence of any yaw moment disturbance.
Result: p-values lower than 0.02 implies that there is significant difference in steering feedback between test drivers and common drivers
Case 2 Null hypothesis: the steering behaviour during disturbance doesn't have association with before and during the yaw moment disturbance for both types of drivers.
Result: p-values higher than 0.02 implies that the test fails to reject null hypothesis.

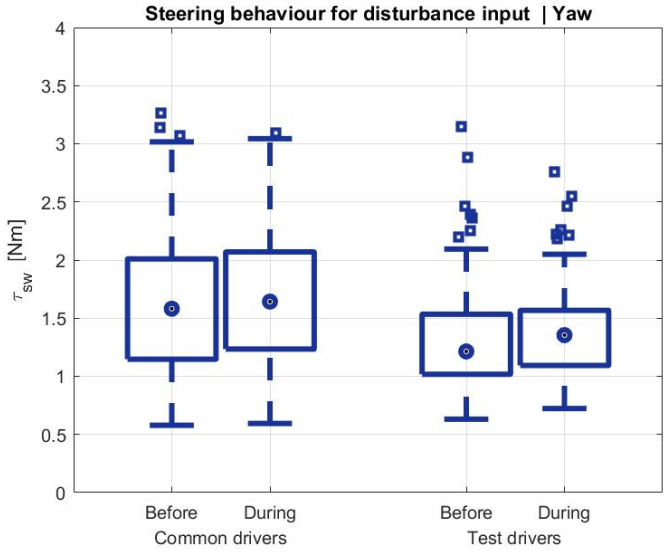


Figure 9. Peak-to-peak steering torque, $\tau_{sw,p2p}$, before and during the yaw moment disturbance input. Box = $25-75\%$ of the sampled data, circle = median, square = outliers

*Response to roll moment input*

Nguyen et al. [14] showed that the ability to discriminate the roll disturbance over the intensity of road disturbances is low. This is because the roll impulse generated is masked by the roll motion caused by inputting the vertical road indentations on each suspension. Here, the real road indentations are fed on the centre of gravity of the vehicle, hence, they are represented in terms of vertical and pitch accelerations. This removes the possibility of masking of roll disturbance response of the vehicle over roll due to road noise. As a result it should be earlier for drivers to notice the roll moment disturbances. However, the results suggest that the drivers are still less likely to observe the roll disturbance than yaw disturbance, which is in line with Huemer et al [12] and Nguyen et al. [14].

The peak-to-peak roll velocity, $\omega_{x,p2p}$, is about 0.35 deg/s at the lowest frequency range, $0.25-0.5$ Hz, regardless of driver type and amplitude as shown in Figure 10. At higher frequencies $\omega_x$ response increases and amplitude gets higher in response to higher disturbance amplitude. The influence of damping of roll moment input by the vehicle dynamics plays a significant role in interpreting and reading the results. The vehicle is more sensitive in the $2-4$ Hz range which contains an eigenfrequency of the vehicle chassis. When comparing other frequency ranges, same input amplitude results in higher measured $\omega_{x,p2p}$. This behaviour is in contrast to yaw disturbance where the measured $\omega_{z,p2p}$ drops of at $2-4$ Hz.

The steering torque $\tau_{sw,p2p}$, feedback by test and common drivers before and during the induced roll moment disturbance is shown in Figure 11. Table 4 shows that the test drivers have significantly lower steering input before and during the disturbance than common drivers. A lot of steering is seen before the disturbances

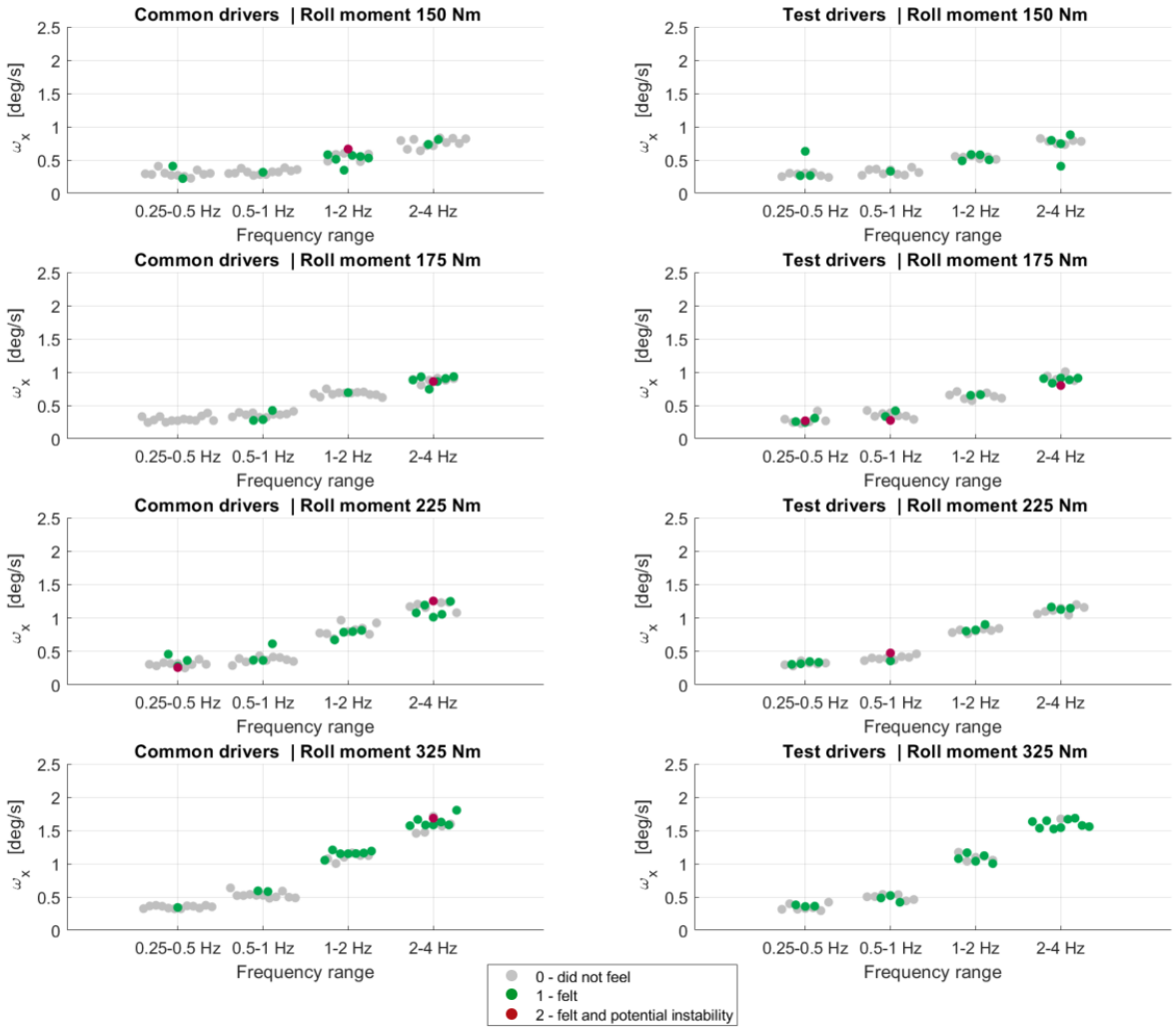


Figure 10. Swarm plot of driver response to roll moment disturbance input. Peak-to-peak roll velocity $\omega_{x,p2p}$ deg/s vs frequency diagrams.

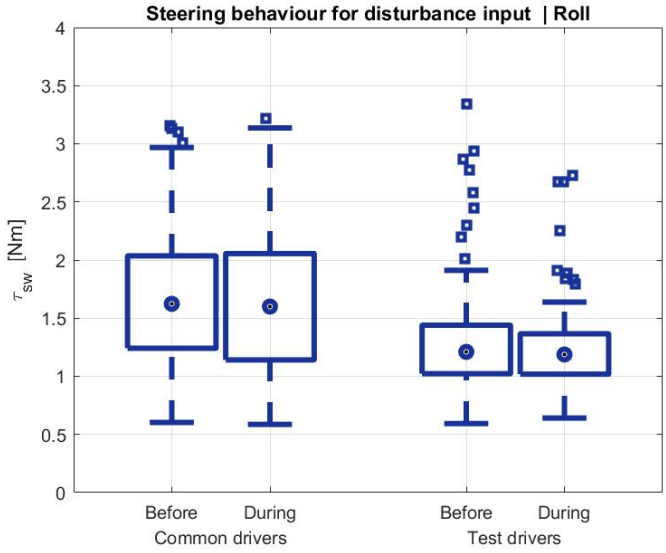


Figure 11. Peak-to-peak steering torque, $\tau_{sw,p2p}$, characteristics of the drivers before and during the roll moment disturbance input. Box = $25-75\%$ of the sampled data, circle = median, square = outliers

and they have nothing to do with the disturbances. As an additional note, just like from the observation in yaw moment disturbance, the pattern for peak-to-peak steering rate, $\dot{\delta}_{sw,p2p}$, feedback for roll moment disturbance is also similar.

Table 4. Paired sample t-test used for analysing the influence of type of driver on peak-to-peak $\tau_{sw,p2p}$ before and during the disturbance.

| | | Common driver | Test driver | p-value |
|---|---|---|---|---|
| Before disturbance | mean value | 1.66 | 1.309 | |
| | standard deviation | 0.574 | 0.458 | $7.12 \cdot 10^{-9}$ |
| During disturbance | mean value | 1.631 | 1.256 | |
| | standard deviation | 0.596 | 0.35 | $2.12 \cdot 10^{-10}$ |
| p-value | | 0.61 | 0.29 | |
| | no. of observations | 214 | 132 | |

Case 1 Null hypothesis: the steering behaviour doesn't have association with the type of driver irrespective of the presence of any roll moment disturbance.
Result: p-values lower than 0.02 implies that there is significant difference in steering feedback between test drivers and common drivers
Case 2 Null hypothesis: the steering behaviour during disturbance doesn't have association with before and during the roll moment disturbance for both types of drivers.
Result: p-values higher than 0.02 implies that the test fails to reject null hypothesis.

### *3.2.3. Drivers test experience*

For the disturbance profiles studied in this paper, after each test, oral feedback from the drivers was noted to understand their perception and experiences during the test. And some common traits can be concluded from the acquired data.

It is a common observation from the phase I study that low frequency and higher amplitude side forces and yaw moments give the drivers an impression of po-

tential instabilities since they need significant post-corrections. Furthermore, at low amplitudes such disturbances can cause the vehicle to drift unnoticed for a relatively long time if one isn't concentrated enough. Drivers are highly prone to occasionally loosing concentration during long straight-line cruising. The vehicle's behaviours at higher frequency yaw moments or side forces might feel unacceptable but not dangerous. This is because the disturbance profiles are more or less symmetric and since the disturbance amplitudes were fairly small the drivers got the intuition of the vehicle being stable and stay in line by itself.

In phase II, the test drivers notice low frequency range yaw moment disturbances as potential instabilities even at low amplitudes. A similar observation to that from phase I. As seen in Figure 7a, most of the disturbances felt are marked '2' by test engineers since their subjective tolerance towards such disturbances are low. The reason for such an intuition is that the vehicle behaviour on such yaw disturbance inputs are uncontrolled slow drifting or swaying which results in a floating feel. A floating feel is never a good quality vehicle dynamic since it does not feel planted on road and provides a lack of confidence for the driver as they feel disconnected with the road. The disturbance continues for a long time hence the intuition of vehicle correction will go wrong since the disturbance and the driver feedback keeps playing simultaneously with an effective phase lag and late corrections. Low frequency flow behaviours exist in vehicles even without external gusts. Whether or not one can notice their influence or intensities on vehicle dynamics coupling depends on the vehicle design and driving expertise. At higher frequency ranges, keeping the same amplitude, the feeling is less alarming since the disturbance input and its reaction is quite fast and gives the test drivers understanding of the disturbance profile. Moreover, higher frequency range of $2-4$ Hz disturbances are short and damped making the drivers less responsive.

### *3.3. Predictive model*

The predictive model is developed from both roll and yaw moment disturbances output. After optimizing, the relevant independent variables (predictors) with significant influence, p-values $< 0.001$, are chosen. They are driver type and standard deviations of steering angle $\delta_{sw,std}$, yaw velocity $\omega_{z,std}$ and roll velocity $\omega_{x,std}$. For driver type, named $DriverType$, value 1 and 2 are assigned to represent common drivers and test drivers, respectively. The standard deviations of these predictors from the beginning of the disturbance and 8 seconds onwards is used.
The resulting $z$ is:

$$z = \beta_0 + \beta_1\ \omega_{x,std} + \beta_2\ \omega_{z,std} + \beta_3\ \delta_{sw,std} + \beta_4\ DriverType \tag{3}$$

The resulting logistic regression over $z$ is plotted as shown in Figure 12 and coefficient properties are shown in Table 5. It has 71% accuracy with 60% accuracy to predict

Table 5. Resulting properties of model parameters

| | values | unit | 95% confidence interval | p-value |
|---|---|---|---|---|
| $\beta_0$ | -3.71 | [-] | -4.70 to -2.71 | $0.23 \cdot 10^{-12}$ |
| $\beta_1$ | 9.86 | [s/deg] | 3.99 to 15.72 | $0.98 \cdot 10^{-3}$ |
| $\beta_2$ | 58.26 | [s/deg] | 47.19 to 69.34 | $0.61 \cdot 10^{-24}$ |
| $\beta_3$ | - 419.42 | [1/deg] | - 508.88 to -329.96 | $0.39 \cdot 10^{-19}$ |
| $\beta_4$ | 0.93 | [-] | 0.55 to 1.31 | $0.14 \cdot 10^{-5}$ |

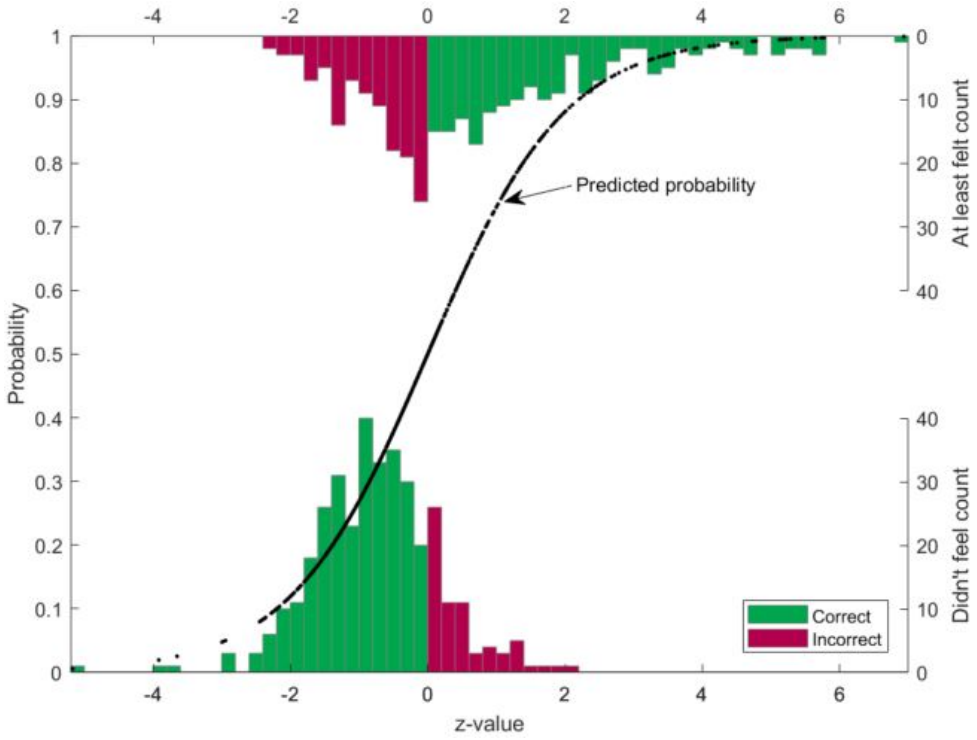


Figure 12. Logistic regression plot over $z$. Histogram plot represents the count of 'at least felt' and 'did not feel'.

'at least felt' and 81% accuracy to predict 'did not feel'. The accuracy and statistical significance can be improved with more tests and resulting data. In the figure, the black dotted curve represents the sigmoidal function. It portraits the predicted probability for 'at least felt' outcome for a given $z$ being the logit value of a given set of values of the selected independent variables.

To understand the influence of each independent variable (predictor) on predicting 'at least felt', the chosen independent variable (predictor) is varied between two standard deviations from its mean standard deviation value and remaining predictors are kept at their mean standard deviation values from all observations. The outcome is compared between the test and common drivers. Figure 13 shows the results. It is clear that the test drivers are more sensitive as their predicted probability tend to move towards 'at least felt' before common drivers.

In Figure 13, steering angle, $\delta_{sw,std}$, suggests that the common drivers are more prone to be oblivious towards disturbances in the presence of more steering fluctuations for a given fixed mean $\omega_{z,std}$ and $\omega_{x,std}$. With an increase in standard deviation of $\omega_{z,std}$ from 0.04 to 0.11 deg/s the probability for identifying a disturbance is raised from around 18 to 90% for the test drivers. While for $\omega_{x,std}$, a raise in standard deviation from 0.04 to around 0.1 deg/s the probability for identifying a disturbance is raised from 55 to 65% for the test drivers. This suggests that at almost negligible roll velocities input there is still a small probability for identifying the disturbance due to presence of mean $\omega_{z,std}$, and $\delta_{sw,std}$ fluctuations. It is clear that the probability is quite sensitive in terms of amplitude fluctuation for yaw velocity, $\omega_z$, provided the steering fluctuation is minimal.

In terms of influence from frequency range, taking previous observations, the

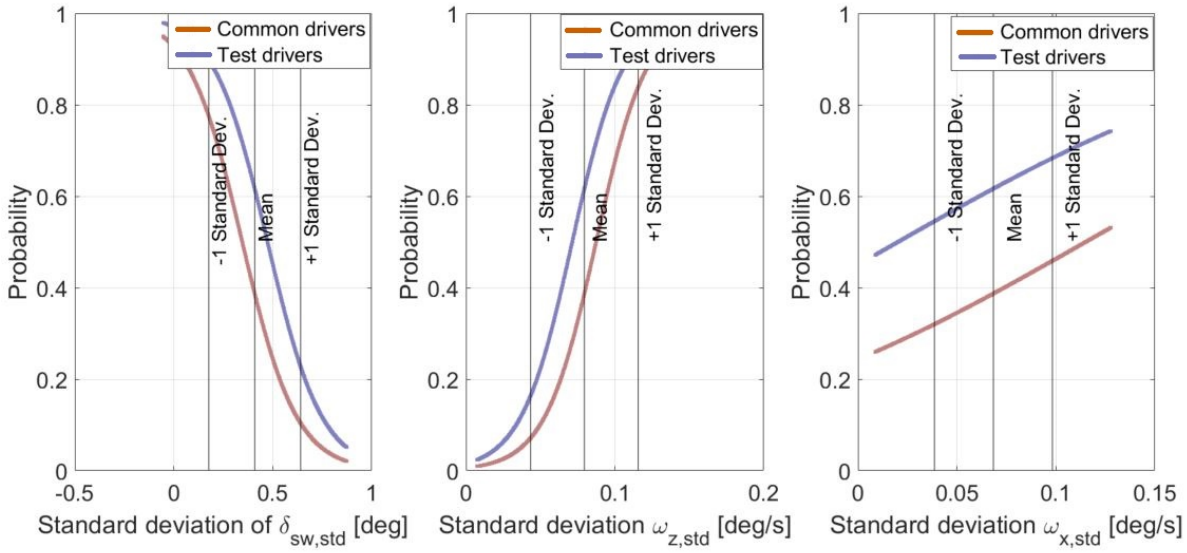


Figure 13. Influence of one independent variable on prediction while remaining variables are kept constant at their mean of standard deviation values from all observations.

drivers are most sensitive to yaw disturbances in the frequency range $0.25 - 2$ Hz and in case of roll moment disturbances frequency range of $2 - 4$ Hz shows higher driver sensitivity.

## 4. Conclusion

It is desirable for vehicle manufactures to be able to identify possible nervous or instable vehicle behavior in the early design and development phase. The costs of finding problems and proposing solutions at late phases, during on-road tests, are extremely undesirable. One potential reason for such behaviours is the coupling between unsteady aerodynamics and vehicle dynamics. In this work, drivers' subjective perceptions under external aerodynamic yaw and roll disturbances of varying amplitudes and frequencies on a straight-line high-speed stability condition is studied with the help of a driving simulator. The main findings from this test are:

- Drivers are much more sensitive to yaw disturbances than roll disturbances. The reason is most likely that roll disturbances do not significantly affect the direction of travel.
- The test drivers are more sensitive than common drivers to yaw disturbances at all tested frequency intervals. The difference is greatest at the lowest frequency interval, $0.25 - 0.5$ Hz, where common drivers are much less sensitive. This suggests that test drivers' sensitivity is so high that their threshold for sensing yaw disturbances is lower than the tested amplitudes.
- In this study, the steering input is not much larger during the disturbances com-

pared to before the disturbances, i.e., the greater steering input is not necessarily a result of the disturbances.
- The driver sensitivity decreases significantly with steering input and that explains a large part of the difference in sensitivity between the two driver types. The test drivers steer less than common drivers on the straight line drive. According to logistical model, even when correcting for the larger steering input from common drivers, professional test drivers are still more sensitive.

From the data, a model was created for predicting which disturbances drivers can feel. The model quantifies the difference in sensitivity between driver types and the difference in sensitivity to yaw and roll disturbances. It can also be used to set a threshold below which disturbances can be ignored when searching for problematic disturbances.

The results obtained from these tests provide a map of reference for assessing and investigating flow behaviour of frequencies and intensities that could result in disturbances in the form of either vehicle nervousness or instabilities. More data collection should be either with a greater and better adjusted range in amplitude or of other components of disturbance. The results from this study will be used for analyzing data from wind tunnel and on road tests to identify potentially problematic unstable aerodynamic behavior.

## Abbreviations

VTI Statnes Väg- och Transportforskninginstitut
(Swedish National Road and Transport Research Institute)
IMU Inertia Measurement Unit


## Acknowledgement(s)

The authors would like to thank VTI for their support and valuable comments to this work. The authors are also very grateful to the Volvo Cars Driving Simulator Group, vehicle test engineers and fellow drivers for their contribution. Special thanks to VI grade for providing support and resources to work on CarReal Time.


## Disclosure statement

The authors declare no conflict of interest. The funders had no role in the design of the study; in the collection, analyses, or interpretation of data; in the writing of the manuscript, or in the decision to publish the results.


## Funding

This research was funded by the Swedish Energy Agency and the Strategic Vehicle Research and Innovation Programme (FFI). Dnr 2015-004986 Projektnr 41038-1

## Notes on contributor(s)

Contribution of the authors are as follows:
Conceptualization, data aqcuration, preliminary analysis and writing main draft is done by Kumar, A. Predictive model development and secondary analysis is done by Sällström., E. and Kumar, A.
Supervision done by Sällström, E., Amiri, K., Jacobson, B.J.H. and Sebben, S.
Test preparation, methodology and validation is done by Kumar, A..
Software: Matlab is used for data analysis by Kumar, A.. with the support from Sällström, E.
Writing-revise, editing and visualization is done by Sällström, E., Amiri, K., Jacobson, B.J.H., Sebben, S. and Kumar, A..

## Nomenclature

| | |
|---|---|
| $a_y$ | Lateral acceleration [m/s$^2$] |
| $a_{y,p2p}$ | Peak-to-peak value of Lateral acceleration [m/s$^2$] |
| $\dot{\omega}_x$ | Roll acceleration [deg/s$^2$] |
| $\omega_x$ | Roll velocity [deg/s] |
| $\omega_{x,p2p}$ | Peak-to-peak value of Roll velocity [deg/s] |
| $\omega_{x,std}$ | Standard deviation value of Roll velocity [deg/s] |
| $\dot{\omega}_z$ | Yaw acceleration [deg/s$^2$] |
| $\omega_z$ | Yaw velocity [deg/s] |
| $\omega_{z,p2p}$ | Peak-to-peak value of Yaw velocity [deg/s] |
| $\omega_{z,std}$ | Standard deviation value of Yaw velocity [deg/s] |
| $\delta_{sw,std}$ | Standard deviation value of Steering angle [deg] |
| $\delta_{sw}$ | Steering angle [deg] |
| $\dot{\delta}_{sw,p2p}$ | Peak-to-peak value of Steering rate [deg/s] |
| $\dot{\delta}_{sw}$ | Steering rate [deg/s] |
| $\tau_{sw,p2p}$ | Peak-to-peak value of Steering torque [Nm] |
| $\tau_{sw}$ | Steering torque [Nm] |

## References


[1] Baker CJ, Reynolds S. Wind-induced accidents of road vehicles. Accident Analysis & Prevention. 1992. p. 559-575 vol.24 no 6. doi 10.1016/0001-4575(92)90009-8.

[2] Macadam CC, Sayers MW, Pointer JD, Gleason M. Crosswind Sensitivity of Passenger Cars and the Influence of Chassis and Aerodynamic Properties on Driver Preferences. Vehicle System Dynamics. 1990. p. 201-236 vol.19 no 4. doi 10.1080/00423119008968942.

[3] Howell J, Panigrahi S. Aerodynamic Side Forces on Passenger Cars at Yaw. SAE World Congress and Exhibition. 2016. doi 10.4271/2016-01-1620.

[4] Theissen P. Unsteady Vehicle Aerodynamics in Gusty Crosswind. PhD thesis, Technical University of Munich; 2012. http://mediatum.ub.tum.de/doc/1096026/520174.pdf.

[5] Hucho WH. Aerodynamics of Road Vehicles. SAE International. 1998. vol.4. ISBN 978-0768000290.

[6] Willumeit HP, Müller K, Dödlbacher G, Matheis A. Method to correlate vehicular behaviour and driver's judgement under side wind disturbance.Vehicle System Dynamics, 17:sup1, 508-524, doi 10.1080/00423118808969292.

[7] Kumar A, Sebben S, Sällström E, Jacobson BJH, Broniewicz A. Analysis of Subjective

Qualitative Judgement of Passenger Vehicle High Speed Drivability due to Aerodynamics. Energies. 2019. 2839 vol.12 no 14. https://www.mdpi.com/1996-1073/12/14/2839.

[8] Brandt A, Sebben S, Jacobson B, Preihs E, Johansson I. Quantitative High Speed Stability Assessment of a Sports Utility Vehicle and Classification of Wind Gust Profiles. WCX SAE World Congress Experience; 2020. doi 10.4271/2020-01-0677.

[9] Yoshihiro O, Takahide N, Takaki N, Satoshi O. Flow Structures above the Trunk Deck of Sedan-Type Vehicles and Their Influence on High-Speed Vehicle Stability 1st Report: On-Road and Wind-Tunnel Studies on Unsteady Flow Characteristics that Stabilize Vehicle Behavior. SAE International Journal of Passenger Cars - Mechanical Systems. 2009. p. 138-156. doi 10.4271/2009-01-0004.

[10] Takuji N, Makoto T, Takahide N, Takaki N, Masashi I. Flow Structures above the Trunk Deck of Sedan-Type Vehicles and Their Influence on High-Speed Vehicle Stability 2nd Report: Numerical Investigation on Simplified Vehicle Models using Large-Eddy Simulation. SAE International Journal of Passenger Cars - Mechanical Systems. 2009. p. 157–167. doi 10.4271/2009-01-0006.

[11] Krantz W, Pitz JO, Stoll D, Nguyen M.T. Simulation des Fahrens unter instationärem Seitenwind. Automobiltechnische Zeitschrift. 2014. p. 64-68 v116. doi 10.1007/s35148-014-0046-6.

[12] Huemer J, Stickel T, Sagan E, Schwarz M, Wolfgang AW. Influence of unsteady aerodynamics on driving dynamics of passenger cars. Vehicle System Dynamics. Vol. 52, No. 11. p. 1470-1488. doi 10.1080/00423114.2014.944191.

[13] Wagner A, Wiedemann J. Crosswind Behavior in the Driver's Perspective. SAE 2002 World Congress & Exhibition. SAE International. mar. 2002. https://doi.org/10.4271/2002-01-0086.

[14] Nguyen M, Pitz J, Krantz W, Neubeck J, Wiedemann J. Subjective Perception and Evaluation of Driving Dynamics in the Virtual Test Drive. SAE International Journal of Vehicle Dynamics, Stability, and NVH. 2017. p. 247–252 vol.1 no 2. doi 10.4271/2017-01-1564.

[15] Heiderich M, Friedrich T, Nguyen MT. New approach for improvement of vehicle performance by using a simulation-based optimization and evaluation method. $7^{th}$ International Munich Chassis Symposium, ATZ, Munich. 2016. doi https://10.1007/978-3-658-14219-3-21.

[16] Fainello M, Ferrari SpA - Diego Minen, VI-grade. Active vehicle ride and handling development by using integrated SIL / HIL techniques in a highperformance driving simulator. 5th International Munich Chassis Symposium; 2014. p. 185-200. doi 10.1007/978-3-658-14219-321.

[17] VI-Grade. https://www.vi-grade.com/en/products/dim-dynamic-simulator/s. accessed on 20 April 2021.

[18] VTI https://www.vti.se/en/research/vehicle-technology-and-driving-simulation/driving-simulation/simulator-facilities. accessed on 20 April 2021.

[19] Volvo Cars. https://www.media.volvocars.com/se/sv-se/media/pressreleases/167927/volvo-cars-anvander-varldens-mest-avancerade-chassisimulator-for-att-utveckla-nasta-generation-bilar. accessed on 20 April 2021.

[20] Kusachov A. Motion Perception and Tire Models for Winter Conditions in Driving Simulators. Thesis of Licentiate, Chalmers University; 2016. https://publications.lib.chalmers.se/records/fulltext/245616/245616.pdf

[21] Jansson J, Sandin J, Augusto B, Fischer M, Blissing B, Källgren L. Design and Performance of the VTI Sim IV. Driving Simulation Conference Paris; 2014. September 4-5. France.

[22] Bruzelius F, Gomez FJ, Augusto B. A Basic Vehicle Dynamics Model for Driving Simulators. International Journal of Vehicle Systems Modelling and Testing, Vol. 8, No. 4, p. 364-385, 2013.

[23] Obialero E. A Refined Vehicle Dynamic Model for Driving Simulators. Master's Thesis. Chalmers University of Technology.

[24] DEWESoft. Documentation on IMU and GPS. 2019. Available online: https://dewesoft.com/products/ interfaces-and-sensors/gps-and-imu-devices. accessed on 20 May 2021.
[25] Williamson AM, Feyer AM, Friswell R. The impact of work practices on fatigue in long distance truck drivers. Accid. Anal. Prev.. 1996. p. 709-719 v26 no 28. doi 10.1016/s0001-4575(96)00044-9.
[26] Lal SKL, Craig A. A critical review of the psychophysiology of driver fatigue. Biol. Psychol.. 2001. p. 173–194 vol.3 no 55. doi 10.1016/s0001-4575(02)00014-3.
[27] Thiffault P, Bergeron J. Monotony of road environment and driver fatigue: A simulator study. Accid. Anal. Prev.. 2003. p381–391 v3 no 35. doi 10.1016/s0001-4575(02)00014-3.
[28] Ranney TA, Simmons LA, Masalonis AJ. Prolonged exposure to glare and driving time: Effects on performance in a driving simulator. Accid. Anal. Prev.. 1999. p. 601–610 vol.6 no 31. doi 10.1016/s0001-4575(99)00016-0.
[29] Kecklund G, Åkerstedt T. Sleepiness in long distance truck driving: An ambulatory EEG study of night driving. Ergonomics. 1993. p. 1007-1017 v12 no 36. doi 10.1080/00140139308967973.
[30] Fisher RA. On the interpretation of 2 from contingency tables, and the calculation of P. Journal of the Royal Statistical Society. 85 (1) p 87–94. 1922. doi:10.2307/2340521. JSTOR 2340521.
[31] Walker SH, Duncan DB. Estimation of the probability of an event as a function of several independent variables. Biometrika. 54 (1/2). p 167–178. 1967. doi:10.2307/2333860. JSTOR 2333860.
[32] David AF. Statistical Models: Theory and Practice. Cambridge University Press. p. 128. 2009.